TU Delft

# Modification of an Asphalt Binder with Altraflex 2006

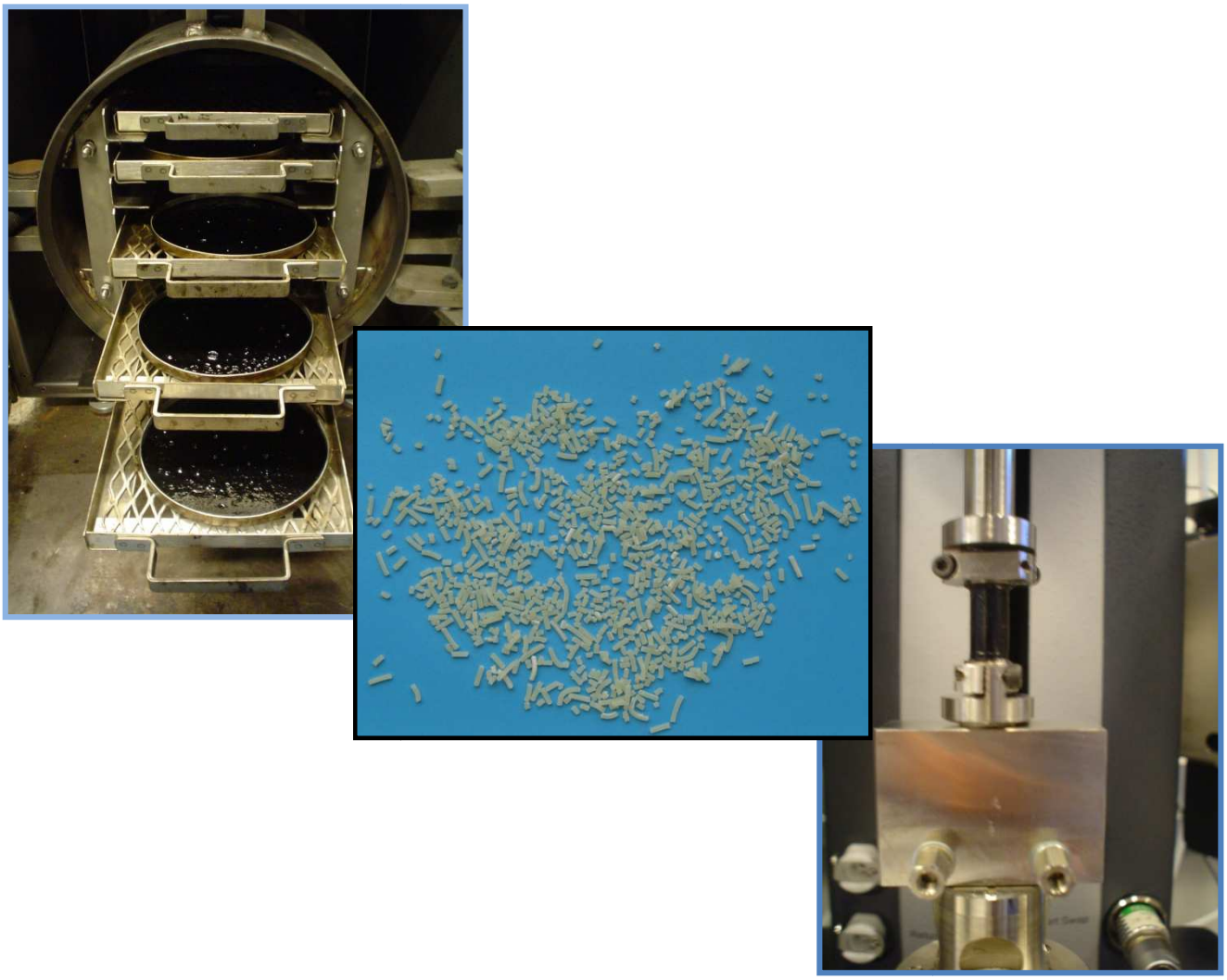

**A.J.D. Adhin**

Januari 2008

ALTRAFLEX

**TECHNISCHE UNIVERSITEIT DELFT**
Faculty of Civil engineering and Geosciences

MSc-Thesis

# "Modification of an Asphalt Binder with Altraflex 2006"

Graduation committee:

| | |
|---|---|
| Prof.dr.ir. A.A.A. Molenaar | TU Delft (Road and Railway Engineering) |
| Dr.ir .A.L.A. Fraaij | TU Delft (Material Science) |
| Ir. M. van de Ven | TU Delft (Road and Railway Engineering) |
| Ir. L.J.M. Houben | TU Delft (Road and Railway Engineering) |
| Drs. J.P. Wortelboer | Altravie B.V. |

A.D.J. Adhin

**Abstract**

In this thesis the effects of modifying B70/100 bitumen with Altraflex 2006 on the rheological and mechanical properties were investigated. Altraflex 2006 is a special modifier developed by Veenvoort which can be added to the bitumen at the pugmill. In this way relative small amounts of bitumen and asphalt mixtures can be modified. Altraflex 2006 contains about 40 % SBS polymers. Rheological and mechanical tests were performed on both the B70/100 and B70/100 containing 6 and 12 percent Altraflex 2006. Penetration and Ring and Ball tests were performed on B70/100 and B70/100 with 6% and 12% Altraflex 2006.
The polymer dispersion in the Altraflex 2006 modified bitumen after 5 and 10 minutes mixing time was visualized by means of an Epifluorescence microscope.
Dynamic Shear tests were performed on B70/100, B70/100 with 6% Altraflex 2006 and B70/100 with 12% Altraflex 2006 at temperatures ranging from $-10^0$ C to $60^0$ C and frequencies ranging from 0.1 rad/sec to 400 rad/sec.

Mortars were made containing B70/100, sand, 6% Altraflex 2006 and two different fillers. These mortars were aged in the Pressure Ageing Vessel (PAV) during 20 hours at a pressure of 21 bars. Dynamic shear tests and Fatigue tests were performed on the aged materials. Dynamic Shear tests were done at temperatures ranging from $-10^0$ C to $60^0$ C including at each temperature a frequency sweep ranging from 0.1 rad/sec to 400 rad/sec on aged B70/100, aged B70/100 with 6% Altraflex 2006 and the four different aged mortars.
Fatigue tests were done on aged B70/100 aged B70/100 with 6% Altraflex 2006 and the four different aged mortars at $10^0$ C at a frequency of 40 Hz.

From all the test we can overall conclude that the rheological behavior of Altraflex 2006 modified bitumen seems to be dependent on the amount of Altraflex 2006 added, the mixing time and the type of bitumen used.

Effect of Altraflex 2006 addition could not be clearly shown on the mechanical behavior of Altraflex 2006 modified mortars.

**Acknowledgement**

I would like to thank my graduation committee: Prof.dr.ir.A.A.A.Molenaar, ir. M. van de Ven, Drs J. Wortelboer, Dr.ir. A.L.A. Fraaij and ir. L.J.M Houben for their time and useful assistance throughout the entire thesis.

I wish to thank the Road and Railway laboratory staff Jan Moraal, Marco Poot, Jan-Willem Bientjes and ir. Radjan Khedoe for their help in conducting the laboratory work in my study.

I wish to thank Dave van Vliet of the Dienst Weg en Waterbouw (DWW) for his help in performing the Microscopic research in my study.

I am also grateful to my aunt Sila Mahabier-Alakhramsing and my uncle Ram Mahabier for letting me stay at their home for a few years.

Sincere thanks to my aunt Emmie Adhin who supported me financially throughout my study.

Countless thanks to my loving parents Arnold Adhin and Indra Adhin-Alakhramsing for giving me the opportunity to study abroad and always supporting and encouraging me.

Last but not least I would like to thank my husband ir. Prewheen Abhelakh for his love, support and patience.

Delft, January 2007

## TABLE OF CONTENTS

# 1 INTRODUCTION

The effect of polymer modification is basically to achieve the following objectives:
a. to increase the resistance to permanent deformation at elevated temperatures,
b. to improve fatigue performance in general and at low temperatures
c. to improve the adhesive/cohesive strength

## 1.1 Raveling resistance

Although all the objectives mentioned above are of importance, their relative importance depends on the type of mixture and the location of the mixture in the pavement. For base course mixtures e.g. especially the resistance to fatigue is of importance while for surface layer mixtures, the resistance to permanent deformations is of prime importance. For porous asphalt concrete however, the resistance to raveling is the key parameter.

Raveling relates to loss of surface aggregate due to traffic and environmental effects without any loss of cohesion of internal fines. If the tensile stress (generated in the bituminous binder) exceeds the breaking strength of the bitumen, cohesive fracture of the bitumen will occur and the aggregate particle will be detached from the road surface. Adhesive failure will occur when the applied stress is higher than the adhesive strength. Raveling is believed to occur mostly at low temperatures and at short loading times when the stiffness of the bitumen is high. As a consequence aged mixtures are more prone to raveling than virgin mixtures.

## 1.2 Research objective

The purpose of this research is to determine to what extend the rheological and mechanical behavior of bitumen can be enhanced by applying the Altraflex 2006 modification.

## 1.3 Structure of report

After this introduction, a literature study on bitumen, polymer modified bitumen and Altraflex 2006 is presented in chapter 2. Chapter 3 gives an overview of the materials used in this research and the background of the tests performed in this research.
In chapter 4 the results of all the tests are presented. Chapter 5 discusses the findings while the thesis is concluded with chapter 6 containing conclusions and chapter 7 containing recommendations.

# 2 LITERATURE STUDY

## 2.1 Bitumen [1]

Here after a short summary is given of the most important properties and characteristics of bitumen and polymer modified bitumens. The text is based on reference [1].

### 2.1.1 Bitumen constitution, structure and rheology

The exact composition of bitumen varies according to the source of the crude oil from which the bitumen originates. Elementary analyses of bitumens manufactured from a variety of crude oils show that most bitumens contain the components given in table 2.1

| Element | Concentration % by mass |
|---|---|
| Carbon | 82 - 88 |
| Hydrogen | 8 - 11 |
| Sulphur | 0 - 6 |
| Oxygen | 0 - 1.5 |
| Nitrogen | 0 - 1 |

**Table 2.1**: Chemical composition of bitumen [1]

Bitumen can be separated into two broad chemical groups: asphaltenes and maltenes. The maltenes can be subdivided into saturates, aromatics and resins (Fig 2.1)

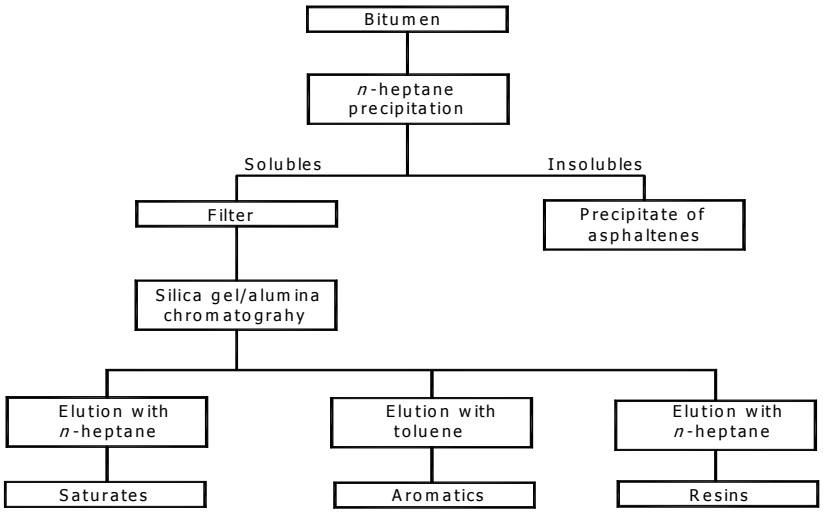


**Fig 2.1**: Schematic representation of the analysis for chemical composition of bitumen [1].

Further analysis of each of the four groups of bitumen show that they are composed as shown in table 2.2

| Type | Color | Molecular weight | Particle size | Hydrogen/Carbon atomic ratio | Soluble in n-heptane | % in bitumen |
|---|---|---|---|---|---|---|
| Asphaltenes | Black or brown | 1000 to 100 000 | 5 to 30 nm | 1:1 | Insoluble | 5 to 25% |
| Resins | Dark brown | 500 to 50 000 | 1 to 5 nm | 1:3 to 1:4 | Soluble | 15 to 30% |
| Aromatics | Dark brown | 300 to 2000 | | 1:5 | | 40 to 65% |
| Saturates | Straw or white | 300 to 2000 | | 1:8 | | 5 to 20 % |

**Table 2.2.**: Analysis on the four groups of bitumen [1]

Asphaltenes

The asphaltene content has a large effect on the rheological characteristics of a bitumen. Increasing this content produces a harder bitumen with a lower penetration, higher softening point and consequently a higher viscosity.

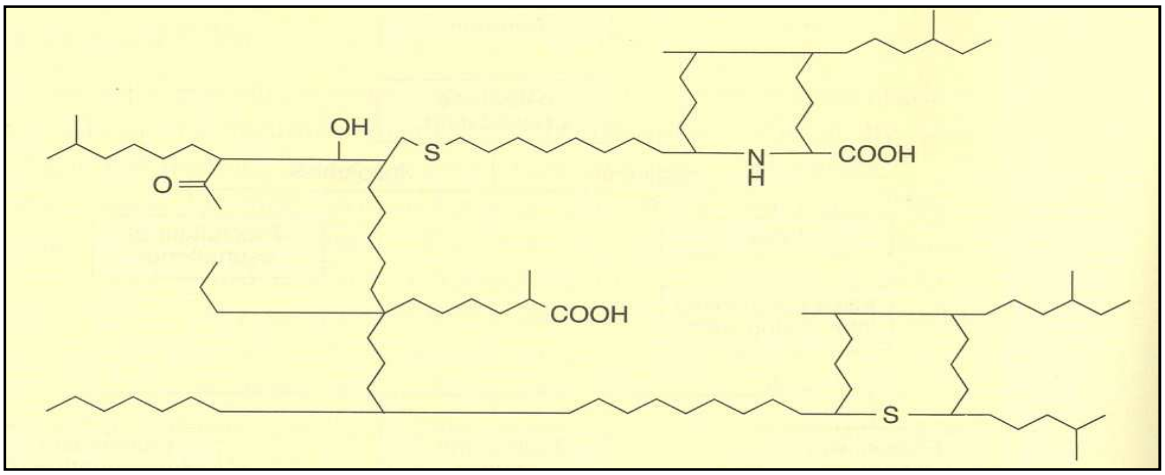


**Fig 2.2:** Typical Asphaltene structure [1]

Resins

Resins are dispersing agents for asphaltenes. The proportion of resins to asphaltenes governs to a degree the solution (SOL) or gelatinous (GEL) type character of a bitumen. This is further explained on page 5.

Aromatics

Aromatics consist of non-polar carbon chains in which the unsaturated ring systems (aromatics) dominate and they have a high dissolving capability for other high molecular weight hydrocarbons.

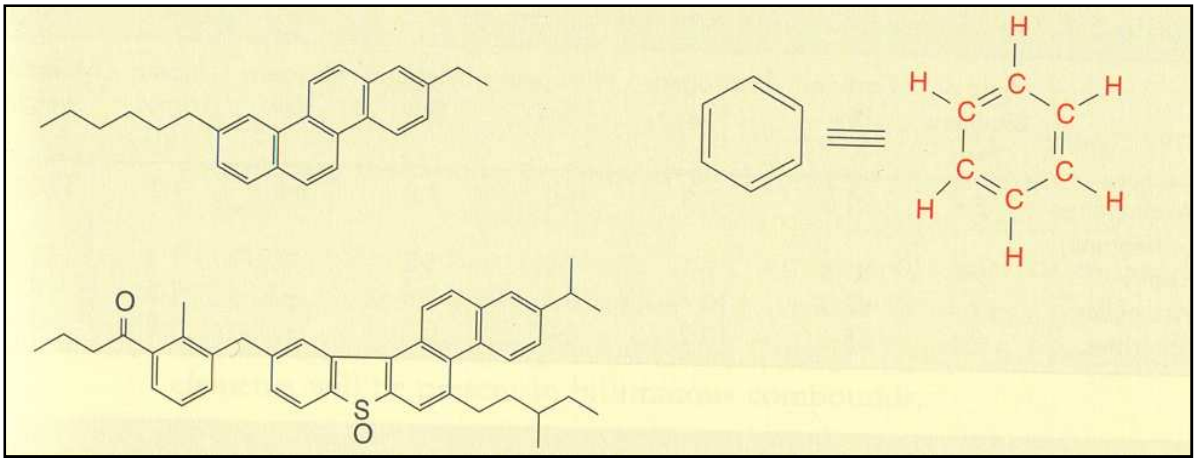


**Fig 2.3**: Typical Aromatic structure [1]

Saturates

Saturates consists of straight and branch chain hydrocarbons together with alkyl-nasphaltenes and some alkyl-aromatics

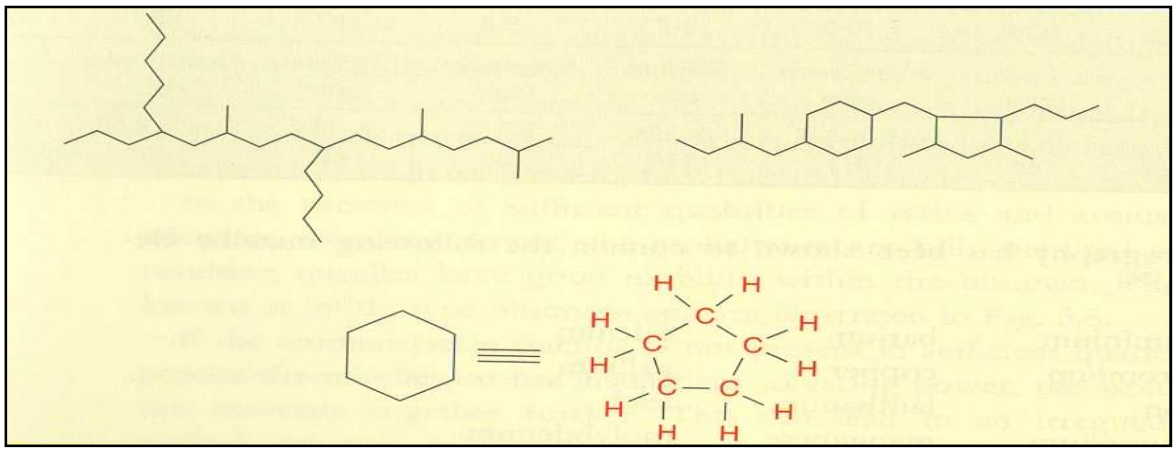


**Fig 2.4:** Typical Saturate structure [1]

### 2.1.2 Bitumen structure

Bitumen is considered to be a colloidal system consisting of high molecular weight asphaltene micelles dispersed or dissolved in a lower molecular weight oily medium (maltenes).

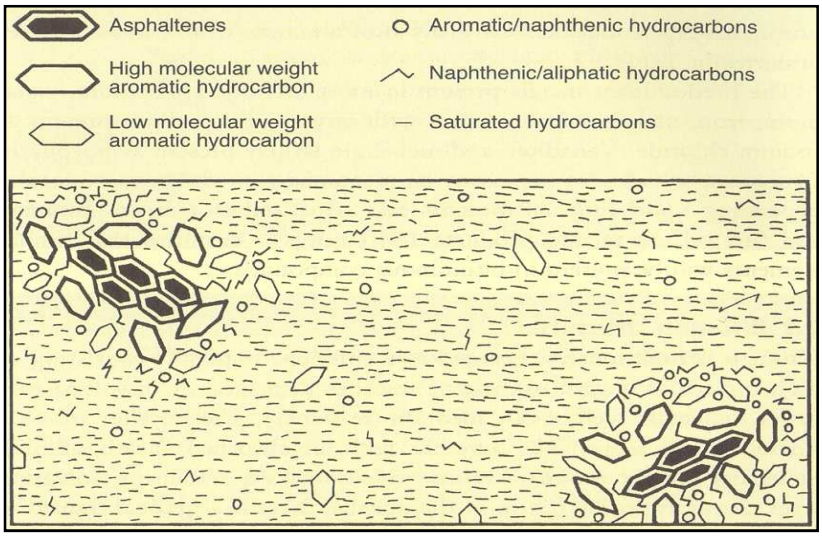


In the presence of sufficient quantities of resins and aromatics of adequate solvating power, the asphaltenes are fully peptized and the resulting micelles have good mobility within the bitumen. These are known as Sol-type bitumens (fig 2.5).

**Fig 2.5**: Schematic representation of a SOL type bitumen [1]

If aromatic/resin fraction is not sufficient to peptize the micelles or has insuffient solvating power the asphaltenes can associate together further. This can lead to an irregular open packed structure or linked micelles in which the internal voids are filled with an intermicellar fluid of mixed constitution. These bitumens are known as GEL types (fig 2.6).

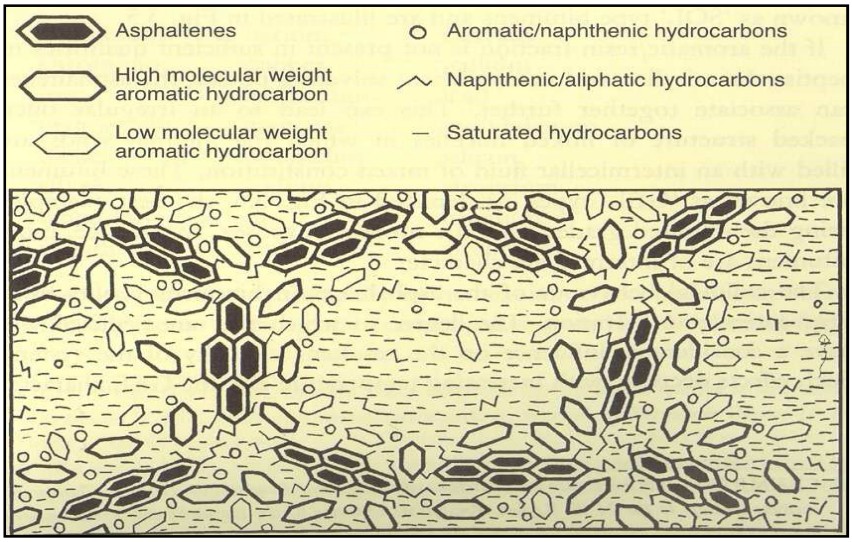


**Fig 2.6**: Schematic representation of a GEL type bitumen [1]

In practice most bitumens are of an intermediate character.

We see that saturates and aromatics can be viewed as carriers for the polar aromatics, i.e. the resins and asphaltenes, who are responsible for the visco-elastic properties of the bitumen at ambient temperatures. Due to the association of the polar molecules it leads to large structures in some case even to three-dimensional networks, i.e. GEL type bitumen.

The degree to which association takes place depends on the temperature , the molecular weight distribution, the concentration of the polar aromatics and on the solvency power of the saturates and aromatics in the maltenes phase. If the concentration and molecular weight of the asphaltenes is relatively low, the result will be a 'SOL" type bitumen.

### 2.1.3 Relationship Constitution and rheology

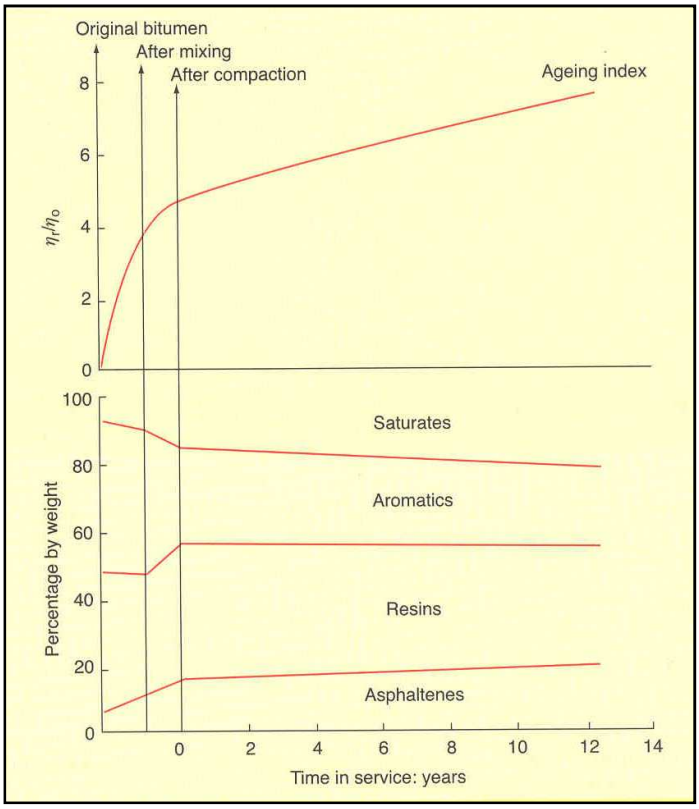


The rheological properties of bitumens depend on the asphaltene content. At constant temperature, the viscosity of bitumen increases as the concentration of the asphaltenes blended into the parent maltenes is increased. This happens when due to ageing, the amount of low molecular fractions decreases. This is shown in figure 2.7.

**Fig 2.7**: Changes in bitumen composition during mixing, laying and in service [1]

## 2.2 Polymer modified bitumen [1]

A modified bitumen is a bitumen where the rheological characteristics are influenced by adding a chemical substance during production {the European standard EN 12597 entitled 'Bitumen Terminology'}.
The bitumen is not chemically changed, but the effect of the modification is based on physical influences on the bitumen characteristics, by adding polymers [2].

One of the prime roles of a bitumen modifier is to increase the resistance of the asphalt to permanent deformation at high road temperatures without adversely affecting the properties of bitumen or asphalt at other temperatures.

The effect of polymer modification is in essence to achieve the next objectives:

a. to increase the resistance to permanent deformation at elevated temperatures,
b. to improve fatigue performance in general and at low temperatures
c. to improve the adhesive/cohesive strength

It is well known that bituminous mixes show a visco-elastic, visco-plastic behavior, which is illustrated properly when a bitumen or asphalt mix specimen is subjected to a step load. The response of the specimen due to this load is given in figure 2.8 [3].

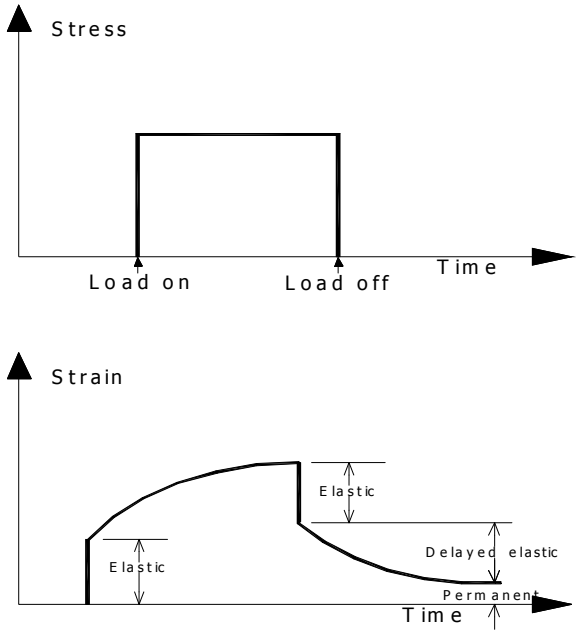


**Fig 2.8**: Visco-elastic responses of a asphalt under a static load

Polymers are built up of one or more types of monomers, which may also be polymerized. If two different polymers are polymerized with each other, the result is a co-polymer. These are split into random co-polymers (i.e. co-polymers in which the monomers appear randomly throughout such as styrene butadiene) and block co-polymers (i.e. co-polymers in which the polymerized monomers are in blocks e.g. styrene-butadiene-styrene block co-polymers). They are also divided into linear and radial (branched) polymers (figure 2.10) [2].

A lot of potential modifiers and additives to be used in bitumen are given in figure 2.9.

| Type of modifier | Example |
|---|---|
| Thermoplastic elastomers | Styrene–butadiene–styrene (SBS)<br>Styrene–butadiene–rubber (SBR)<br>Styrene–isoprene–styrene (SIS)<br>Styrene–ethylene–butadiene–styrene (SEBS)<br>Ethylene–propylene–diene terpolymer (EPDM)<br>Isobutene–isoprene copolymer (IIR)<br>Natural rubber<br>Crumb tyre rubber<br>Polybutadiene (PBD)<br>Polyisoprene |
| Thermoplastic polymers | Ethylene vinyl acetate (EVA)<br>Ethylene methyl acrylate (EMA)<br>Ethylene butyl acrylate (EBA)<br>Atactic polypropylene (APP)<br>Polyethylene (PE)<br>Polypropylene (PP)<br>Polyvinyl chloride (PVC)<br>Polystyrene (PS) |
| Thermosetting polymers | Epoxy resin<br>Polyurethane resin<br>Acrylic resin<br>Phenolic resin |
| Chemical modifiers | Organo-metallic compounds<br>Sulphur<br>Lignin |
| Fibres | Cellulose<br>Alumino-magnesium silicate<br>Glass fibre<br>Asbestos<br>Polyester<br>Polypropylene |
| Adhesion improvers | Organic amines<br>Amides |
| Antioxidants | Amines<br>Phenols<br>Organo-zinc/organo-lead compounds |
| Natural asphalts | Trinidad Lake Asphalt (TLA)<br>Gilsonite<br>Rock asphalt |
| Fillers | Carbon black<br>Hydrated lime<br>Lime<br>Fly ash |

**Fig 2.9**: Additives used to modify bitumen [1].

The most polymers used can be split into elastomers and thermoplastic resins.
Elastomers exhibit a rubber-like behavior (if the material is stretched it will try to jump back to its original form). This behavior is lost at high temperatures. Compared to elastomers thermoplastic resins exhibit a less elastic behavior. Thermoplastic resins differ from elastomers through a melting phase and a relatively low molecular weight [2].

The benefits of different types of modifiers are given in table 2.3.

| Modifier | Permanent deformation | Thermal cracking | Fatigue cracking | Moisture damage | Ageing |
|---|---|---|---|---|---|
| Elastomers | x | x | x | | x |
| Plastomers | x | | | | |
| Tyre rubbers | | x | x | | |
| Carbon black | x | | | | x |
| Lime | | | | x | x |
| Sulphur | x | | | | |
| Chemical modifiers | x | | | | |
| Antioxidants | | | | | x |
| Adhesion inprovers | | | | x | x |
| Hydrated lime | | | | x | x |

**Table 2.3**: Benefits of different types of modifiers [1]

### 2.2.1 The modification of bitumen using thermoplastic elastomers [1]

Of the four main groups of thermoplastic elastomers –polyurethane, polyether-polyester copolymers and styrenic block copolymers- the styrenic block copolymers that have proved to present the most potential when blended with bitumen.

Styrenic block polymers (thermoplastic rubbers or thermoplastic elastomers) may be produced by a chronological operation of successive polymerization of styrene-butadiene-styrene (SBS) or styrene-isoprene-styrene (SIS). Then again, a di-block precursor can be produced by successive polymerization of styrene and mid-block monomer, followed by a reaction with a coupling agent. Not only linear copolymers but also multi-armed copolymers can be produced; these are often referred to as radial or branched copolymers as shown in fig 2.10

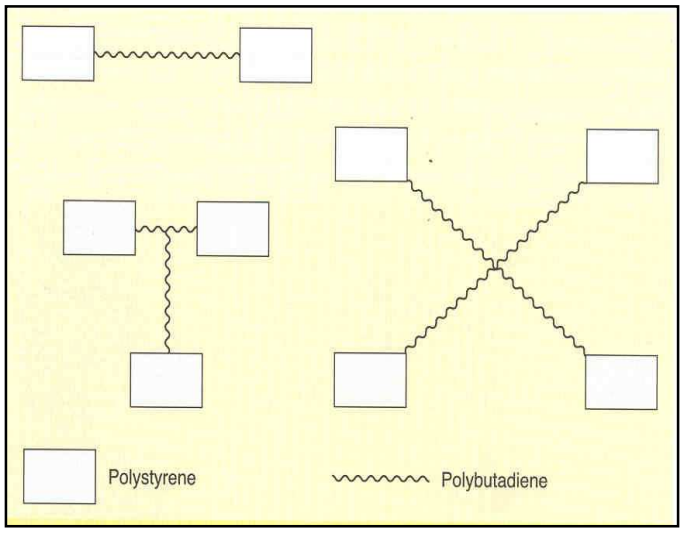


**Fig 2.10**: A linear and branched thermoplastic elastomer [1]

Thermoplastic elastomers derive their strength and elasticity from a physical cross-linking of the molecules into a three dimensional network. This is achieved by the agglomeration of the polystyrene end-blocks into separate domains (figure 2.11) providing the physical cross-links for a three-dimensional polybutadiene or polyisoprene rubbery matrix. The polystyrene end-

blocks impart strength to the polymer and the mid-block that gives the material its incomparable elasticity. At temperature above the glass transition point of polystyrene, it softens as the domains weaken and will even dissociates under stress allowing easy processing. Upon cooling, the domains re-associate and the strength and elasticity is restored, i.e. the material is thermoplastic.

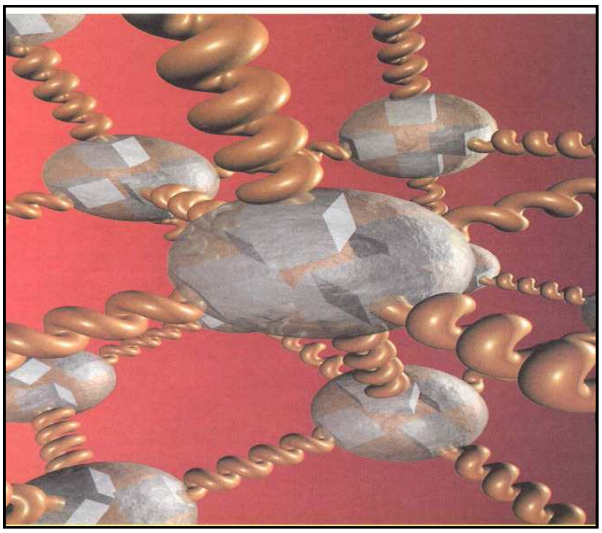

**Fig 2.11**: Schematic structure of thermoplastic elastomer [1]

The quality of the polymer dispersion reached is influenced by a number of factors:

- The constitution of the bitumen
- The type and concentration of the polymer
- The shear rate applied by the mixer

When the polymer is added to the hot bitumen, the bitumen instantly starts to penetrate the polymer particles the styrene domains of the polymer to become solvated and swollen. Once this has occurred, the level of shear exerted on the swollen particles is critical if a satisfactory dispersion is to be achieved within a realistic blending time. For this high shear mixers are required to sufficiently disperse thermoplastic elastomers into the bitumen. In Chapter 2.1 it is seen that bitumens are complex mixtures that can be subdivided into groups of molecules that have common structures:

- Saturates
- Aromatics
- Resins
- Asphaltenes

Saturates and aromatics can be viewed as carriers for the polar aromatics, i.e. the resins and asphaltenes. The polar aromatics are responsible for the visco-elastic properties of the bitumen at ambient temperatures. This is because of association of the polar molecules that leads to large structures, in some cases even to three-dimensional networks, i.e. 'GEL' type bitumen. The degree to which this association takes place depends on the temperature, the molecular weight distribution, the concentration of the polar aromatics and on the solvency power of the saturates and aromatics in the maltenes phase. If the concentration and molecular weight of the asphaltenes is rather low, the result will be a 'SOL' type bitumen.

The addition of thermoplastic elastomers with a molecular weight similar to or higher than that of the asphaltenes disturbs the phase equilibrium. The polymer and the asphaltene compete for the solvency power of the maltenes phase and if insufficient maltenes are available, phase separation may possibly take place

### 2.2.2 The modification of bitumen by the addition of non-rubber thermoplastic polymers [1]

The principal non-rubber thermoplastic polymers used in modified binders are Polyethylene, polypropylene, polyvinyl chloride, polystyrene and ethylene vinyl acetate (EVA).
As thermoplastics, they are characterized by softening on heating and hardening on cooling. These polymers tend to influence the penetration more than the softening point, which is the opposite tendency of thermoplastic elastomers. Thermoplastic polymers, when mixed with bitumen associate below certain temperatures increasing the viscosity of the bitumen. On the other hand they do not significantly increase the elasticity of the bitumen and, when heated, they can separate which may give rise to a coarse dispersion on cooling.

## 2.3 Altraflex 2006

Altraflex 2006 is a special modifier, which can be added to the bitumen at the pugmill. Altraflex 2006 contains about 40 % SBS polymers.

Altraflex 2006 contains several components:
-for polymer modification: an SBS-type elastomer material

-for ageing resistance: a material that can absorb free radicals so that the oxidation process is slowed down

-an adhesion improving substance on stone, which at the same time ensures better water-resistance

The philosophy behind these additives is to ensure that oxygen, and UV light have as little as possible influence on the interaction between the mortar and the stone area.

Due to commercial reasons there is no further information available about the composition of Altraflex 2006.

# 3 BACKGROUND ON MATERIALS AND TESTS

As mentioned before, Altraflex 2006 is a modification that can be added to the bitumen at the pugmill. This makes Altraflex 2006 very interesting to be used in the production of small or dedicated quantities of SBS modified asphalt mixtures. The question however is how much Altraflex 2006 can be added to the base bitumen without mixing problems and what the characteristics are of Altraflex 2006 modified bitumen. In order to determine this a test program was developed that consisted of two phases.

The first part of the test program is a preliminary analysis in which an indication of the ease of mixing the Altraflex 2006 with bitumen B70/100 is investigated. In this part also the viscosity rheological properties of Altraflex 2006 modified B70/100 are determined. Use is made of the penetration test, the Ring and Ball softening point test and the Dynamic Shear Rheometer. Also a microscopic investigation of the dispersion of the Altraflex 2006 in the bitumen is done (Scheme 3.1).
In the second part mortars are made with B70/100, different fillers, sand and 6% Altraflex 2006 (Scheme 3.2 & 3.3).
These mortars are aged in the PAV and with this material DSR tests and fatigue test are done (Scheme 3.3).

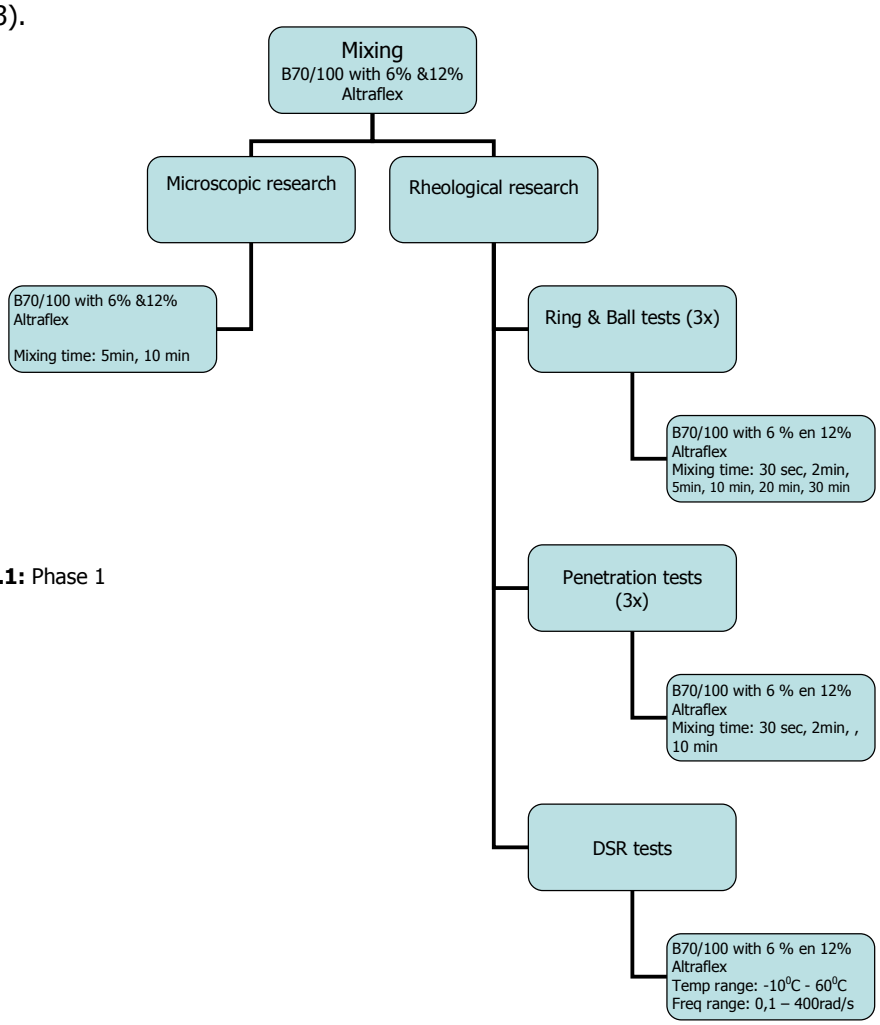


**Scheme 3.1:** Phase 1

**Scheme 3.2:** Phase 2A

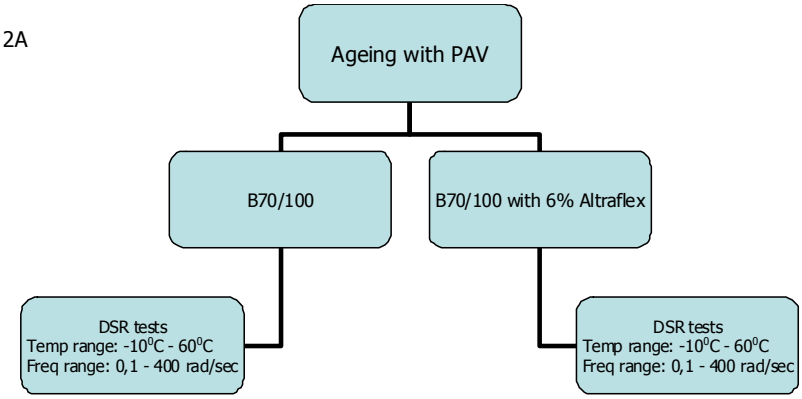


**Scheme 3.3:** Phase 2B

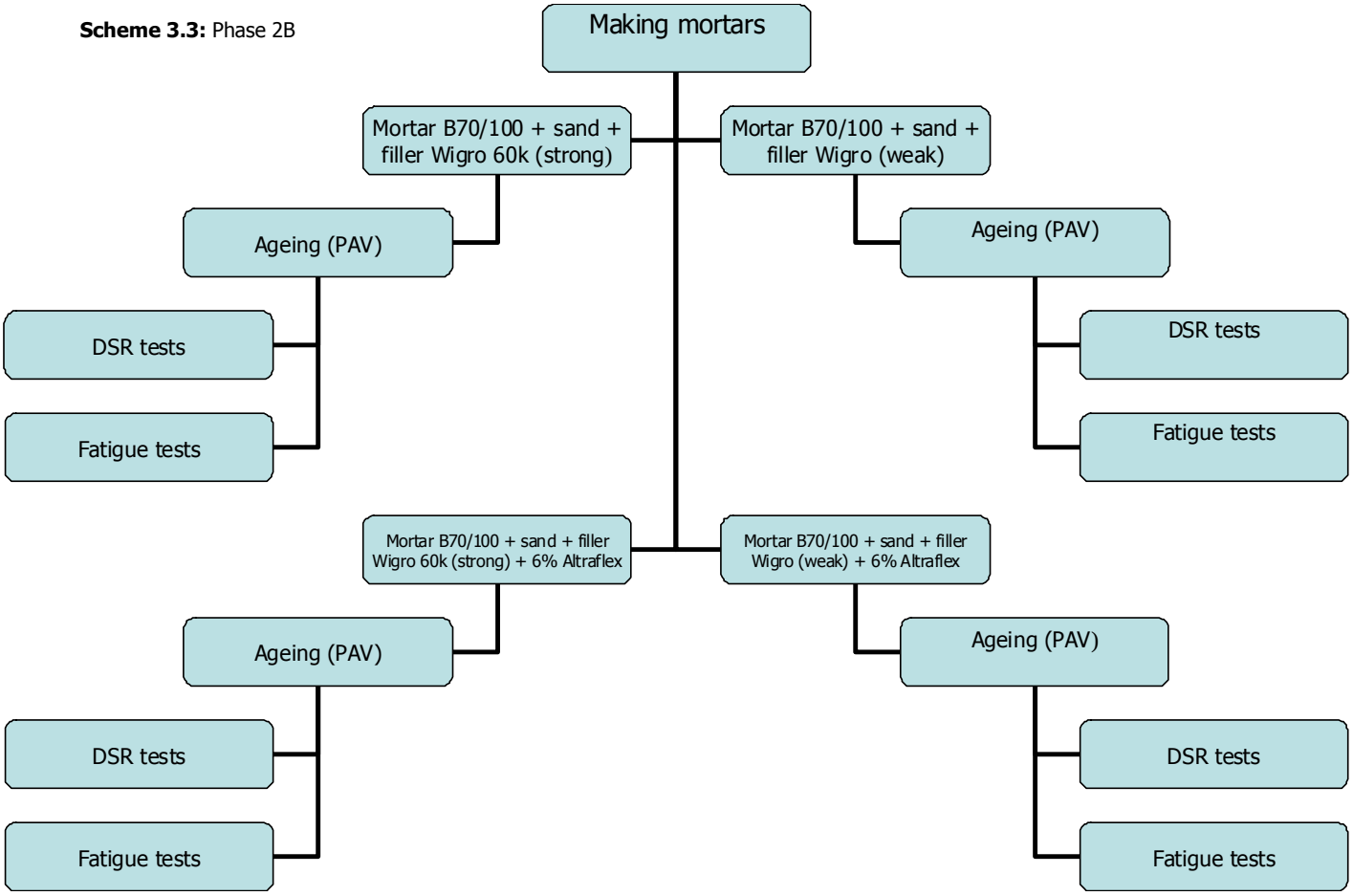

## 3.1 Background on materials

### 3.1.1 Bitumen

The bitumen used in this investigation is a Q8 (Kuwait) Bitumen B70/100
The specifications for a B70/100 are given in table 3.1:

| **Characteristic** | **Bitumen 70/100** |
|---|---|
| Penetration at 25$^0$C , in 0.1 mm | 70 – 100 |
| Saturation point, $^0$C | 43 - 51 |
| Penetration index | -1.5 - + 0.7 |
| Flash point, minimum, $^0$C | 230 |
| Solubility, minimum , % | 99 |
| Dynamic viscosity 60 $^0$C, minimum, mm$^2$/s | 90 |
| Kinematic viscosity at 135 $^0$C, minimum, mm$^2$/s | 230 |

**Table 3.1**: The characteristics of the B70/100

### 3.1.2 Altraflex 2006

As mentioned before Altraflex 2006 consists of an SBS type elastomer, a material that can absorb free radicals so that the oxidation process is slowed down and an adhesion improving substance on stone, which at the same time ensures better water-resistance.

The amount of SBS is roughly 40% of the total amount of Altraflex 2006. Quantities of 6% and 12% of Altraflex 2006 are added to the bitumen implying an addition of approximately 3% and 6% SBS.

### 3.1.3 Fillers

Two types of fillers are used in this research being Wigro and Wigro 60K. The characteristics of these fillers are given in table 3.2

| **Type** | **Wigro** | **Wigro 60k** |
|---|---|---|
| Specification | weak | strong |
| Producer | Ankerpoort Winterswijk | Ankerpoort Winterswijk |
| Location of fabrication | Winterswijk | Winterswijk |
| Rigden Air voids % V/V (min-max) | 34 - 40 | 44 - 50 |
| Density (kg/m$^3$) (min-max) | 2675 - 2875 | 2475 - 2675 |
| Composition %(m/m) | Limestone 100 | Limestone 65 - 75<br>Calcium hydroxide 25 - 35 |
| Bitumen number | 42 - 48 | 56 - 62 |

**Table 3.2**: Characteristics of fillers

The effects on the rheological properties of the mortars are investigated after using two different types of fillers: Filler Wigro 60k that contains calcium hydroxide and filler Wigro that does not contain calcium hydroxide.

### 3.1.4 Mortars

With the materials mentioned above mortars are made with the following composition [4] (by mass)
Sand: Bitumen: Filler = 0.88 : 1: 1.06

Characteristics sand: fine sand , diameter smaller than 0.5 mm [4]

The mortars contain:

Mortar 1: B70/100 with Wigro 60K and sand
Mortar 2: B70/100 with Wigro 60 and sand
Mortar 3: B70/100 with Wigro 60K, Altraflex 2006 and sand
Mortar 4: B70/100 with Wigro 60, Altraflex 2006 and sand

In the cases where Altraflex 2006 is added the percentage used is 6% of the bitumen weight.

## 3.2 Background on tests

In this section some background information is given about the tests that were performed during this investigation.

### 3.2.1 Mixing Altraflex 2006 into Bitumen B70/100


The B70/100 is mixed with 6 % and 12 % Altraflex 2006 with a high shear mixer during 10 minutes The high shear mixer used was a Silverson mode L4R. After mixing the Altraflex 2006 for at least 10 minutes in the bitumen at 170 $^0$C, a homogenous mix was obtained.

Because in practice a polymer modifier is mixed in the pug mill for maximum 30 to 45 seconds, Altraflex 2006 modified samples were taken after 30 seconds and 2 minutes mixing time with the high shear mixer to determine their rheological behavior.
To investigate influence of mixing time further rheological investigation was done on samples of Altraflex 2006 modified bitumen after 20 minutes and 30 minutes mixing time.

**Fig 3.1**: The high shear mixer

The high shear mixer (figure 3.1) works with the principle Stator and Rotor: The fluids (with Altraflex 2006 grains) go in, as a normal centrifugal pump, through the machine and go out

with a certain intensified pressure. During this pace through the machine the substances must move themselves between the Stator and the twisting Rotor and the present canals. The speed of the rotor was kept at 5000 rpm during the mixing period. Before mixing, the required amount of Altraflex 2006 is put in the tin with the required amount of bitumen, which has a temperature of $170^0$ C.
Then the tin is put on top of a electrically heated plate to keep the temperature of the whole at $170^0$ C, underneath the high shear mixer and the mixing is started at 5000 rpm during 10 minutes.

### 3.2.2 The Penetration test

This test is done according to norm NEN-EN 1426.

In this test, a needle of specified dimensions is allowed to penetrate a sample of bitumen, under a known load (100 g), at a fixed temperature (25 or 40 $^0$C0, for a known time (5 sec). Figure 3.2 shows the test set up as well as close up of the needle penetrating the bitumen.
The penetration is defined as the distance traveled by the needle into the bitumen. It is measured in tenths of millimeters.

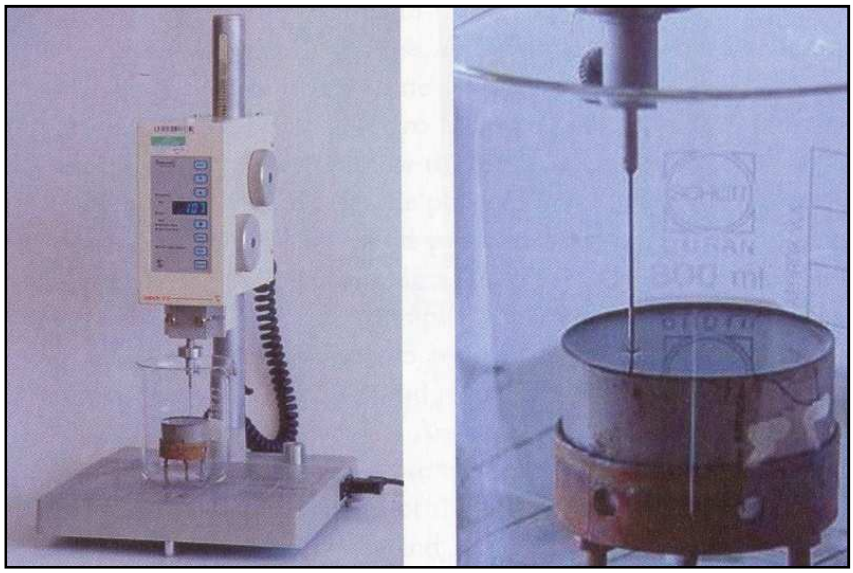

**Fig 3.2:** The penetration test

The penetration test is done for different samples containing pure bitumen B70/100, B70/100 with 6% Altraflex 2006 and B70/100 with 12% Altraflex 2006.
The Altraflex 2006 modified samples were prepared by mixing Altraflex 2006 in B70/100 during 30 seconds, 2 minutes and 10 minutes.

### 3.2.3 Softening point test

This test is performed according to NEN-EN 1427.
For the ring and ball softening point the hot liquid bitumen is poured into two brass rings placed on a silicone proofed glass plate.
The rings are filled to the brim and the excess bitumen struck off with a metal edge. After cooling the bitumen filled rings are freed from the glass plate and mounted over holes on a twin holder. A steel ball bearing weighing 3.5g is placed on each bitumen ring. The holder, with a thermometer clipped onto it, is then placed in a water filled glass beaker. The beaker is then placed on a controlled heating ring and the water temperature is raised at a defined rate of 5°C per minute. The temperature of the water in the beaker is kept evenly distributed using a magnetically driven stirrer. At the bitumen's softening point, the bitumen in the ring deforms under the weight of the ball and both flow down through the ring. The temperature is recorded when the bitumen touches a metal plate mounted 25 mm below the ring. This is the softening point.
Figure 3.3 shows some details of the test.

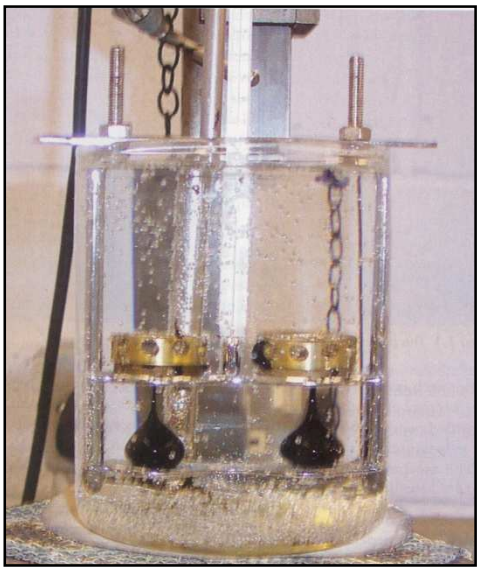

**Figure 3.3**: The ring and ball softening test

The softening point test is done for different samples containing pure bitumen B70/100, B70/100 with 6% Altraflex 2006 and B70/100 with 12% Altraflex 2006.
The Altraflex 2006 modified samples were prepared by mixing Altraflex 2006 in B70/100 during 30 seconds, 2 minutes, 5 minutes and 10 minutes.

### 3.2.4 Dynamic Shear test as used for rheology and fatigue measurements

#### 3.2.4.1 Rheology measurement

The Dynamic Shear Rheometer (DSR) tests were performed according to norm NEN-EN 14770. Figure 3.4 shows the test device (type AR 2000ex).

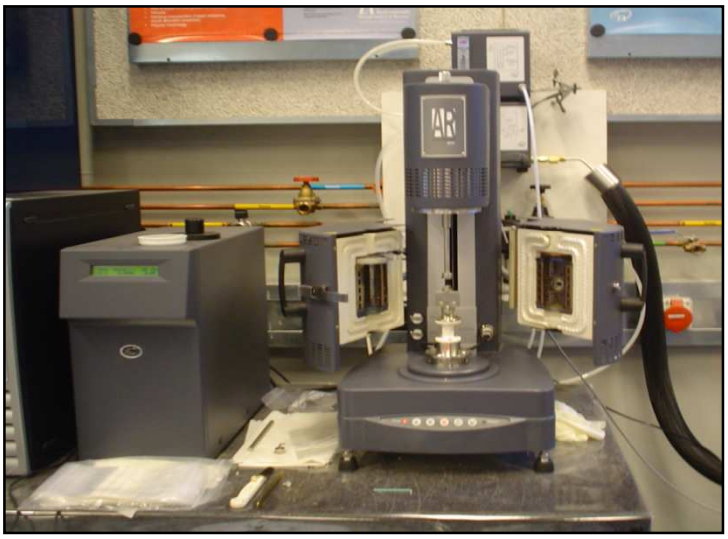

**Fig 3.4**: The Dynamic Shear Rheometer

The DSR consists of two parallel metal plates, an environmental chamber, a loading device, and a control and data acquisition system.
Two upper plate sizes are used. A small plate, 8 mm in diameter, is used for moderate temperatures ($-10^0$ C to $20^0$ C) and stiffnesses (G*) ranging between 100 kPa to 10 000 kPa. The large plate, with a diameter of 25 mm, is used to perform tests at higher temperatures ($20^0$ C to $60^0$ C) and lower stiffness (G*) values (between 1 kPa to 100 kPa). During testing, one of the plates is oscillating with respect to the other plate, at preselected frequencies and rotational deformation amplitudes. Figure 3.5 gives a schematic representation of the test.

Long or static loads or very low frequency loading will show the viscous characteristics of the binder. When the loading time is short at high frequencies then the elastic properties will dominate. The influence of temperature is similar; high temperatures will reveal viscous behavior and will reverse (elastic) at lower temperatures. The complex shear modulus and the phase angle define the asphalt binder's resistance to shear deformation in the linear visco-elastic region.
The complex shear modulus and the phase angle are related to rutting and fatigue of the asphalt mixture.

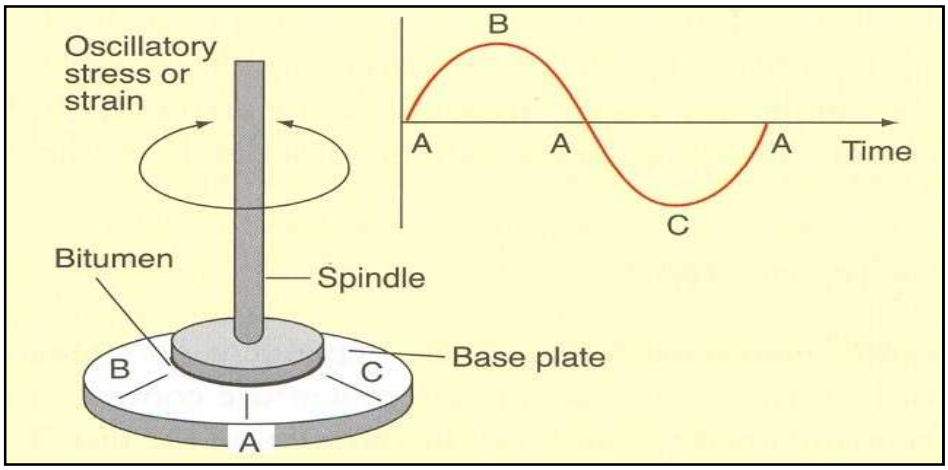


**Fig 3.5**: Schematic representation of the DSR mode testing

As mentioned before the Dynamic Shear Rheometer or DSR is used to characterize the viscous and elastic behavior of asphalt binders. This is done by measuring the complex shear modulus (G*) and phase angle (δ) of asphalt binders at the desired temperature and frequency of loading. Complex shear modulus G* is a measure of the total resistance of a material to deforming when repeatedly sheared. It consists of two components: the storage modulus (G') or the part that is elastic (recoverable), and the loss modulus (G"), the part that is viscous (non-recoverable).

$$G^* = \sqrt{(G^{"})^2 + (G^{'})^2}$$

In which
G* = the complex shear modulus
G' = the storage modulus
G" = the loss modulus

A graphical representation of the complex modulus as well as the storage and loss modulus is given in figure 3.6.

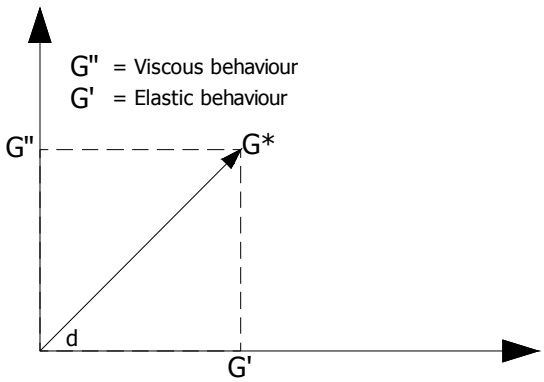


**Fig 3.6**: Relationship between G*, G', G" and δ (d)

The time lag between the applied stress and the resulting strain is the phase angle δ (figure 3.7).
For a perfectly elastic material

there is an instantaneous response and the time lag between the applied stress and the resulting strain or the phase angle δ is zero. For a viscous liquid the time lag between the applied stress and the resulting strain or the phase angle δ is 90 degrees.

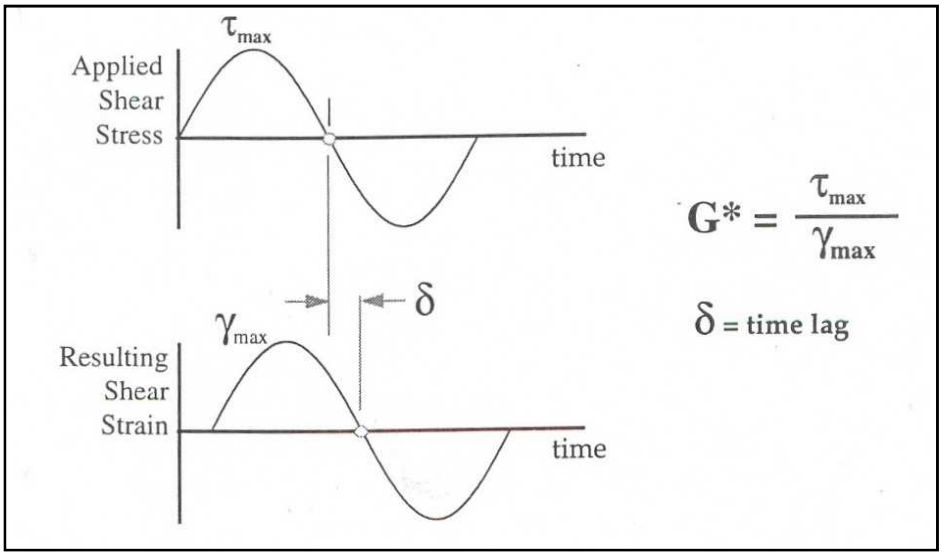


**Fig 3.7**: Stress-Strain response of a visco-elastic material

Both temperature and loading time have an influence on the stiffness characteristics of both bitumen and asphaltic mixes. It is however not practical to perform test over the entire temperature and loading time domain in order to determine this dependency. Stiffness values covering the entire time and temperature domain however can be obtained by making use of the equivalency principle between frequency and temperature. This equivalency is a result of the thermo rheological simple behavior of bitumens and asphalt mixes, it allows to construct a master curve relating stiffness to load frequency given a certain temperature. The shift factor for all the different temperatures and loading time can be calculated with the William, Landel and Ferry formula [21].

$$\log a_T = \frac{1}{2.3} \ln a_T = -\frac{C_1(T - T_r)}{C_2 + T - T_r}$$

Where:
$a_T$ = shift factor
$T_r$ = reference temperature ($^0$C)
T = test temperature ($^0$C)
$C_1$ , $C_2$ = material dependent parameters

If one desires then to know the stiffness modulus at e.g. loading frequency of 5*10-² HZ at the reference temperature level Ts = 20°C this value can be obtained then from measurements taken at a frequency of f Hz made at temperature T = 30°C. This frequency can be calculated from [3]:

$$f_{T=30°C} = f_r / a_{T=30°C}$$

where: $f_r$ = in this case $5*10^{-2}$
$f_{T=30°C}$ = frequency at which stiffness modulus has to be determined at 30°C
$a_{T=30°C}$ = shift factor between 30°C curve and the curve at the reference temperature of 15°C

Rheology tests were done on pure B70/100 and B70/100 bitumen modified with 6% and 12% Altraflex 2006. In the table 3.3 beneath an overview is given of the materials on which the DSR test is performed:

| | B70/100 | B70/100 with 6% Altraflex 2006 | B70/100 with 12% Altraflex 2006 |
|---|---|---|---|
| Pure | x | x | x |
| Aged | x | x | - |

**Table 3.3**: Overview of the materials on which the DSR test is performed

Rheology tests were also done on aged mortars of B70/100 and aged mortars B70/100 bitumen modified with 6% Altraflex 2006. In the table 3.4 beneath an overview is given of the mortars on which the DSR test is performed:

| | Mortar 1 B70/100 + Wigro60K+ sand | Mortar 2 B70/100 + Wigro + sand | Mortar 3 B70/100 + Wigro60K + sand + Altraflex 2006 | Mortar 4 B70/100 + Wigro + sand + Altraflex 2006 |
|---|---|---|---|---|
| Pure | - | - | - | - |
| Aged | x | x | x | x |

**Table 3.4:** Overview of the mortars on which the DSR test is performed

The tests were done at temperatures ranging from $-10^0$ C to $60^0$ C in steps of $10^0$ C. Frequencies ranging from 0,1 rad/second to 400 rad/second were used. For details about the ageing protocol, the reader is referred to section 3.2.6.

### 3.2.4.2 Fatigue measurements

The fatigue tests are also done with the Dynamic Shear Rheometer.
In this test, mortar columns with a height of 20 mm and a diameter of 6 mm are subjected to torque in a stress-controlled mode. The mortar columns for DSR shear testing are enclosed in steel rings over a height of 4 mm at both ends.
Figure 3.8 shows a sample as used in the fatigue tests. For details about the specimen preparation the reader is referred to [4].

**Fig 3.8**: Fatigue mortar columns

G* is the ratio of maximum shear stress ( $\tau_{max}$ ) to maximum shear strain ( $\gamma_{max}$ ) or

$$G^* = \frac{\tau_{max}}{\gamma_{max}} \quad (1)$$

To calculate the maximum shear stress ( $\tau_{max}$ ) and the maximum shear strain ( $\gamma_{max}$ ) we use:

$$\tau_{max} = \frac{2T}{\pi r^3} \quad (2)$$

$$\gamma_{max} = \frac{\theta r}{h} \quad (3)$$

In which:

$\tau_{max}$ = maximum shear stress
$\gamma_{max}$ = maximum shear strain
T = maximum applied torque
r = radius of binder specimen
θ = deflection (rotation) angle
h = specimen height

The $N_{failure}$ is calculated with

$$N_f = a.\tau^{-b} \quad (4)$$

$$\log N_f = \log a - b \log \tau \quad (5)$$

In which:

$\tau$ = applied shear stress
a,b = constants

From the fatigue test we can calculate the dissipated energy [3]. It is the dissipated energy that causes the specimen to fail.
The dissipated energy per cycle per unit volume can be expressed by:

$$W = \pi \tau \gamma \sin\phi \quad (6)$$

Where
$\tau, \gamma$ = stress and strain amplitude
Φ = phase angle between stress and strain

The total amount of dissipated energy per volume to fatigue can be written as:

$$W_{FAT} = A_F (N_{FAT})^z \quad (7)$$

Where
$W_{FAT}$ = total amount of dissipated energy
$N_{FAT}$ = number of load repetitions to fatigue
$A_F$, z =material constants

Since σ, ε and Φ will change during the cycle we can say:

$$W_{FAT} = N_{FAT} W_{in} / \psi \quad (8)$$

Where
$\psi$ = factor that takes into account the variation in dissipated energy per cycle during the test

The relation between $\gamma$ and N can be determined with:

$$\gamma_0 = \sqrt{\frac{A_F.\psi}{\pi.G^*\sin\phi_0}} N^{(\frac{z-1}{2})} \quad (9)$$

If we assume that:

$$\gamma_0 = \alpha N^{\beta} \quad \text{then} \quad (10)$$

$$\alpha = \sqrt{\frac{A_F.\psi}{\pi.G^*\sin\phi_0}} \quad (11)$$

$$\beta = \frac{z-1}{2} \quad (12)$$

Then N can be calculated with:

$$N = \left(\frac{1}{\alpha}\right)^{\frac{1}{\beta}} \gamma^{\frac{1}{\beta}} \quad (13)$$

We can also calculate what the relation is with the slope m of the DSR curves for the different mortars.

$$\frac{1}{\beta} = \frac{x}{m} \quad (14)$$

In which m is the slope of the graph for the G* at a certain frequency and temperature. The value for x can then be calculated.

Fatigue tests were done on:

| | Mortar 1<br>B70/100 + Wigro60K+ sand | Mortar 2<br>B70/100 + Wigro + sand | Mortar 3<br>B70/100 + Wigro60K + sand + Altraflex 2006 | Mortar 4<br>B70/100 + Wigro + sand + Altraflex 2006 |
|---|---|---|---|---|
| Pure | - | - | - | - |
| Aged | x | x | x | x |

The Fatigue tests are done at $10^0$C and a frequency of 40 Hz

### 3.2.5 Microscopic visualization

The NEN-EN 13632 (en) specifies a method for visualization of the polymer distribution in polymer modified bitumen by fluorescent microscopy.
The principle is that a sample of polymer modified bitumen is homogenized by gentle stirring and poured into a preheated mould. After a controlled cooling procedure to ambient temperature the sample is cooled below -20 $^0$C for a minimum period of time. The bitumen layer is broken into small pieces and the freshly broken surface is viewed through an epifluorescence microscope with a magnification of 25 times to 500 times.

### 3.2.6 Ageing with the Pressure Ageing Vessel

As mentioned before, samples for several tests were subjected to an ageing protocol.
Ageing throughout the in-service life (the so-called long term ageing) is a process that is difficult to simulate because it is a complex process involving temperature, oxygen, UV radiation, moisture etc. Therefore procedures have been developed to simplify the ageing process and one of these procedures is the so-called Pressure Ageing Vessel (PAV). This test is developed to age 500 grams of bitumen at a certain temperature during a certain period of time.

The procedure followed implied exposure of the mortar in the PAV to 90ºC at a pressure of 21 bars during 20 hours.

The ageing is done according to NEN-EN 14769.

Figure 3.9 shows the PAV and figure 3.10 shows in more detail the placement of the trays in the oven.

**Fig 3.9**: The Pressure Ageing Vessel

**Fig 3.10**: The aged material

# 4 INFLUENCE OF AMOUNT OF ALTRAFLEX 2006 AND MIXING TIME ON VISCOSITY CHARACTERISTICS

## 4.1 The Penetration Test

### 4.1.1 B70/100 with different percentages Altraflex 2006

The penetration tests are performed at $25^0$ C en 40 $^0$C.
The mixing time with the High Shear Mixer was 10 minutes and the mixing temperature was $170^0$C.
The results are the average of three tests and are presented in table 4.1, graph 4.1 and graph 4.2.

| Penetration (x 0,1 mm) | | | |
|---|---|---|---|
| Temp ($^0$C) | B70/100 | B70/100 with 6% Altraflex 2006 | B70/100 with 12% Altraflex 2006 |
| 25 | 73.6 | 93.3 | 105.0 |
| 40 | 327.7 | 361.7 | 339.9 |

**Table 4.1**: Results penetration tests at 25 $^0$C en 40 $^0$C, mixing time 10 minutes

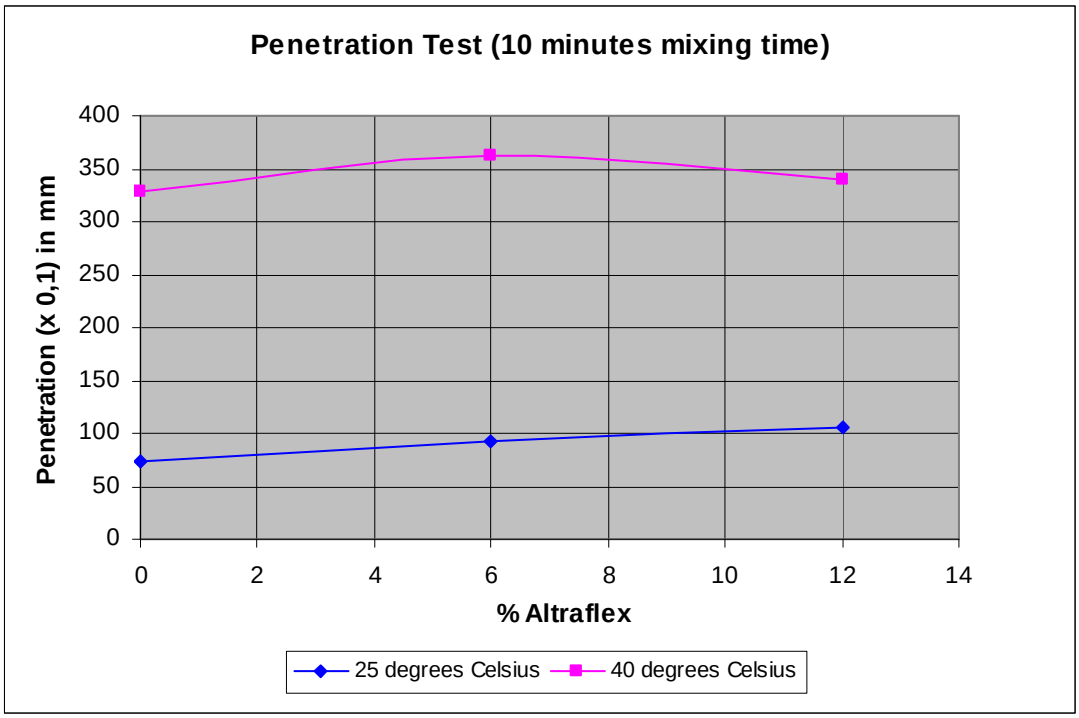


**Graph 4.1**: Penetration tests at 25 $^0$C en 40 $^0$C for different percentages of Altraflex 2006

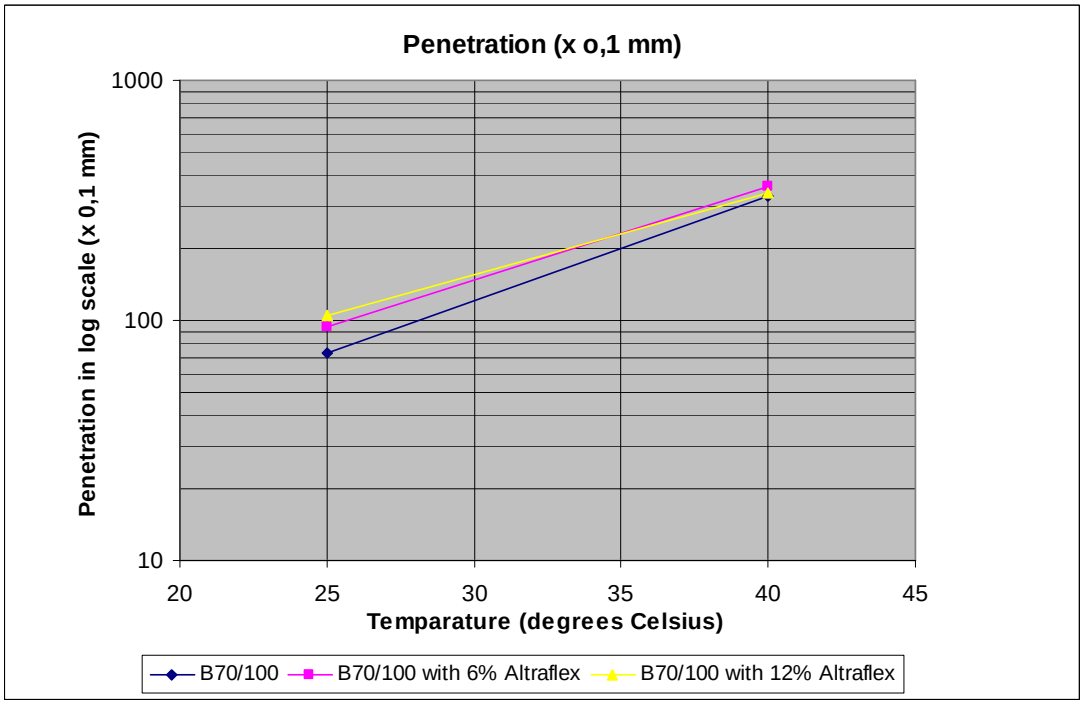


**Graph 4.2**: Penetration of bitumen and Altraflex 2006 modified bitumen as a function of temperature

### 4.1.2 B70/100 with different percentages Altraflex 2006 at different mixing times

It was suggested to do penetration tests on samples of the Altraflex 2006 modified bitumen after mixing times of 30 seconds and 2 minutes.

The penetration tests are performed at $25^0$ C en 40 $^0$C.
The mixing time with the High Shear Mixer was 30 seconds and 2 minutes and the mixing temperature was $170^0$C.

Figure 4.1 shows that the structure of the mixes was not homogeneous.

**Fig 4.1**: Inhomogeneous structure of the mix

The results are shown in tables 4.2 and 4.3.

| | Penetration in mm (0,05 sec, 25 degrees) | | | |
|---|---|---|---|---|
| | B70/100 met 6% Altraflex (x 0,1) 30 seconds mixing time | B70/100 met 6% Altraflex (x 0,1) 120 seconds mixing time | B70/100 met 12% Altraflex (x 0,1) 30 seconds mixing time | B70/100 met 12% Altraflex (x 0,1) 120 seconds mixing time |
| | 76.5 | 87.0 | 83.0 | 75.0 |
| | 73.0 | 85.0 | 82.5 | 62.0 |
| | 98.0 | 80.0 | 86.0 | 84.0 |
| | 95.0 | 86.5 | 72.0 | 73.0 |
| | 75.0 | 75.0 | 60.0 | 75.0 |
| | | | | |
| average x | 83.5 | 82.7 | 76.7 | 73.8 |
| standard deviation σ | 12.0 | 5.1 | 10.7 | 7.9 |

**Table 4.2**: Results penetration of Altraflex 2006 modified bitumen tests at 25 $^0$C, mixing time 30 seconds and 2 minutes

| | Penetration in mm (0,05 sec, 40 degrees) | | | |
|---|---|---|---|---|
| | B70/100 met 6% Altraflex (x 0,1) 30 seconds mixing time | B70/100 met 6% Altraflex (x 0,1) 120 seconds mixing time | B70/100 met 12% Altraflex (x 0,1) 30 seconds mixing time | B70/100 met 12% Altraflex (x 0,1) 120 seconds mixing time |
| | 383.0 | 374.0 | 360.0 | 377.0 |
| | 393.0 | 379.5 | 355.0 | 335.0 |
| | 380.0 | 386.0 | 360.0 | 353.0 |
| | 391.0 | 360.0 | 330.0 | 372.0 |
| | 376.0 | 386.0 | 380.0 | 370.0 |
| | | | | |
| average x | 384.6 | 377.1 | 357.0 | 361.4 |
| standard deviation σ | 7.2 | 10.8 | 17.9 | 17.3 |

**Table 4.3**: Results penetration of Altraflex 2006 modified bitumen tests at 40 $^0$C, mixing time 30 seconds and 2 minutes

The variation of the results of table 4.2 and 4.3 are not in accordance with the norm (NEN-EN 1426). The differences in penetration values within one group of values obtained at specific mixing time/ test temperature combination (e.g. 30 second mixing time/ test temperature 25$^0$C) are larger than the differences allowable in NEN-EN 1426. It is recalled that the maximum allowed difference between the individual readings is 4 (x 0,1 mm) at test temperatures of 25 $^0$C. These large differences are due to the inhomogeneous structure of the mixture. In spite of this the average and standard deviation for each combination is calculated.

Given the fact that inhomogeneous mixtures were obtained at mixing times of 30 and 120 seconds, it was concluded that these mixing times were too short.

### 4.1.3 B40/60 with different percentages of Altraflex 2006

To compare the influence of the bitumen, tests were also done on a B40/60 bitumen and a B40/60 bitumen with 6% Altraflex 2006. Again the penetration tests were performed at 25$^0$ C en 40 $^0$C. The mixing time with the High Shear Mixer was 10 minutes and the mixing temperature was 170$^0$C.

| Penetration (x 0,1 mm) | | |
|---|---|---|
| Temp ($^0$C) | B40/60 | B40/60 with 6% Altraflex 2006 |
| 25 | 40,3 | 51,8 |
| 40 | 166,3 | 228,2 |

**Table 4.4**: Results penetration tests for B40/60

### 4.1.4 Evaluation of the results

In graph 4.3 and 4.4 the results of the different test are compared with each other:

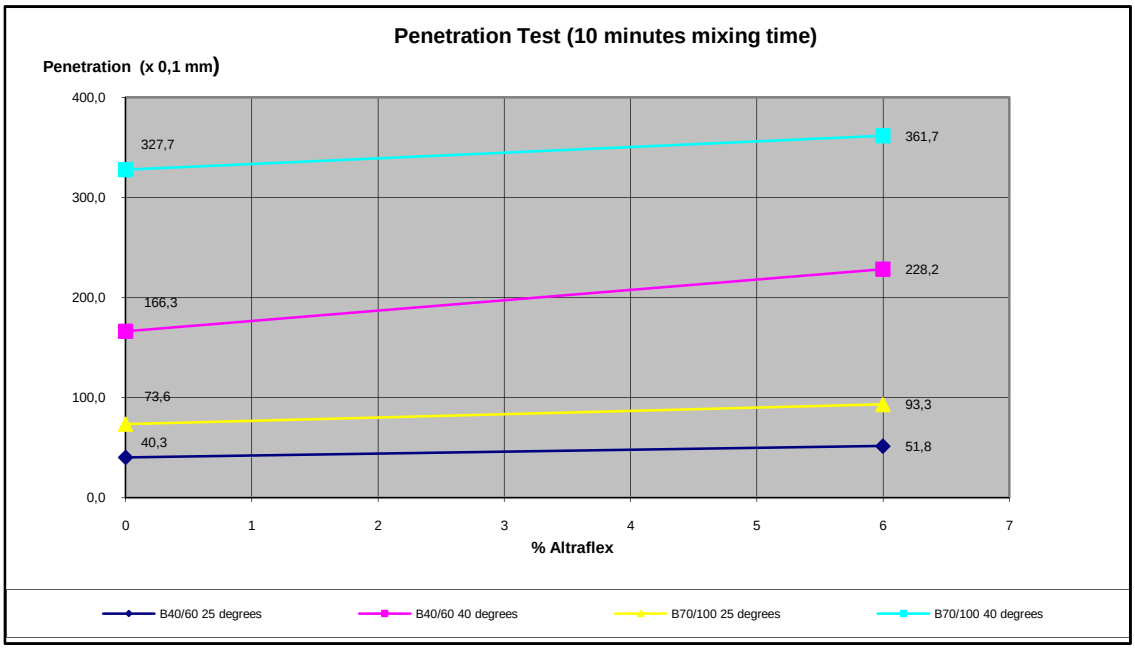


**Graph 4.3**: Penetration test for B70/100 and B40/60 with 0% and 6% Altraflex 2006 at 25 $^0$C en 40 $^0$C

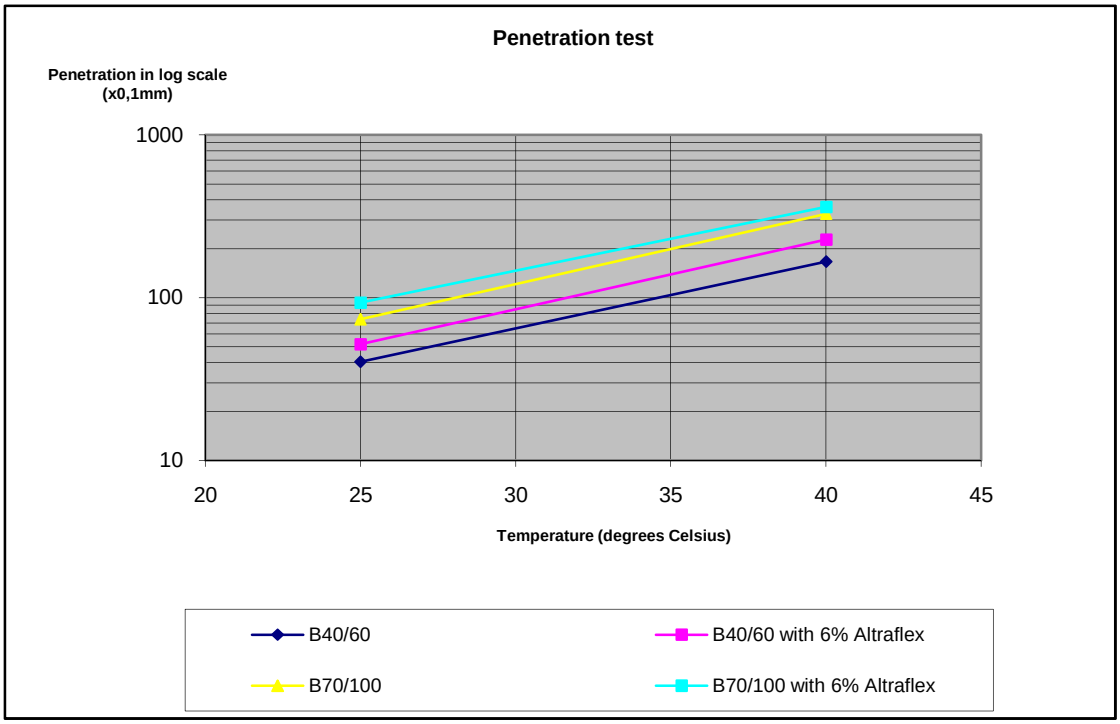


**Graph 4.4:** Penetration test for B70/100 and B40/60 with 0% and 6% Altraflex 2006 at 25 $^0$C en 40 $^0$C

The influence of the mixing time on the penetration at 25$^0$C and 40$^0$C is to be seen in graph 4.5 and 4.6.

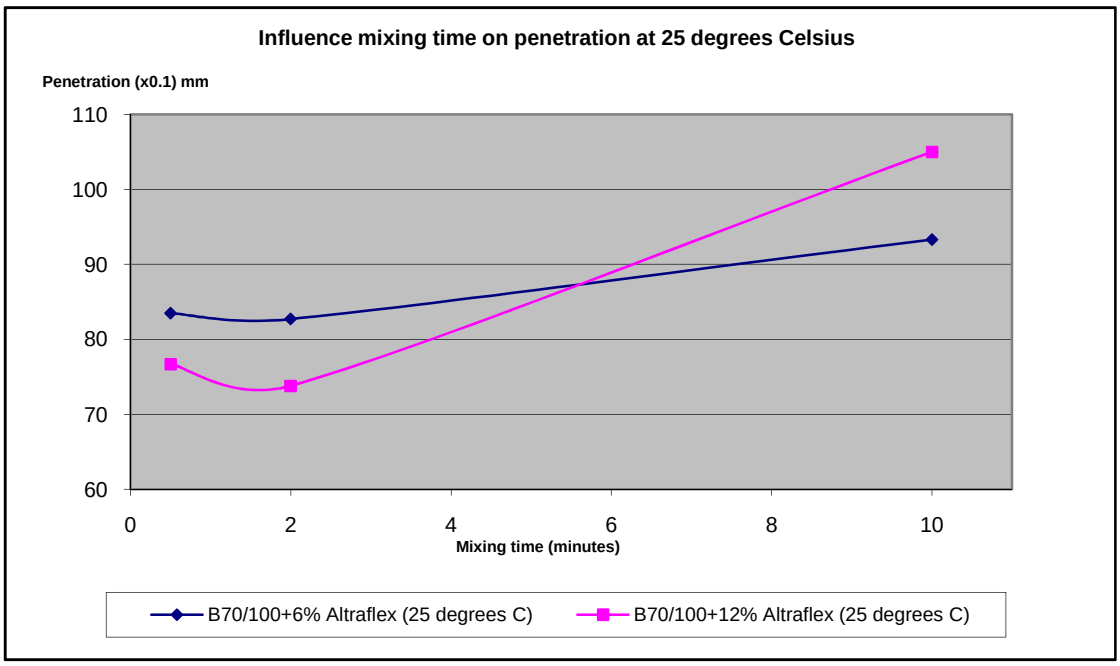


**Graph 4.5**: Influence of mixing time on penetration at 25 $^0$C

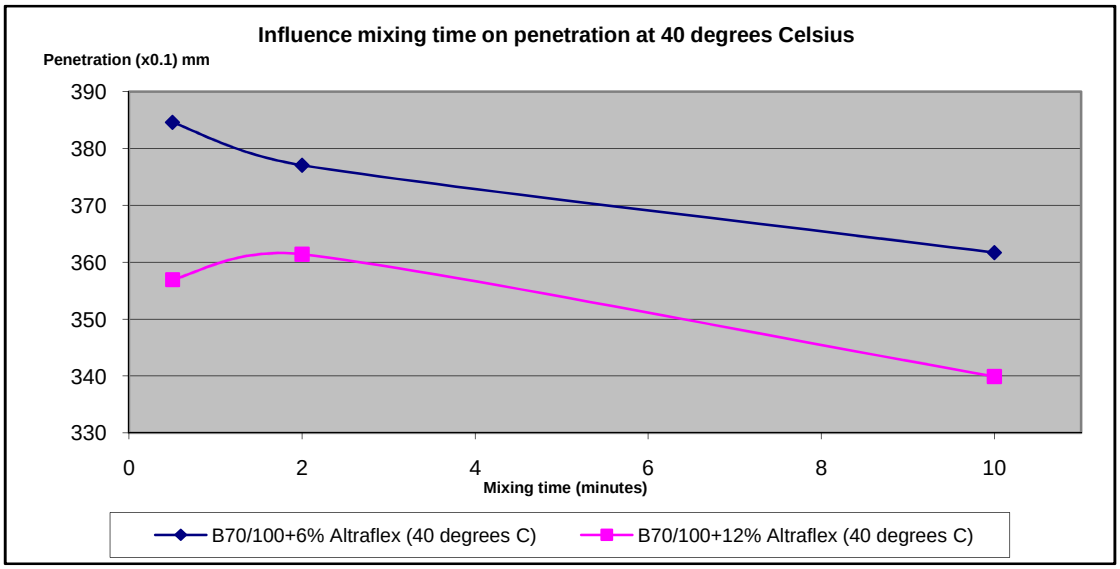


**Graph 4.6**: Influence of mixing time on penetration at 40 $^0$C

### 4.1.5 Conclusion

From graph 4.1 it can be observed that the penetration measurement at 25$^0$C increases as the level of modification gets higher. At 40$^0$C the penetration measurement decreases as the level of modification gets higher.
In graph 4.4 it can be seen that the use of a harder bitumen results in a lower penetration.
When adding 6% of Altraflex 2006 into a harder bitumen the penetration is lower compared with adding 6% of Altraflex 2006 into a softer bitumen.
The penetration gets lower by adding 12% Altraflex 2006 to B70/100 than by adding 6% Altraflex 2006 to B70/100 in the case of penetration tests at 40 degrees Celsius.
From these results it can be seen that the mixing time has a considerable influence effect on the penetration value. It is important to realize that the penetration test is a empirical test and relations are only based on results of unmodified bitumen. Here the penetration is only used to show the effect of the high shear mixing time on this parameter.
In the case of penetration tests performed at 25 degrees Celsius the penetration eventually gets higher with larger mixing times for both B70/100 with 6% Altraflex 2006 and B70/100 with 12% Altraflex 2006. At 40 degrees Celsius the penetration gets lower with larger mixing times for both B70/100 with 6% Altraflex 2006 and B70/100 with 12% Altraflex 2006.

## 4.2 The Ring and Ball Softening Test

### 4.2.1 B70/100 with different percentages of Altraflex 2006 at different mixing times

Te Ring & Ball tests are performed for mixtures mixed during 5, 10, 20 en 30 minutes.
The mixing device was the High Shear Mixer and the mixing temperature was 170$^0$C. The result are presented in table 4.5.

The R&B temperature of B70/100 is 47 $^0$C.

| | Tr&b (degrees Celsius) | | | |
|---|---|---|---|---|
| | mixing time (minutes) | Test1 | Test 2 | average |
| B70/100 met 6% Altraflex | 5 | 46.6 | 46.7 | 46.7 |
| | 10 | 47.5 | 47.9 | 47.7 |
| | 20 | 50.0 | 49.3 | 49.6 |
| | 30 | 50.2 | 49.3 | 49.7 |
| | | | | |
| B70/100 met 12% Altraflex | 5 | 46.3 | 46.3 | 46.3 |
| | 10 | 76.2 | 75.0 | 75.6 |
| | 20 | 84.3 | 85.0 | 84.7 |
| | 30 | 75.0 | 76.0 | 75.5 |
| | | | | |

**Table 4.5**: Results R&B tests for different mixing time for Altraflex 2006 modified bitumen

The Ring & Ball tests were performed in a water bath. The Ring & Ball test of the samples with a mixing time of 20 minutes is first done in a water bath but because the R&B temperature exceeded 80$^0$C ($Ring_1$ = 81 $^0$C and $Ring_2$ = 81 $^0$C) the test is repeated in a glycerol bath. The result obtained in the glycerol bath is reported in table 4.5 and graph 4.7.

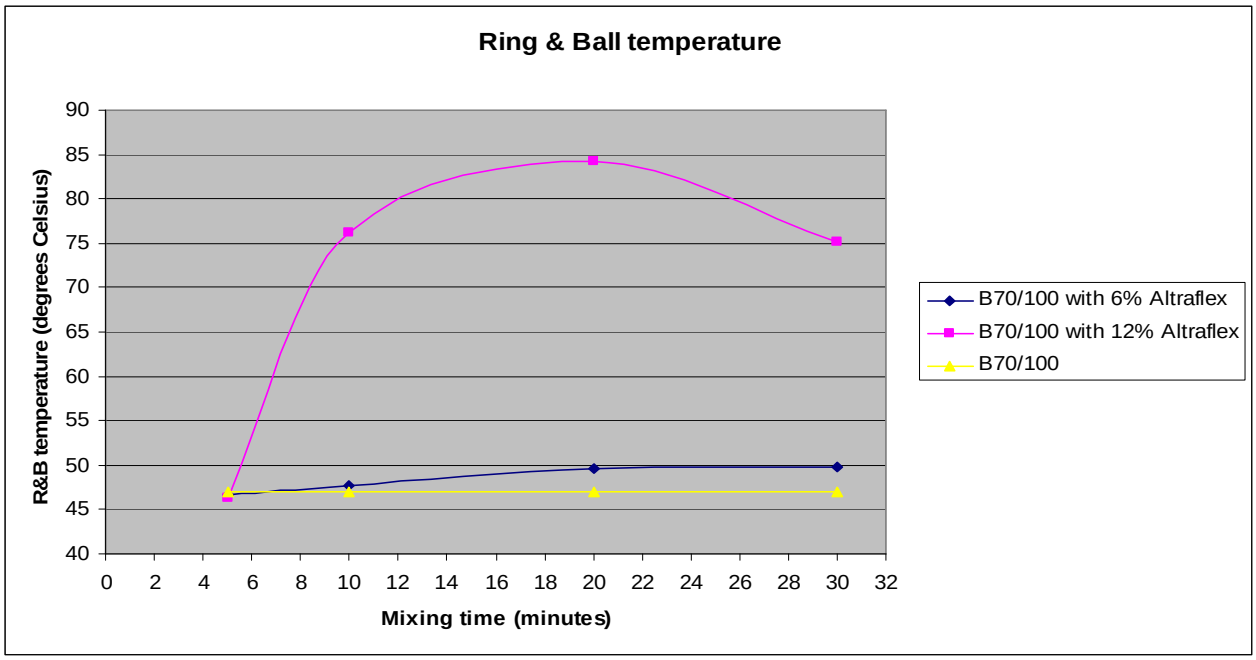


**Graph 4.7**: Ring & Ball temperatures for Altraflex 2006 modified bitumen

### 4.2.2 B70/100 with different percentages Altraflex 2006 at different mixing times

It was suggested to take do ring and ball tests of samples of the Altraflex 2006 modified bitumen after mixing times of 30 seconds and 2 minutes.
After taking these samples it was clear that the structure of the mixes was not homogeneous.

The mixing device is the High Shear Mixer and the mixing temperature was 170$^0$C.

| | | Tr&b (degrees Celsius) | | |
|---|---|---|---|---|
| | mixing time (minutes) | Test1 | Test 2 | average |
| B70/100 met 6% Altraflex | 0,5 | 47,4 | 47,2 | 47,3 |
| | 2 | 47,4 | 47,6 | 47,5 |
| | | | | |
| B70/100 met 12% Altraflex | 0,5 | 46,0 | 47,0 | 46,5 |
| | 2 | 47,2 | 47,8 | 47,5 |

**Table 4.6**: Results R&B tests for mixing time of 0,5 and 2 minutes

Due to the inhomogeneous structure of the mixture, even though it is not to be seen in the results of table 4.6, these results cannot be used further. According to NEN-EN 1427 the difference between the two measurements should not exceed 2 $^0$C in the case of modified bitumen.

### 4.2.3 B40/60 with 6% Altraflex 2006

To compare the influence of the bitumen, tests were also done for B40/60 with 6% Altraflex 2006.
The mixing time with the High Shear Mixer was 10 minutes and the mixing temperature was 170$^0$C.

| | Tr&b (degrees Celsius) | | |
|---|---|---|---|
| | Test1 | Test 2 | average |
| | | | |
| B40/60 | 52,4 | 52,7 | 52,6 |
| | 52,4 | 52,9 | 52,7 |
| | 52,8 | 52,4 | 52,6 |
| | | | |
| B40/60 met 6% Altraflex | 52,0 | 52,2 | 52,1 |
| | 52,2 | 52,6 | 52,4 |
| | 52,0 | 52,2 | 52,1 |

**Tabel 4.7**: Results B40/60 and B40/60 with 6% Altraflex 2006 for mixing time of 10 minutes

From table 4.7 we can calculate the average for B40/60, these are presented in table 4.8.

| | T r&b ($^0$C) |
|---|---|
| B40/60 | 52,6 |
| B40/60 with 6% Altraflex 2006 | 52,2 |

**Table 4.8**: Results B40/60

### 4.2.4 Evaluation of the results

In graph 4.8 the results of the different types of bitumen are compared with each other

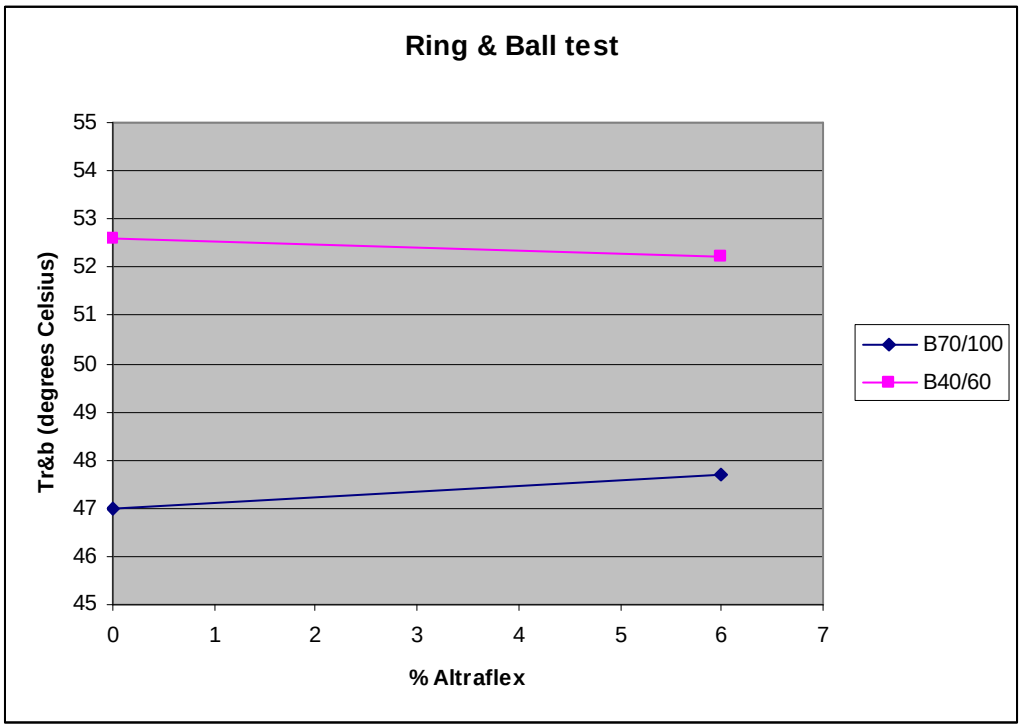


**Graph 4.8**: Ring & Ball temperatures voor B40/60 en B70/100 for mixing time of 10 minutes

The influence of the mixing time on the $T_{R\&B}$ are presented in graphs 4.9 and 4.10:

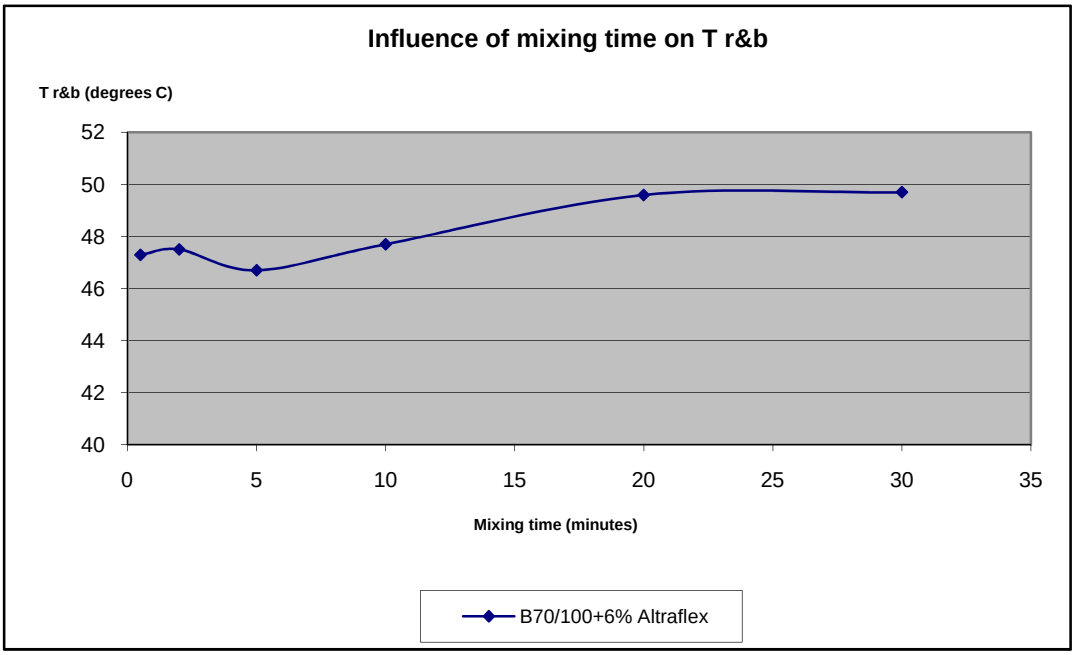


**Graph 4.9**: Influence of the mixing time on the $T_{R\&B}$ for B70/100 with 6% Altraflex 2006

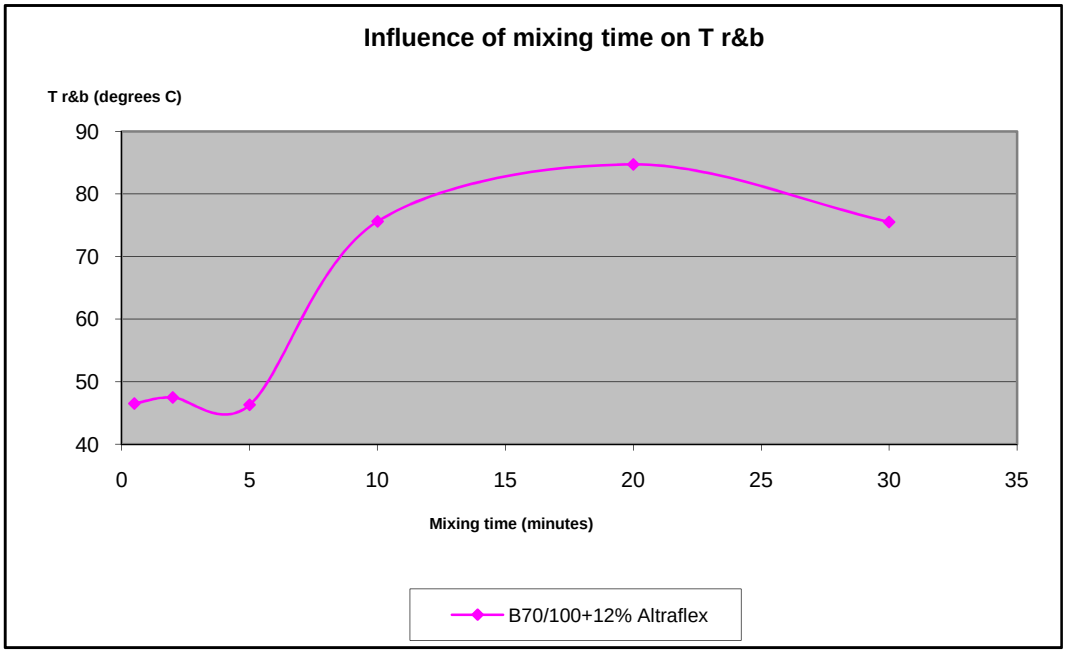


**Graph 4.10**: Influence of the mixing time on the $T_{R\&B}$ for B70/100 with 12% Altraflex 2006

### 4.2.5 Conclusion

In graph 4.5 we can see that adding Altraflex 2006 to B70/100 results into higher ring and ball temperatures.
When the mixing time is increased the ring and ball temperature also increases in case we add 6% Altraflex 2006 concentration, but decreases after a very high maximum (12%) Altraflex 2006 concentration is added.

In case we use harder bitumen, in this case B40/60 (graph 4.8), the ring and ball temperature decreases when adding 6% Altraflex 2006 concentration in comparison with B70/100, where it increases.

From the results it seems clear that the mixing time of the Altraflex 2006 into the base bitumen should be of at least 10 minutes.

## 4.3 The Penetration Index

For PMB it is not allowed to use the empirical tests to predict the behavior of the binder. The relations given below are in principle not valid for SBS modified bitumen.
With the results of the penetration test and the Ring & Ball tests the penetration index can be calculated with:

$$P.I. = \frac{20T_{R\&B} + 500LOG(pen) - 1952}{T_{R\&B} - 50LOG(pen) + 120}$$

We calculate:

| | B70/100 | B70/100 with 6% Altraflex 2006 | B70/100 with 12% Altraflex 2006 |
|---|---|---|---|
| Penetration (x 0.1mm) | 73.6 | 93.3 | 105.0 |
| $T_{R\&B}$ ($^0$C) | 47.0 | 47.7 | 75.6 |
| Penetration Index | -1.07 | -0.19 | 6.04 |

**Table 4.9**: Penetration Index for B70/100 and modified B70/100, mixing time of 10 minutes

| | B40/60 | B40/60 with 6% Altraflex 2006 |
|---|---|---|
| Penetration (x 0.1mm) | 40.3 | 51.8 |
| $T_{R\&B}$ ($^0$C) | 52.6 | 52.2 |
| Penetration Index | -1.05 | -0.59 |

**Table 4.10**: Penetration Index for B40/60 and modified B40/60, mixing time of 10 minutes

### 4.3.1 Conclusion

The value of PI ranges from around -3 for highly temperature susceptible bitumens to around +7 for highly blown low-temperature susceptible bitumens.
It is not permitted to perform these calculations but based on the PI it is clear that addition of Altraflex 2006 improves temperature susceptibility considerably .

In Appendix 1 the results of the penetration tests and the ring and ball test are put together in the Shell Bitumen Test Data Chart. It is just done to show the outcome of the empirical tests. The result of the pure B70/100 is a straight line and the PI can easily be determined from the Shell Bitumen Test Data Chart. However for the 6% Altraflex 2006 modified bitumen the line is not very straight and in case of 12 % Altraflex 2006 modification the line is not straight at all. This shows that other fundamental rheological tests are necessary to measure the real performance.

## 4.4 Microscopic Visualization

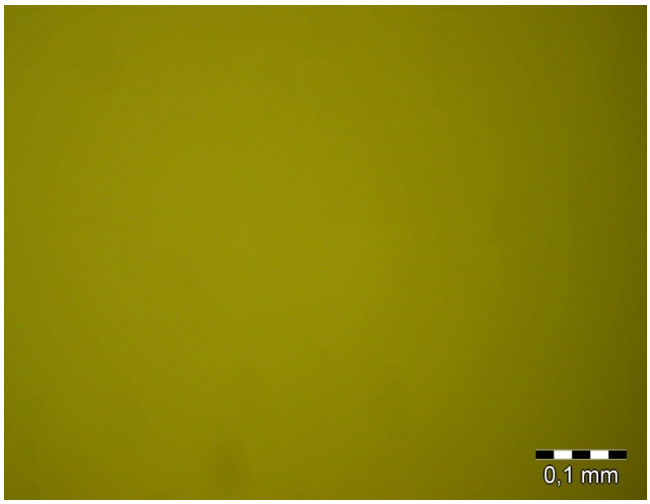


By means of an Epifluorescence microscope it was tried to see the dispersion of the polymer in the bitumen. During the mixing of Altraflex 2006 in the bitumen B70/100 samples were taken after 5 minutes mixing and after complete mixing (10 minutes).The results are shown in figures 4.2 to 4.6 (magnification is 25 times).
Results:

**Fig 4.2** : B70/100

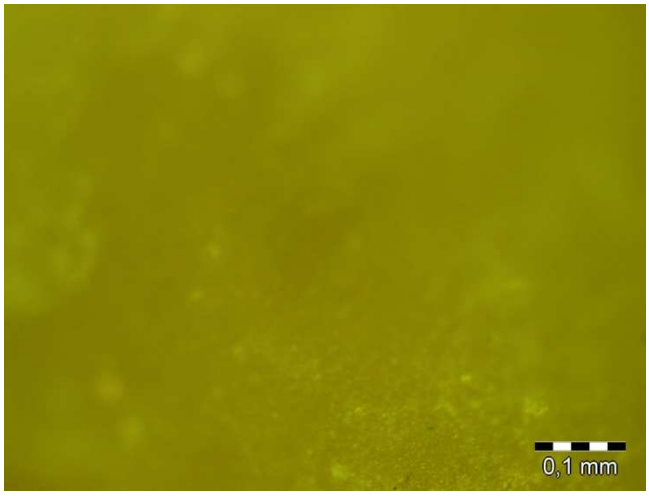


**Fig 4.3** : B70/100 with 6% Altraflex 2006 after 5 minutes mixing

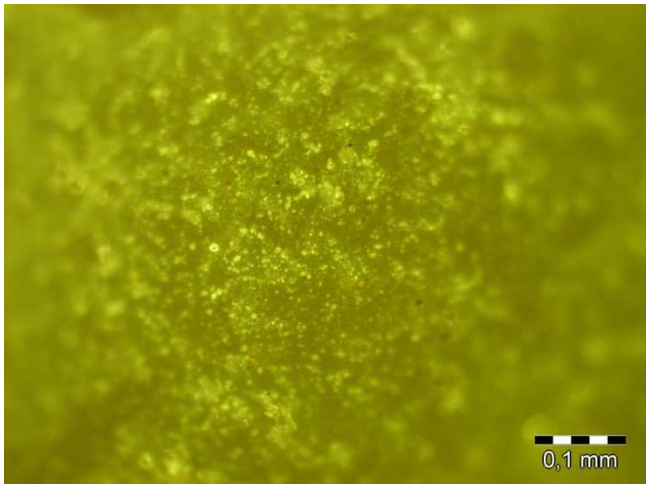


**Fig 4.4:** B70/100 with 6% Altraflex 2006 after 10 minutes mixing

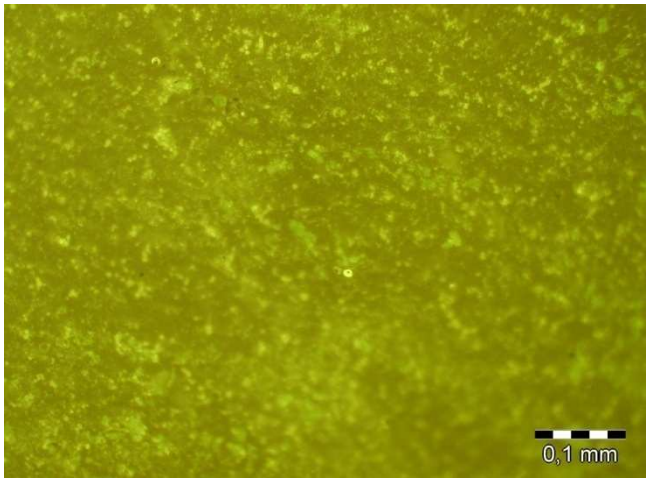


**Fig 4.5**: B70/100 with 12% Altraflex 2006 after 5 minutes mixing

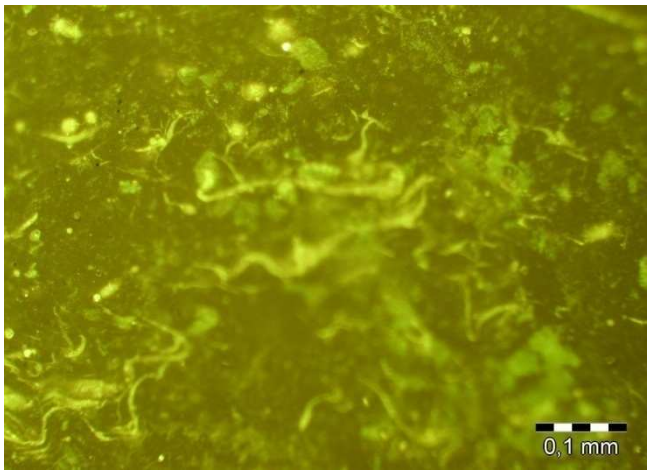


**Fig 4.6**: B70/100 with 12% Altraflex 2006 after 10 minutes mixing

### 4.4.1 Conclusion

The yellow spores in figure 4.3 to 4.6 represent the polymers in the bitumen. The number of these spots increases as the content of polymer is increased. The microscopic observations show that the yellow spots show up as independent tiny dots at 6% and start to merge at 12% concentration forming continuity in structure.
From the distribution of the yellow spots it is assumed that the polymer is evenly distributed in the base bitumen. However for the 12% concentration an irregular pattern starts to develop after 10 minutes of mixing. This tends to lead to the assumption that getting a well-dispersed structure seems to be dependent on the amount of Altraflex 2006 added and the mixing time. However it must be mentioned that it is very difficult to decide on the dispersion of the polymer in the bitumen.

## 4.5 Dynamic Shear Rheometer (DSR) Tests

The DSR test program shown in table 3.3 has been executed.
The following test conditions were used:
tempearture range: -10, 0, 10, 20, 30, 40, 50, 60
frequency range per temperature: 0,1 – 400 rad/sec

In order to compare the materials a master curve is constructed.
The master curve is constructed with the William, Landel and Ferry formula [21] . The master curves have been created using the data obtained in the temperature range from -10 to 60°C whereby the angular frequency is shifted to a reference temperature of 20°C.

### 4.5.1 DSR results for B70/100

The results of the DSR for B70/100 are presented in graph 4.11 till graph 4.10.

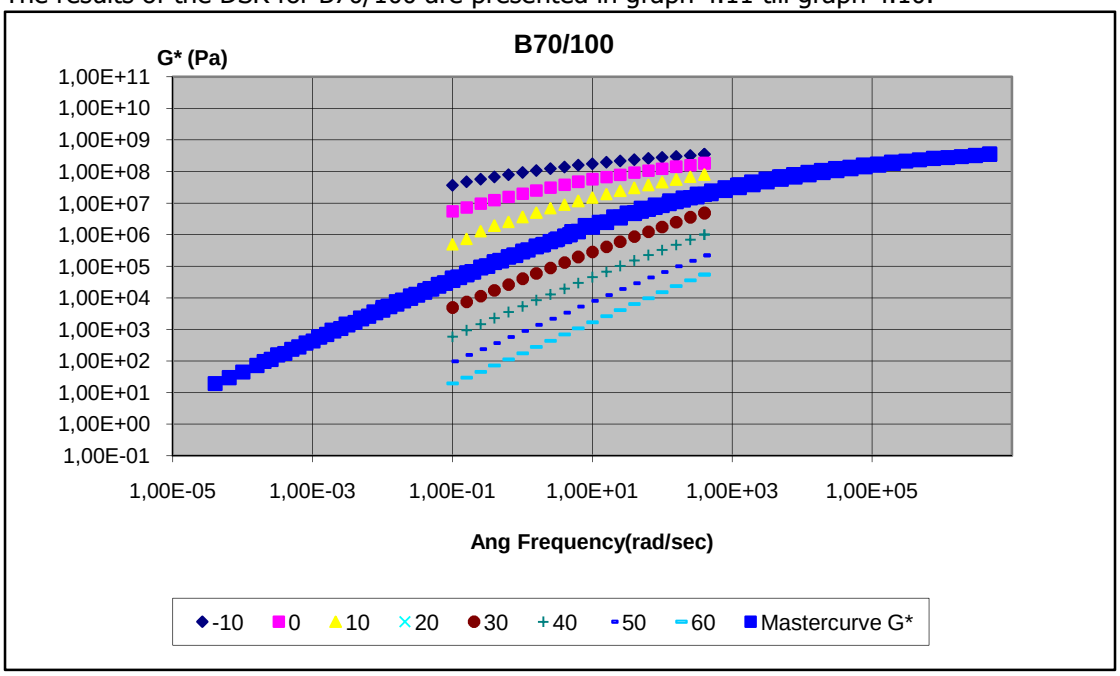


**Graph 4.11**: Mastercurve G* at 20$^0$C for B70/100

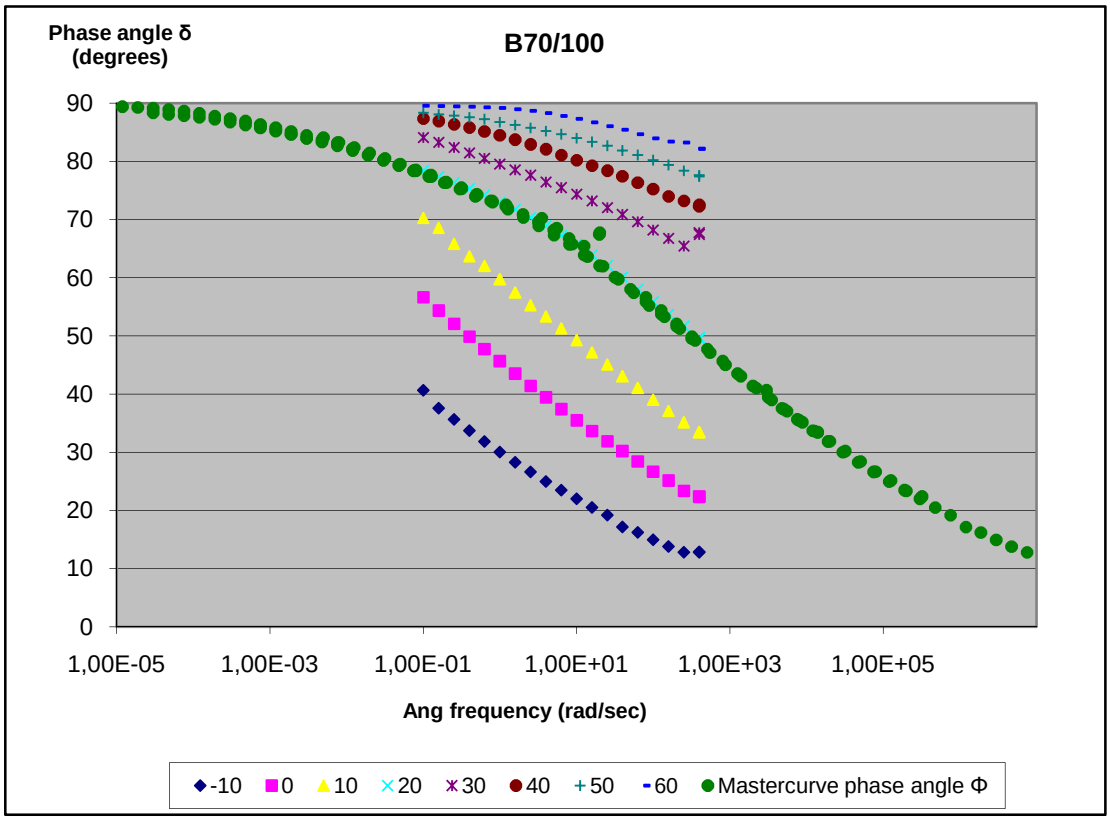


**Graph 4.12**: Mastercurve Phase angle δ at 20$^0$C for B70/100

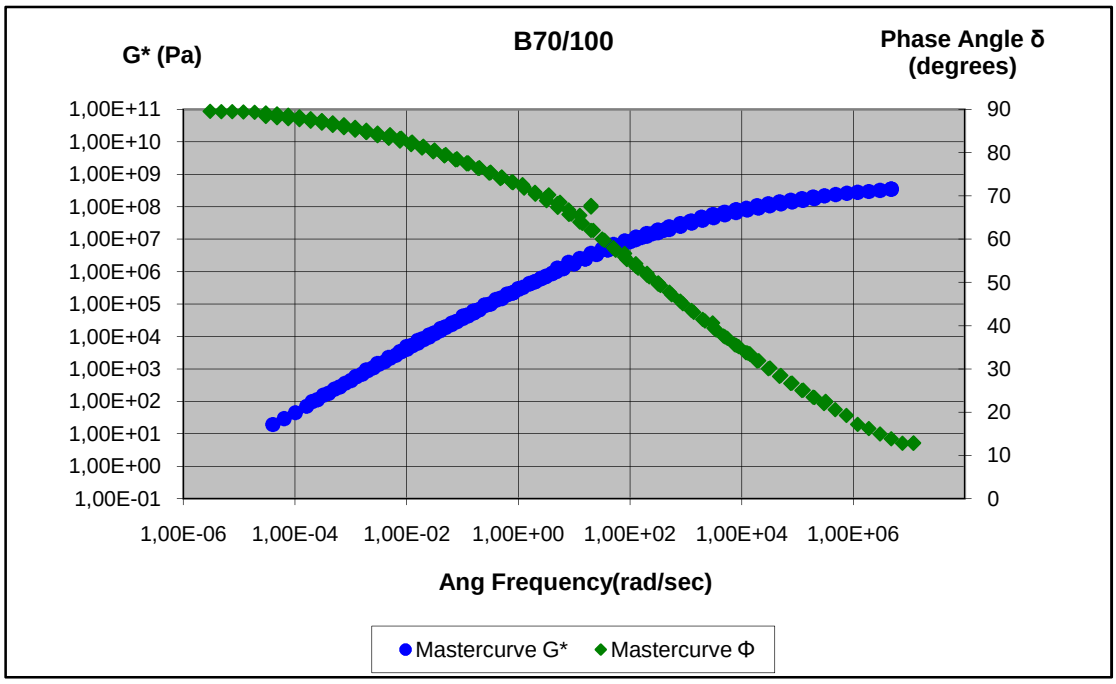


**Graph 4.13**: Mastercurves B70/100 at $20^0$C for G* and δ

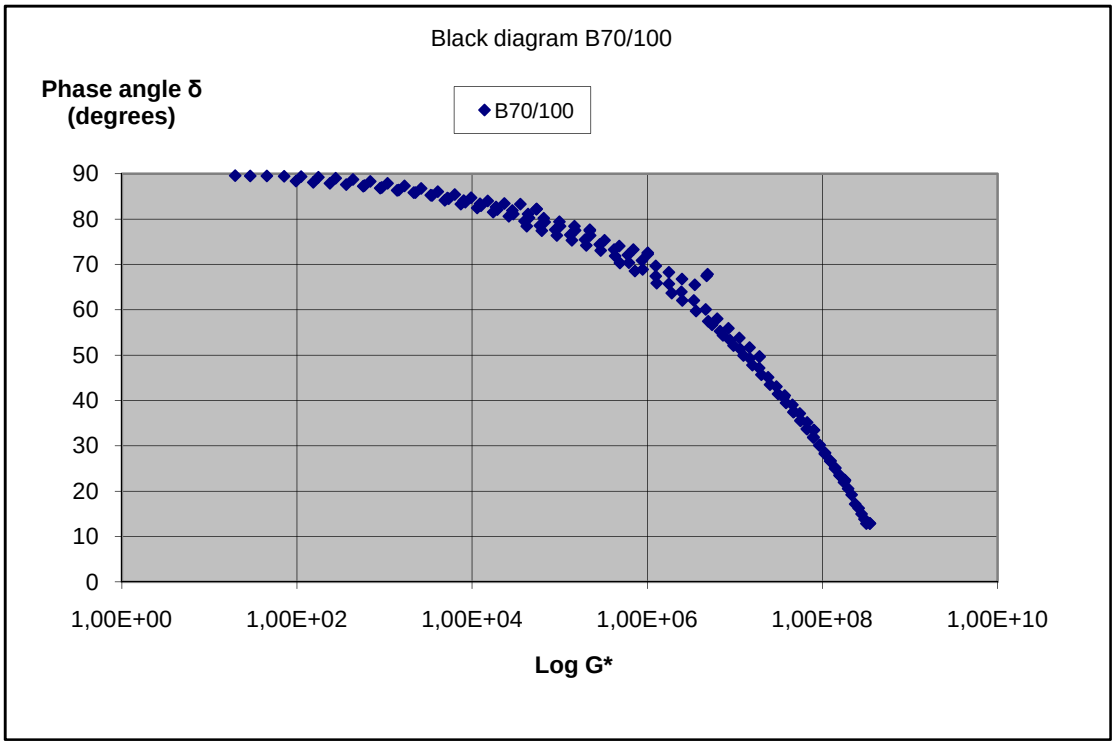


**Graph 4.14** : Black Diagram B70/100

To get to these mastercurves we used shift factor $\alpha$ for the mastercurve G* and shift factor β for the mastercurve Phase angle δ. (See table 4.11).

| Temperature ($^0$C) | Shift factor $\alpha$ | Shift factor β |
|---|---|---|
| -10 | 12000 | 30000 |
| 0 | 500 | 800 |
| +10 | 20 | 35 |
| +20 | 1 | 0.8 |
| +30 | 0.1 | 0.05 |
| +40 | 0.012 | 0.003 |
| +50 | 0.002 | 0.0003 |
| +60 | 0.0004 | 0.00003 |

**Table 4.11**: Shift factors for mastercurves for G* and δ for B70/100

In graph 4.15 the dependency of the shift factors on temperature are given for B70/100:

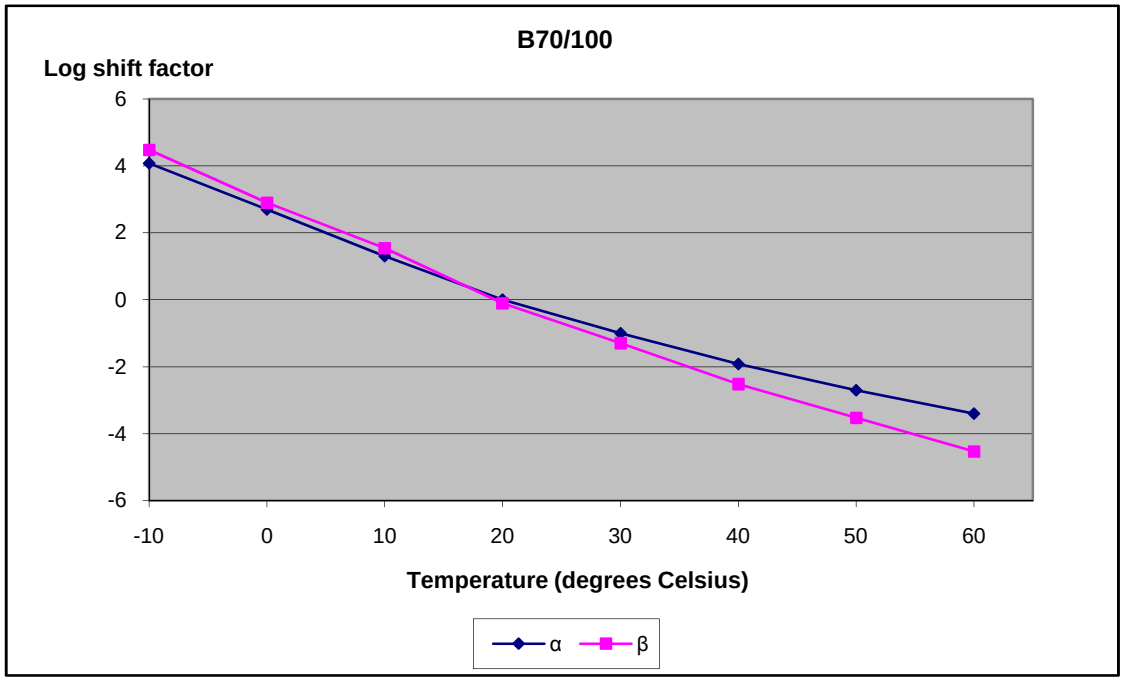


**Graph 4.15**: Dependency of the shift factors on temperature for B70/100

### 4.5.2 DSR results for B70/100 with 6% Altraflex 2006

The results of the DSR for B70/100 with 6% Altraflex 2006 are presented in graph 4.11 till graph 4.14.

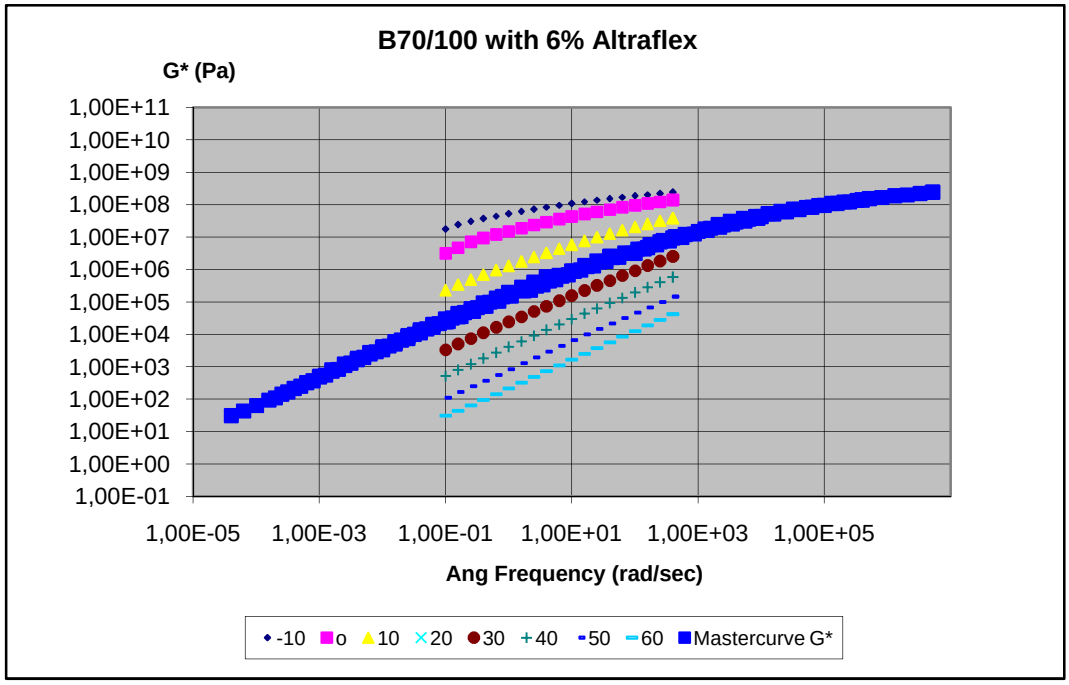


**Graph 4.16**: Mastercurve G* at 20$^0$C for B70/100 with 6% Altraflex 2006

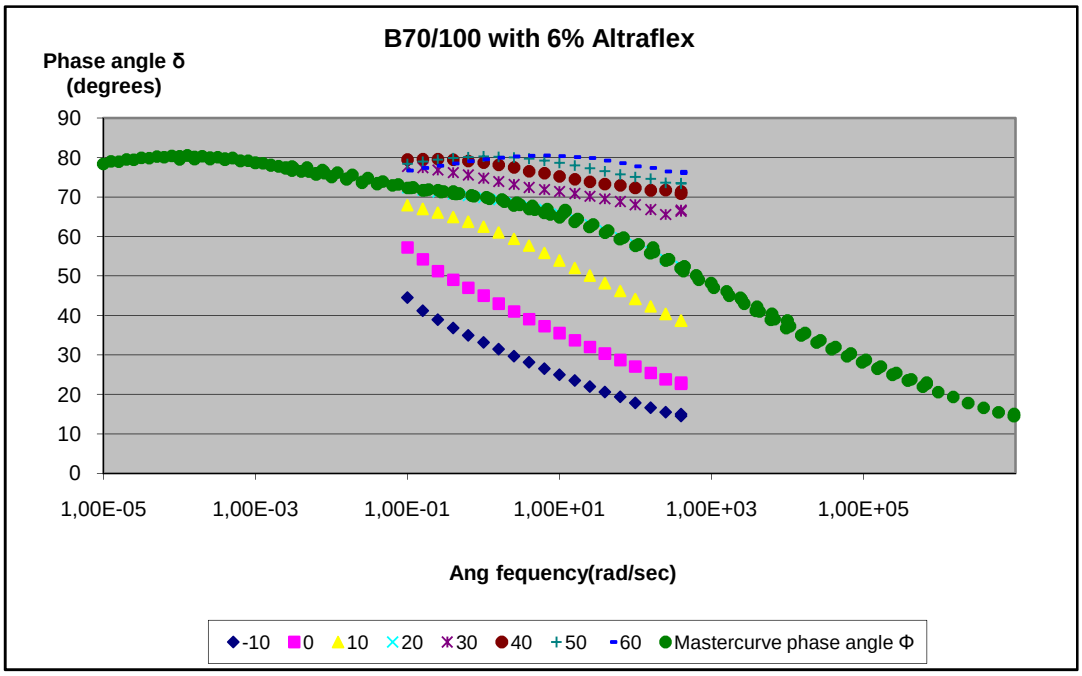


**Graph 4.17**: Mastercurve Phase angle δ at 20$^0$C for B70/100 with 6% Altraflex 2006

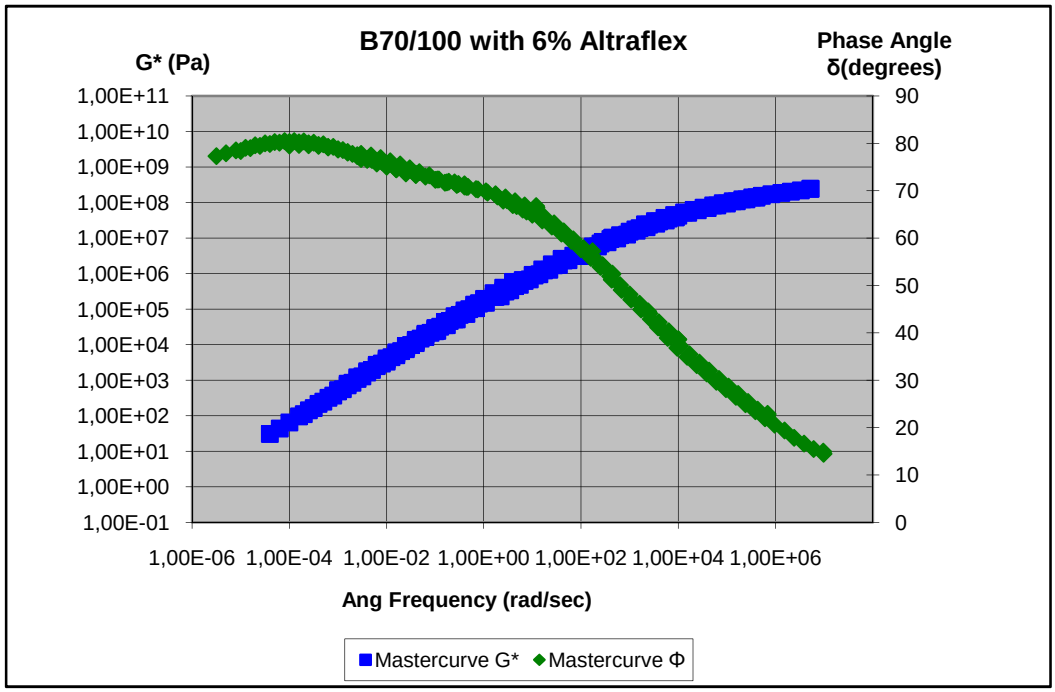


**Graph 4.18**: Mastercurves for G* and δ at 20$^0$C for B70/100 with 6% Altraflex 2006

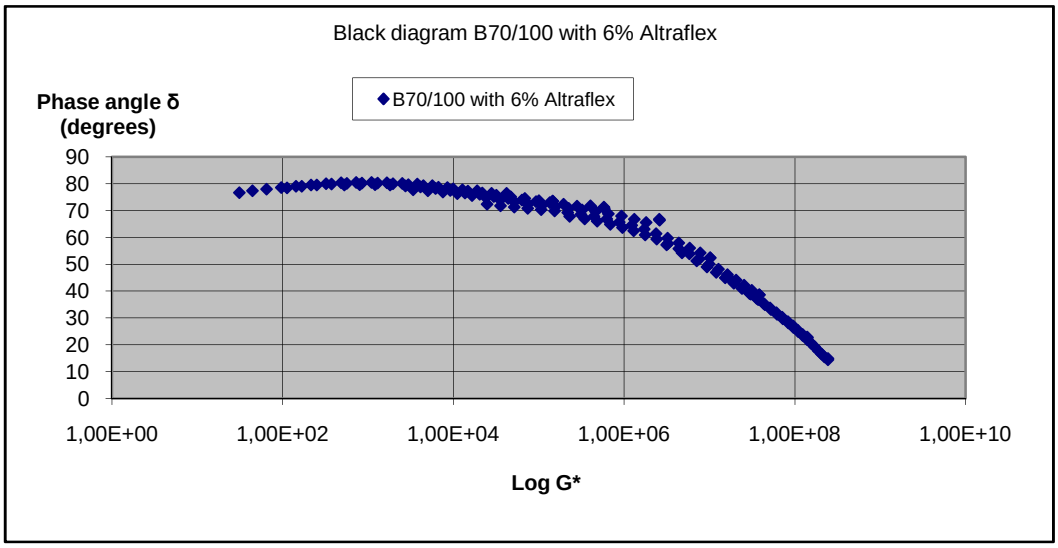


**Graph 4.19:** Black Diagram B70/100 with 6% Altraflex 2006

To get to these mastercurves we used shift factor $\alpha$ for the mastercurve G* and shift factor β for the mastercurve Phase angle δ. (See table 4.12).

| Temperature ($^0$C) | Shift factor $\alpha$ | Shift factor β |
|---|---|---|
| -10 | 13000 | 24000 |
| 0 | 1000 | 1700 |
| +10 | 22 | 25 |
| +20 | 1.1 | 1.1 |
| +30 | 0.1 | 0.03 |
| +40 | 0.01 | 0.001 |
| +50 | 0.002 | 0.0001 |
| +60 | 0.0004 | 0.00002 |

**Table 4.12:** Shift factors for mastercurves for G* and δ as determined for B70/100 with 6% Altraflex 2006

In graph 4.20 the dependency of the shift factors on temperature are given for B70/100 with 6% Altraflex 2006:

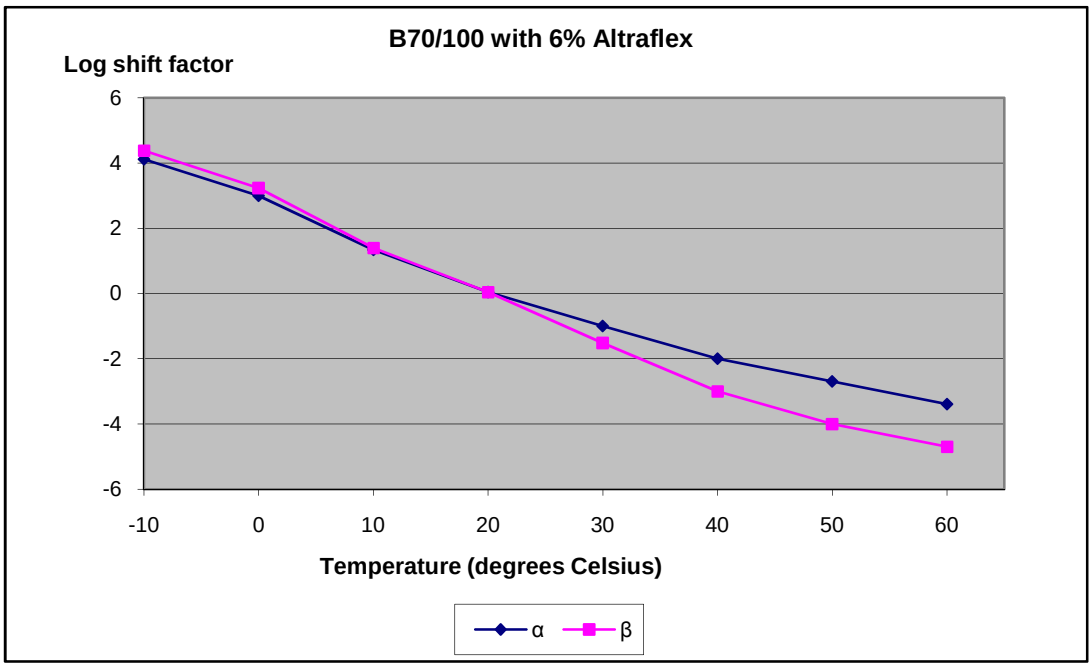


**Graph 4.20**: Dependency of the shift factors on temperature for B70/100 with 6% Altraflex 2006

### 4.5.3 DSR results for B70/100 with 12% Altraflex 2006

The results of the DSR for B70/100 with 12% Altraflex 2006 are presented in graph 4.21 till graph 4.24.

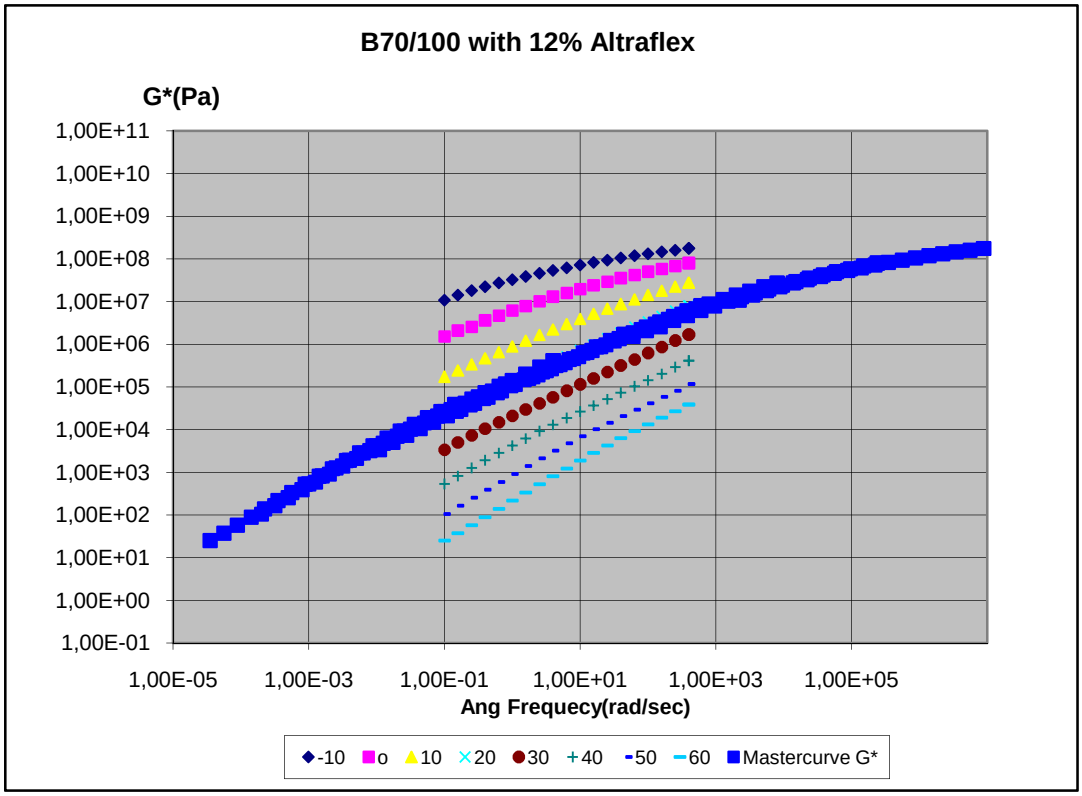


**Graph 4.21**: Mastercurve G* at 20$^0$C for B70/100 with 12% Altraflex 2006

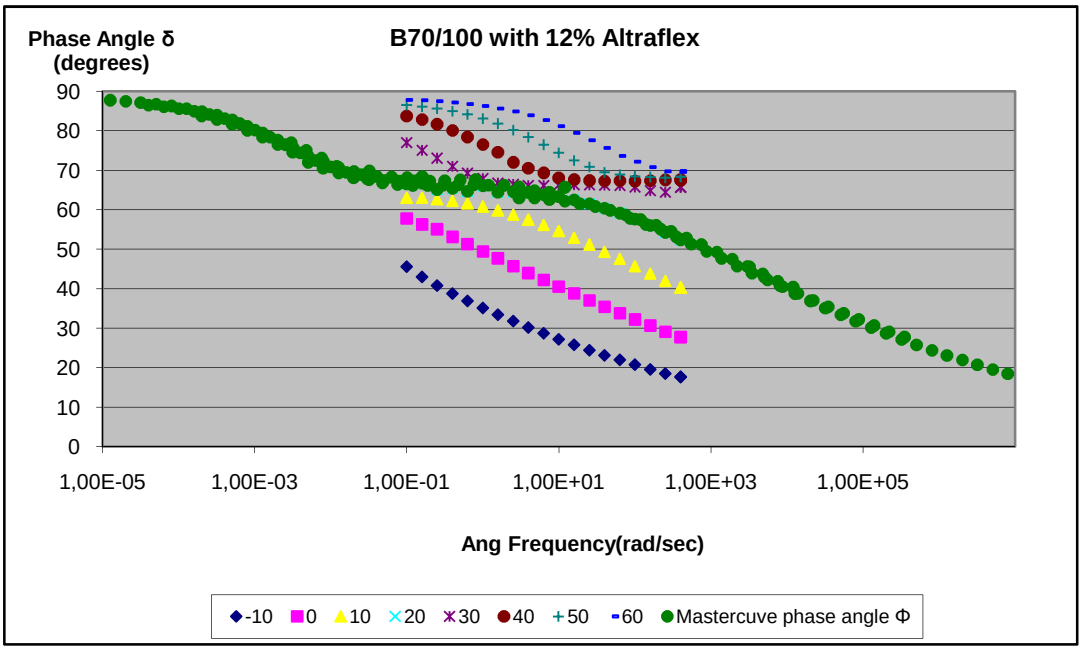


**Graph 4.22:** Mastercurve Phase angle δ at 20$^0$C for B70/100 with 12% Altraflex 2006

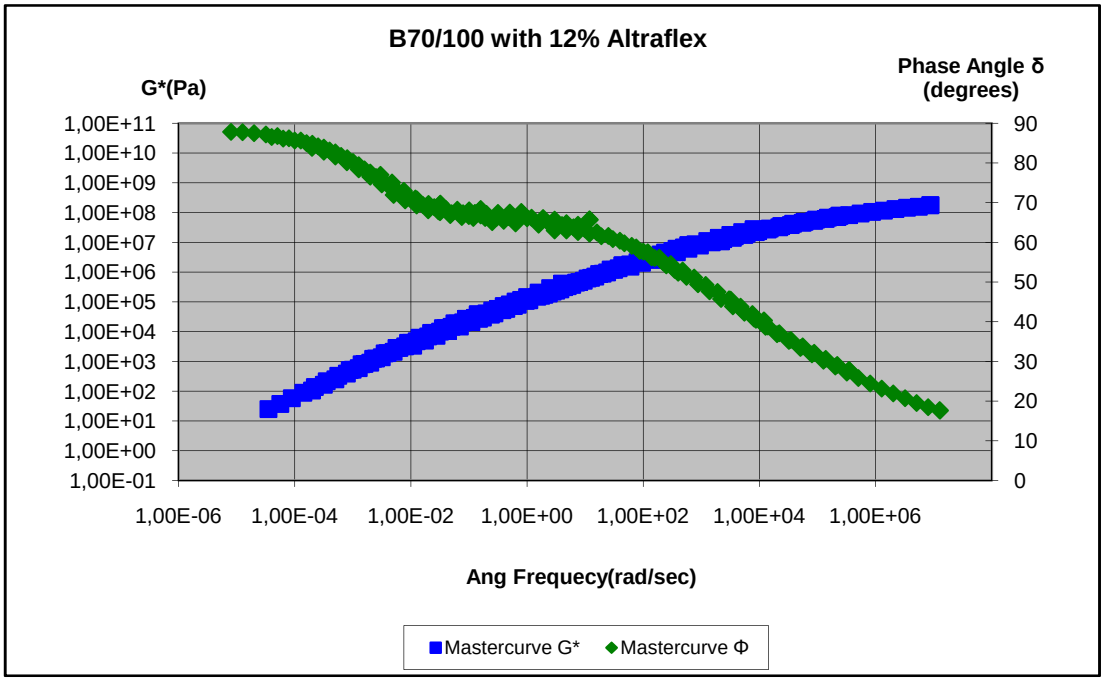


**Graph 4.23:** Mastercurves for G* and δ at $20^0$C for B70/100 with 12% Altraflex 2006

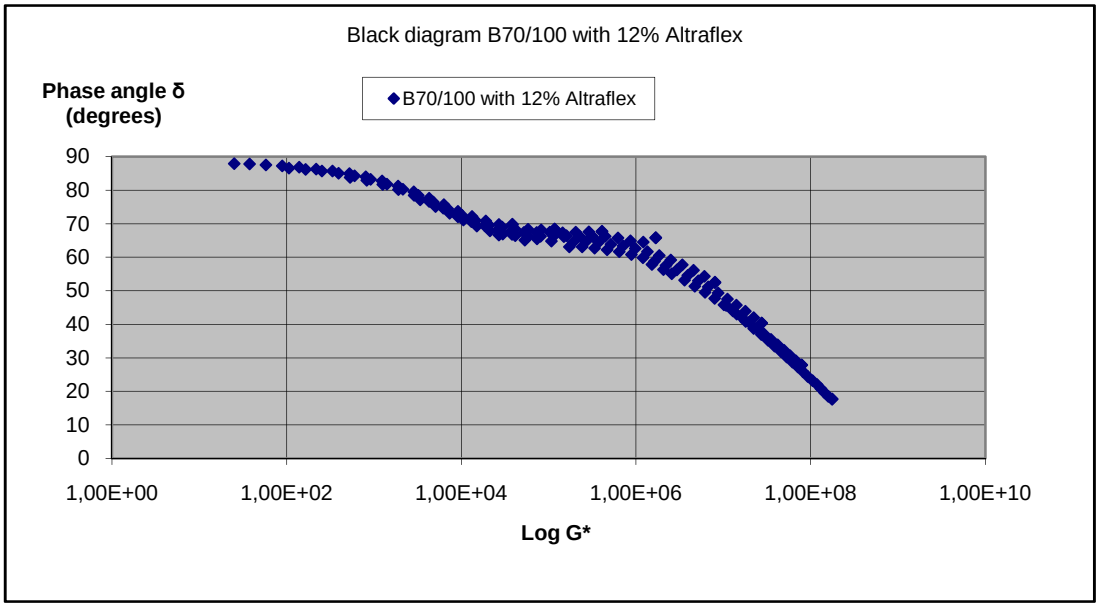


**Graph 4.24:** Black Diagram B70/100 with 12% Altraflex 2006

To get to these mastercurves we used shift factor $\alpha$ for the mastercurve G* and shift factor β for the mastercurve Phase angle δ. (See table 4.13)

| Temperature ($^0$C) | Shift factor $\alpha$ | Shift factor β |
|---|---|---|
| -10 | 22000 | 32000 |
| 0 | 600 | 875 |
| +10 | 20 | 30 |
| +20 | 1.5 | 1 |
| +30 | 0.11 | 0.03 |
| +40 | 0.01 | 0.002 |
| +50 | 0.002 | 0.0004 |
| +60 | 0.000355 | 0.00008 |

**Table 4.13**: Shift factors for mastercurves for G* and δ for B70/100 with 12% Altraflex 2006

In graph 4.25 the dependency of the shift factors on temperature are given for B70/100 with 6% Altraflex 2006:

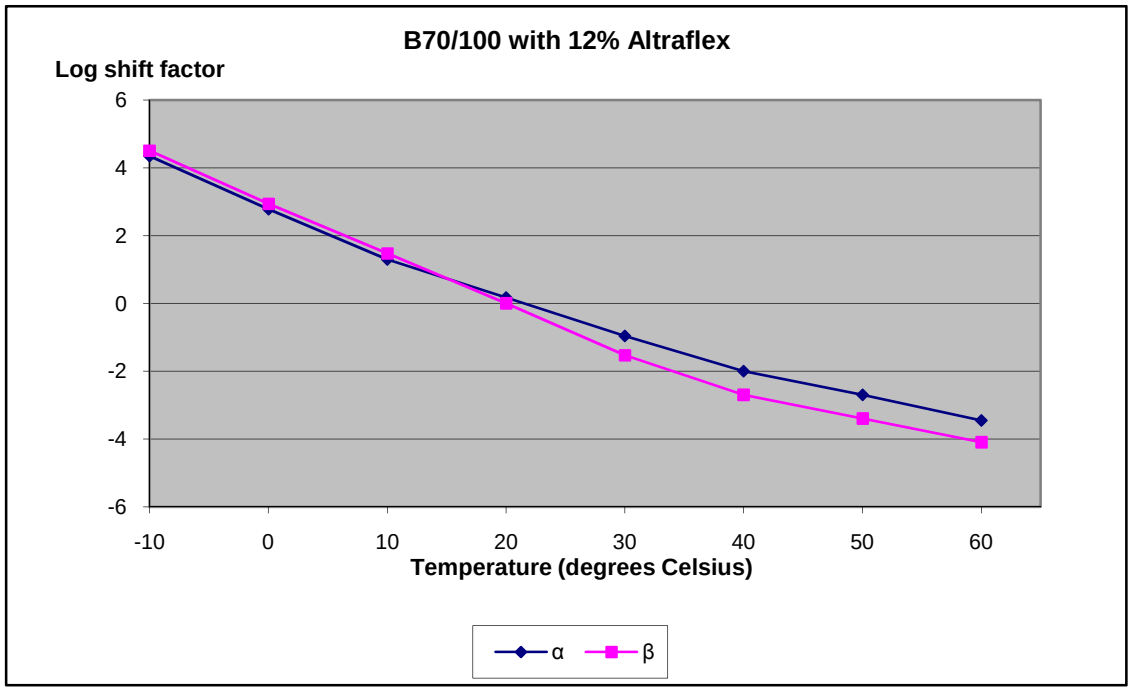


**Graph 4.25:** Dependency of the shift factors on temperature for B70/100 with 6% Altraflex 2006

### 4.5.4 Comparison

The different mixtures are compared, the results are plotted in graph 4.26.

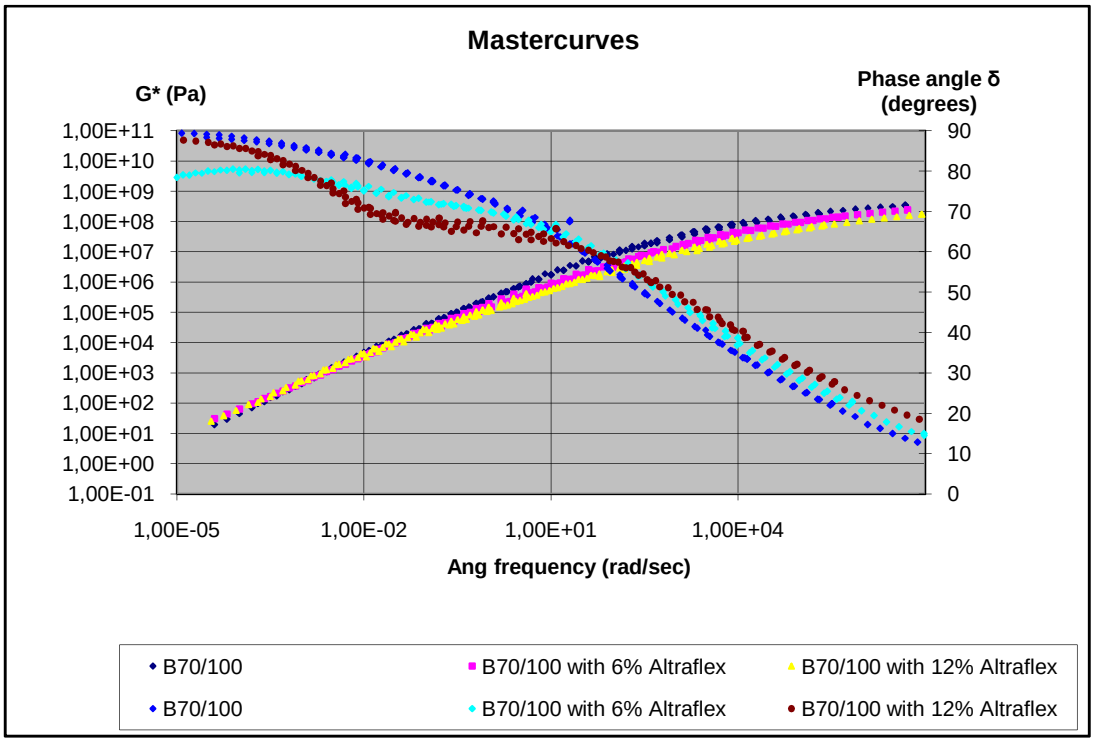


**Graph 4.26**: Mastercurves at 20$^0$C

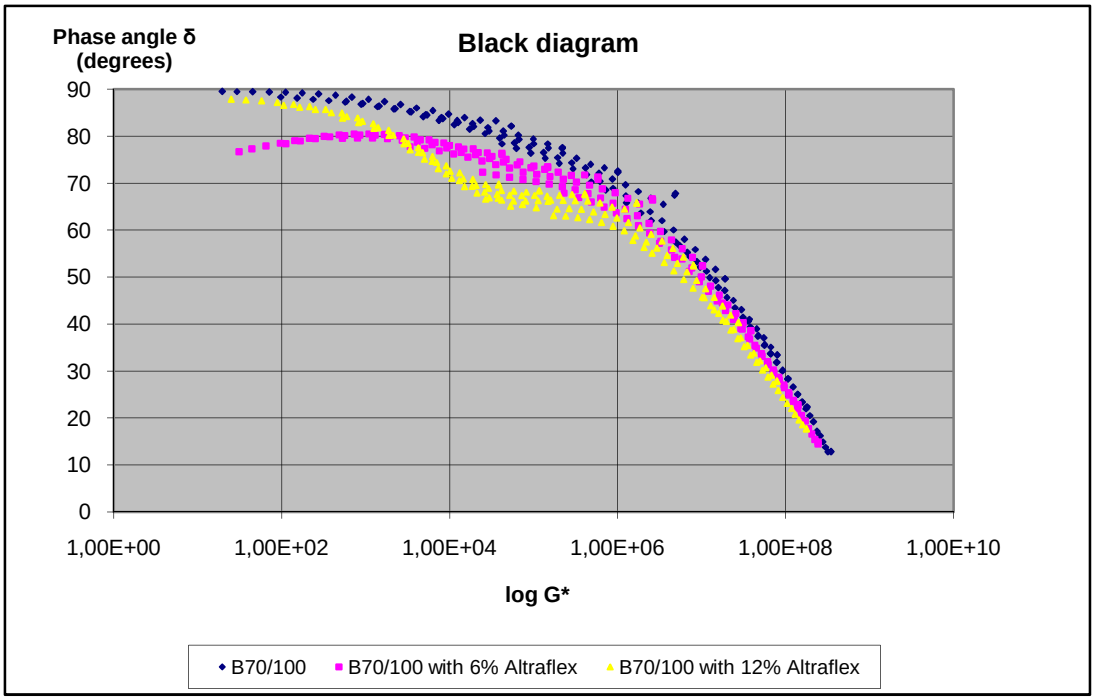


**Graph 4.27:** Black diagram

### 4.5.5 Conclusion

When comparing the mastercurves for G* and δ we must realized that the frequency range which is important for practice is somewhere between $10^{-2}$ Hz and $10^{2}$ Hz.
In graph 4.19 we see that the G* (Pa) does not vary much when we compare B70/100 with B70/100 with 6% Altraflex 2006 and B70/100 with 12% Altraflex 2006. The G* at low angular frequencies starts for all three materials around 30 Pa and reaches at high angular frequencies values between 1.0 x $10^{8}$ and 5.0 x $10^{8}$ Pa.

The comparison of the mastercurves for the phase angle is somewhat complicated due to the irregular patterns obtained for B70/100 + 6% Altraflex 2006 and especially B70/100 + 12% Altraflex 2006.
In the low frequency range (< 1Hz) both Altraflex 2006 mixtures have a lower phase angle than the B70/100 indicating that these materials have a higher elastic and less viscous behavior than the B70/100.In the higher frequency range (> $10^{3}$ Hz) this is just the other way around.

In order to obtain a better indication of the differences between the three materials, values of G* and δ are given for 0.1 Hz, 10 Hz and 100 Hz as well as the slope m of the G* curve are given in table 4.13a.

| | **B70/100** | | | **B70/100+6% Altraflex 2006** | | | **B70/100+12% Altraflex 2006** | | |
|---|---|---|---|---|---|---|---|---|---|
| Frequency (Hz) | G* (Pa) | δ (degrees) | m | G* (Pa) | δ (degrees) | m | G* (Pa) | δ (degrees) | m |
| 0,1 | 1,95E+05 | 74,0 | 0,710 | 1,35E+05 | 70,1 | 0,7697 | 1,03E+05 | 64,8 | 0,637 |
| 10 | 8,00E+06 | 55,4 | 0,903 | 5,00E+06 | 59,4 | 0,7990 | 1,92E+06 | 59,1 | 0,633 |
| 100 | 2,70E+07 | 48,5 | 0,716 | 1,21E+07 | 50,1 | 0,5914 | 8,15E+06 | 50,9 | 0,631 |

**Table 4.13a:** Values for the G* and δ for different frequencies.

Based on the high PI values for the B70/100 + 12% Altraflex 2006 samples, it was expected that the G* mastercurve of that material would be much flatter i.e. implying a less temperature (frequency) dependency of G*. This however was not observed. This might partly be due to the fact that the PI concept is not applicable for polymer modified bitumen but there also might be other reasons for this.

## 4.6 Dynamic Shear Rheometer (DSR) Tests on Aged material

DSR test are performed on B70/100 and B70/100 with 6% Altraflex 2006 that are aged in the PAV (table 3.3).
Also the aged mortars (table 3.4) are studied with the DSR and compared with each other.

The following test conditions were used:
temperature range: -10, 0, 10, 20, 30, 40, 50, 60
frequency range at each temperature: 0,1 – 400 rad/sec

The mastercurves for G* and δ are determined for a reference temperature of $20^0$C.

### 4.6.1 Aged B70/100

The results of the DSR for B70/100 aged are presented in graph 4.28 till graph 4.31.

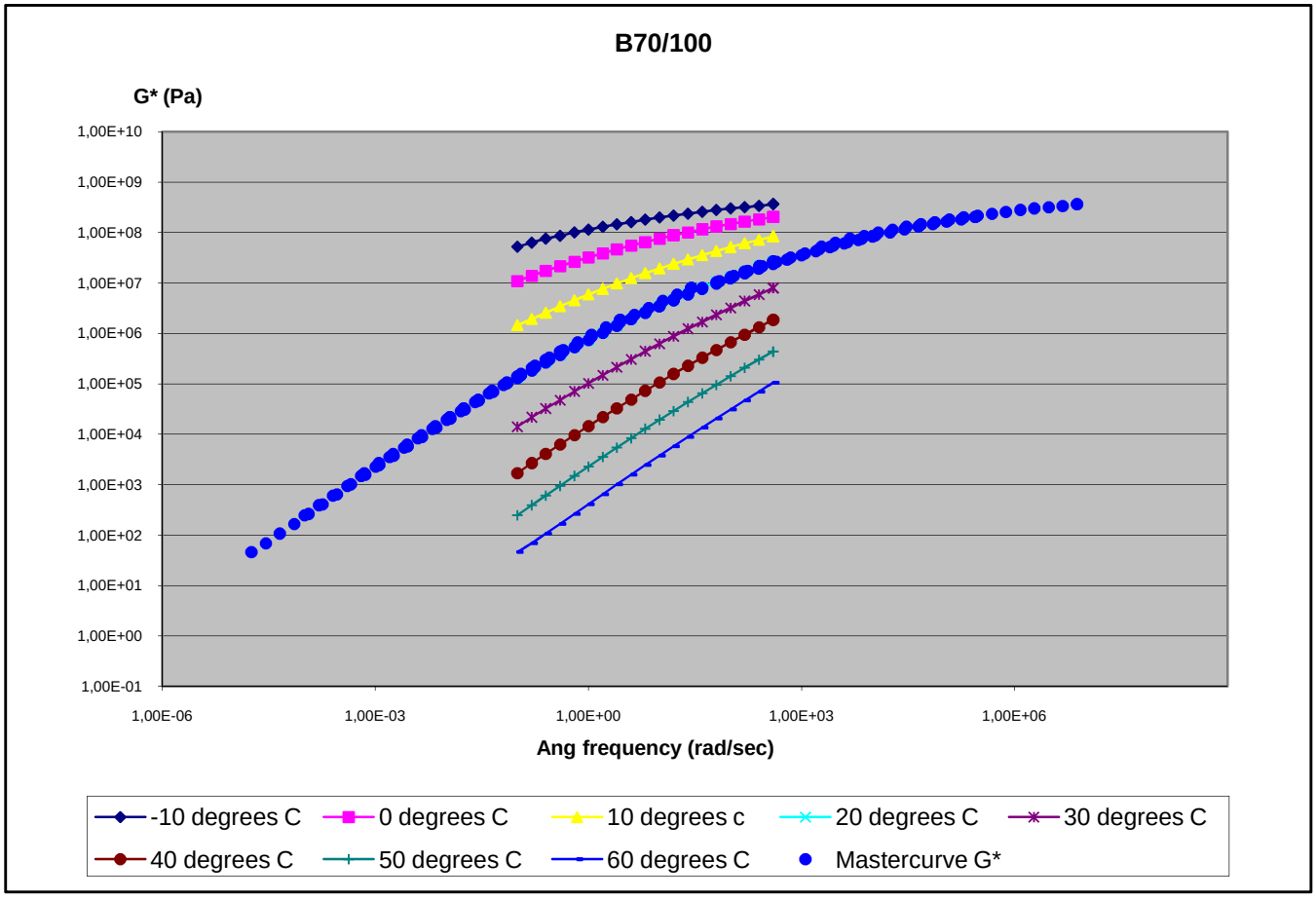


**Graph 4.28**: Mastercurve G* at $20^0$C for B70/100 aged

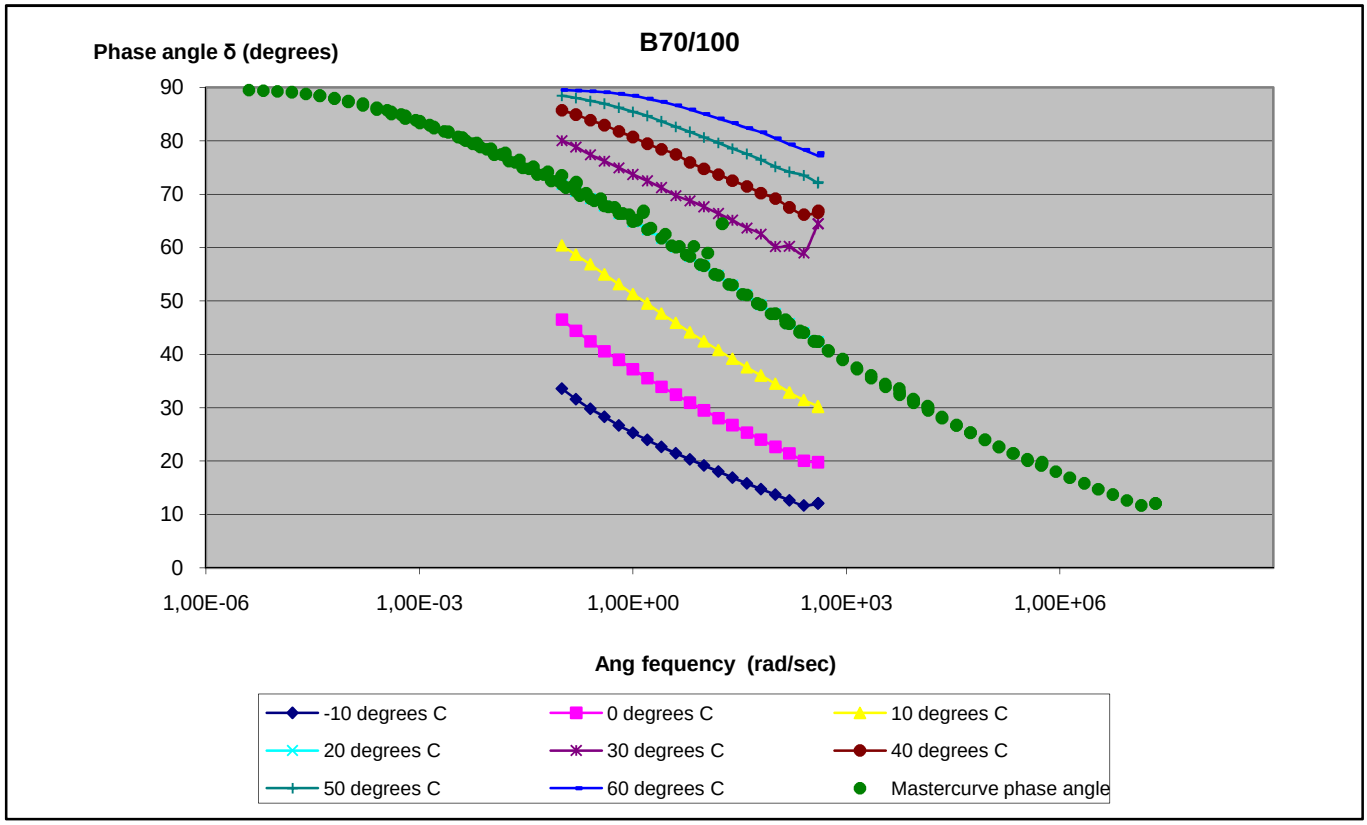


**Graph 4.29**: Mastercurve Phase angle δ at 20$^0$C for B70/100 aged

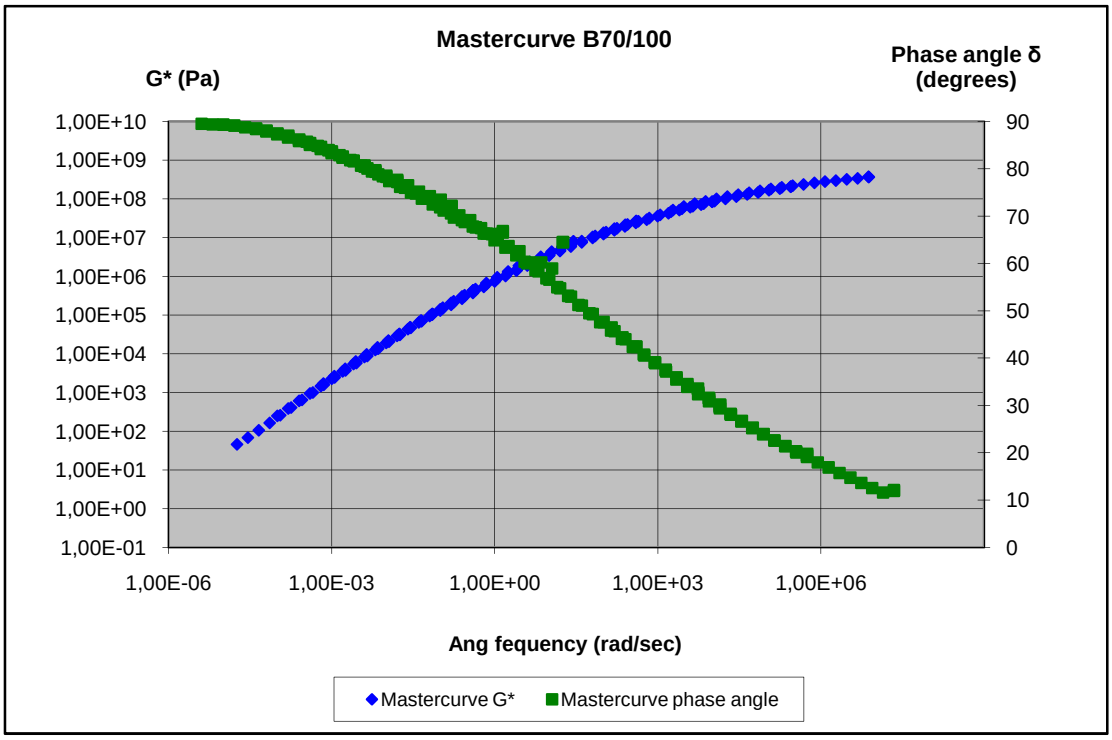


**Graph 4.30**: Mastercurves for G* and δ at 20$^0$C for B70/100 aged

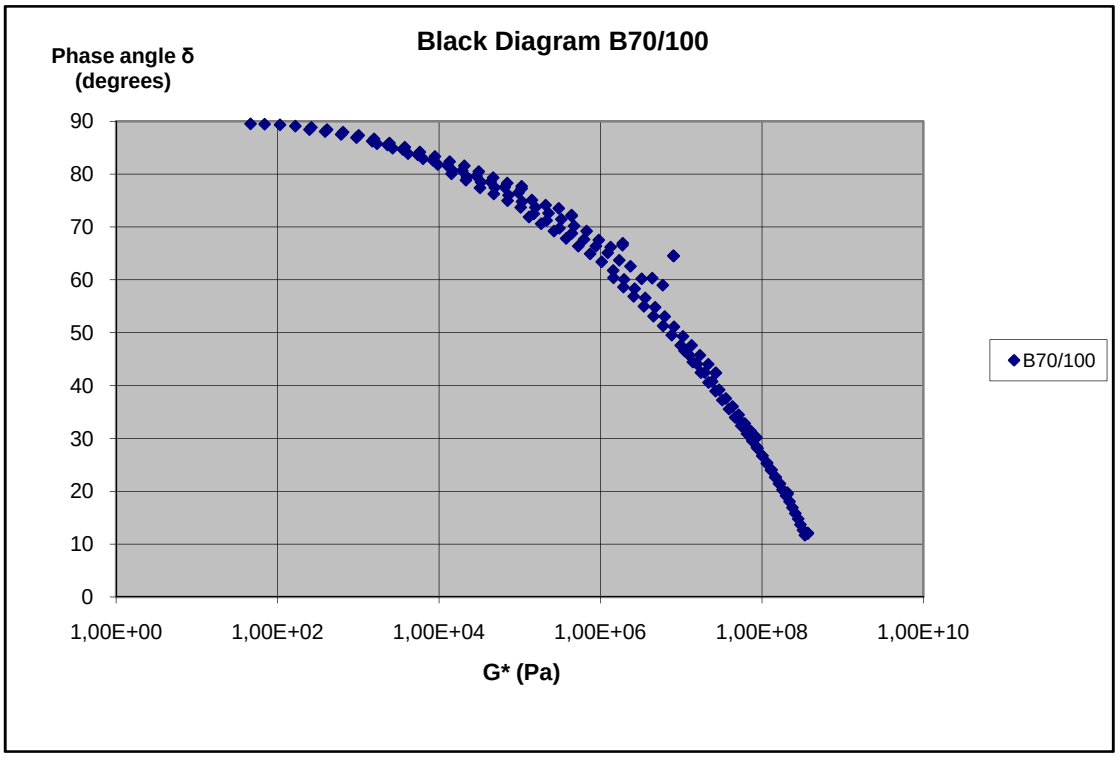


**Graph 4.31**: Black Diagram for B70/100 aged

The dependency of the shift factors on temperature for B70/100 is to be seen in graph 4.32

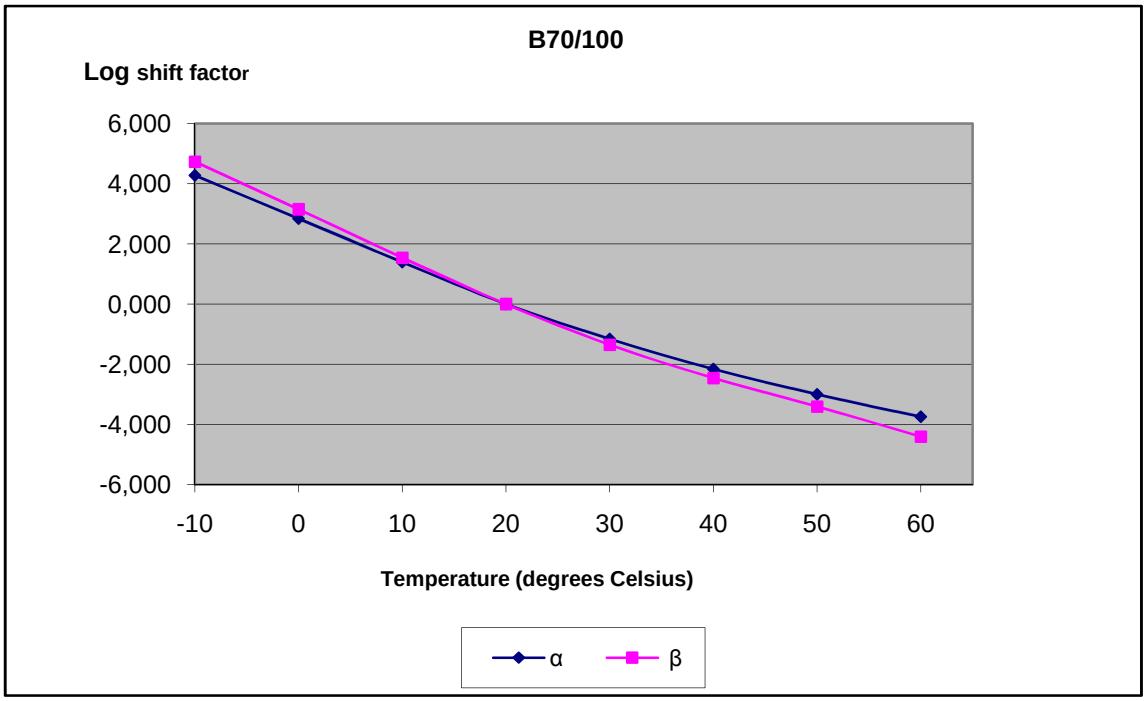


**Graph 4.32**: Dependency of the shift factors on temperature for B70/100

### 4.6.2 Aged B70/100 with 6% Altraflex 2006

The results of the DSR for B70/100 with 6% Altraflex 2006 aged are presented in graph 4.33 till graph 4.36.

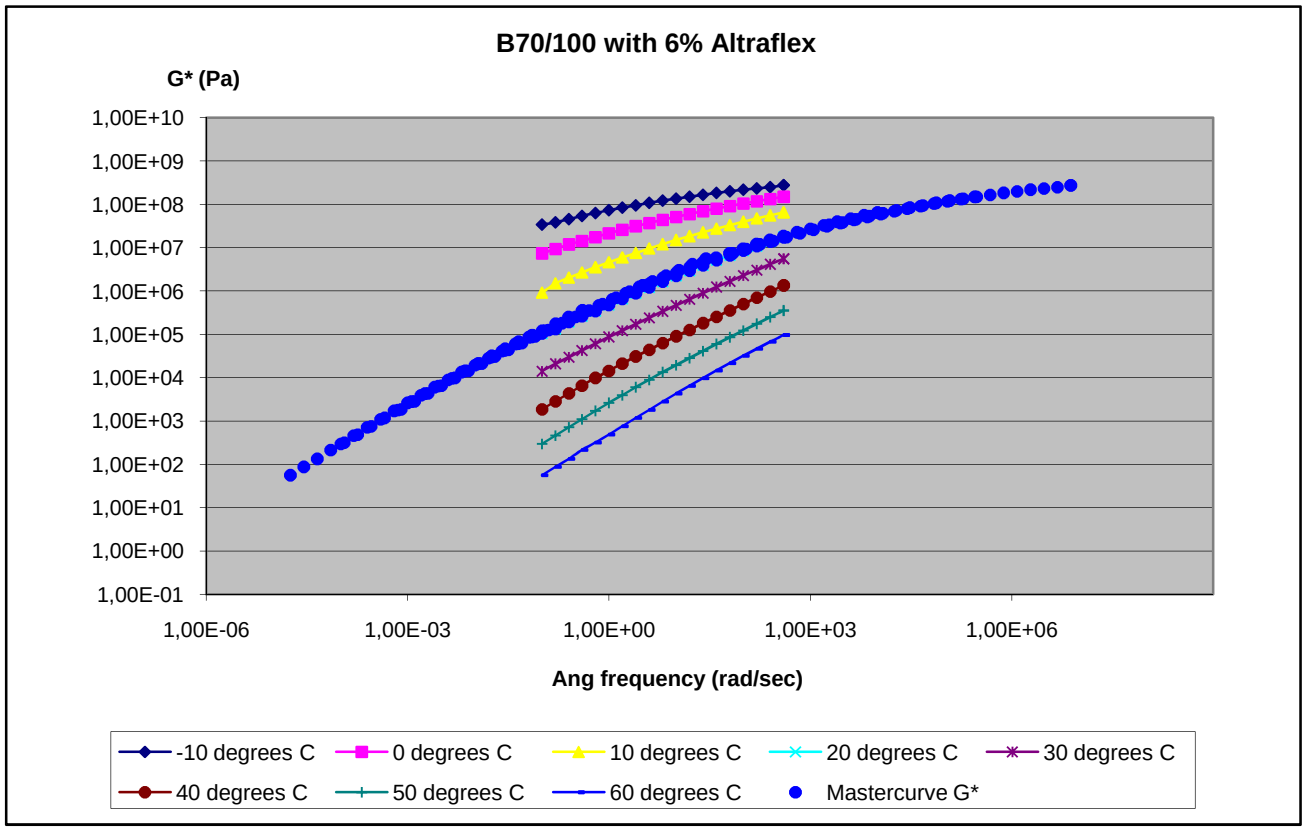


**Graph 4.33 :** Mastercurve G* at 20$^0$C for B70/100 with 6% Altraflex 2006 aged

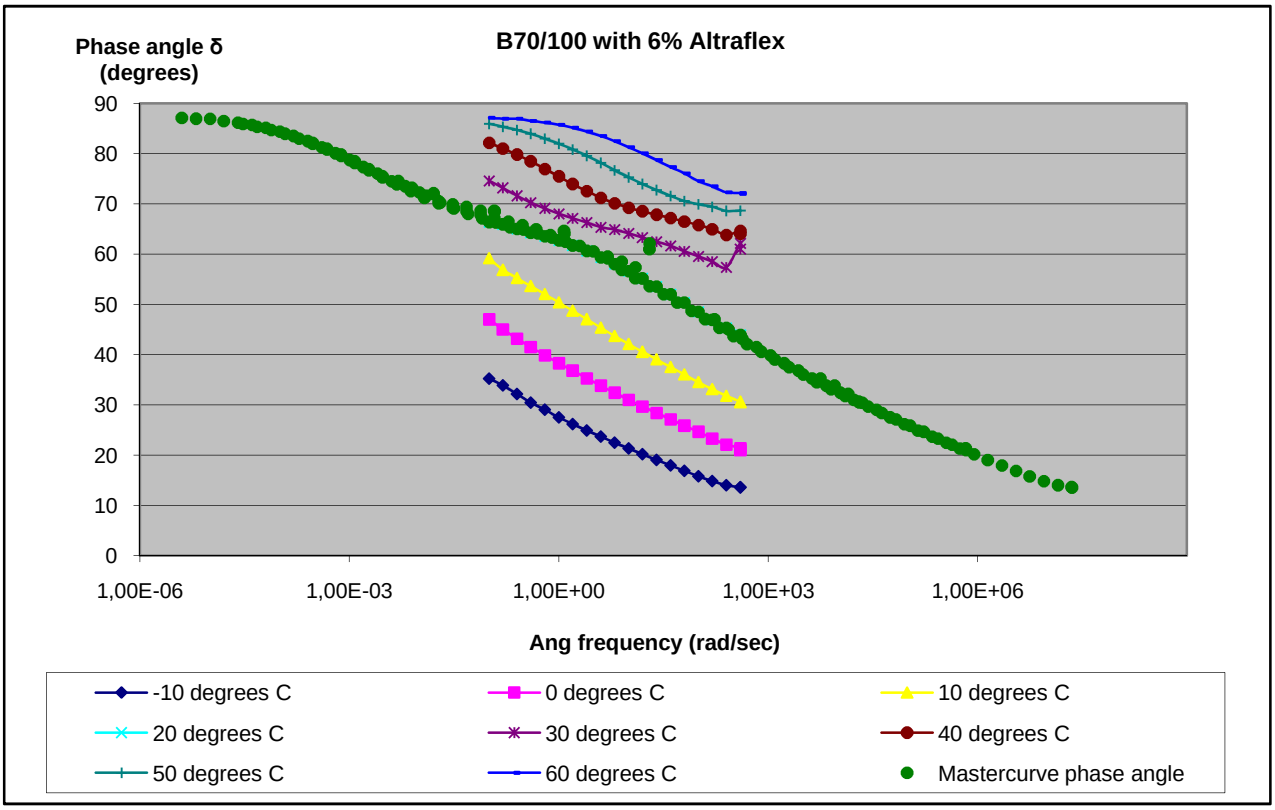


**Graph 4.34**: Mastercurve Phase angle δ at 20$^0$C for B70/100 with 6% Altraflex 2006 aged

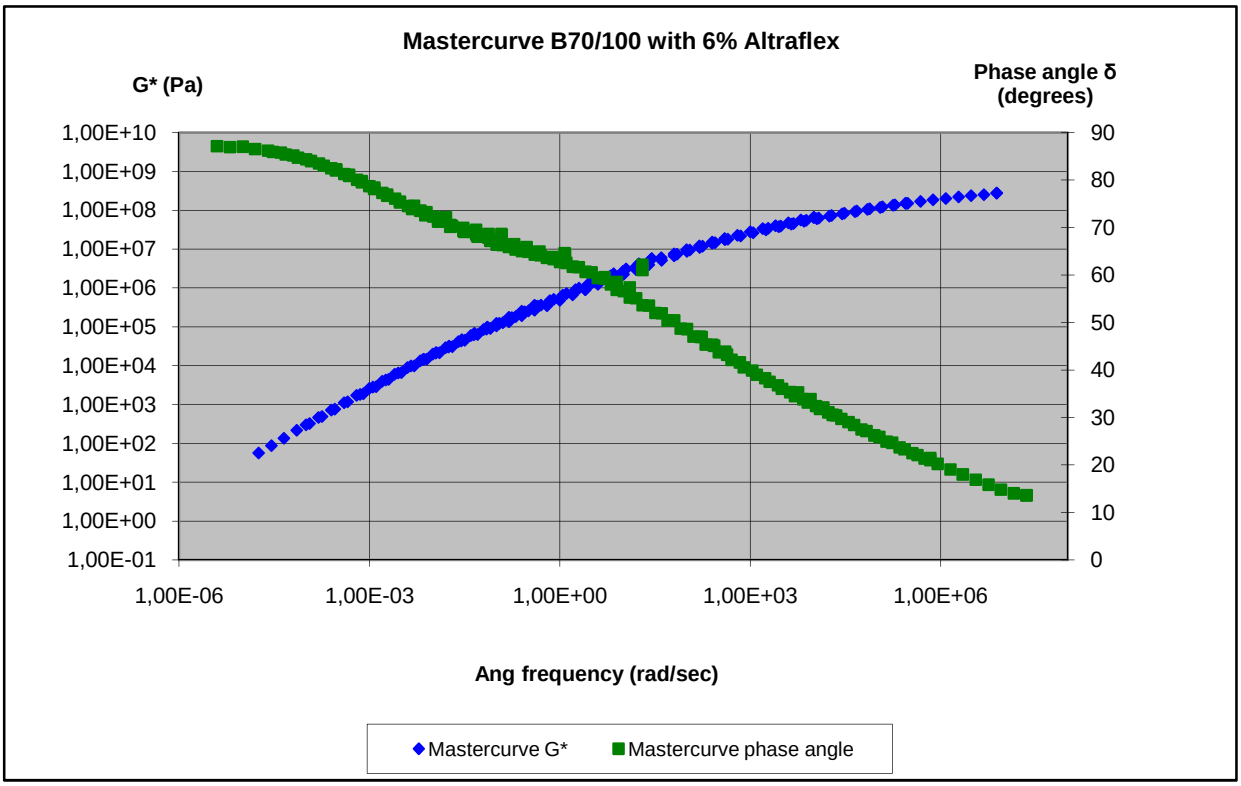


**Graph 4.35:** Mastercurves for G* and δ at 20$^0$C for B70/100 with 6% Altraflex 2006 aged

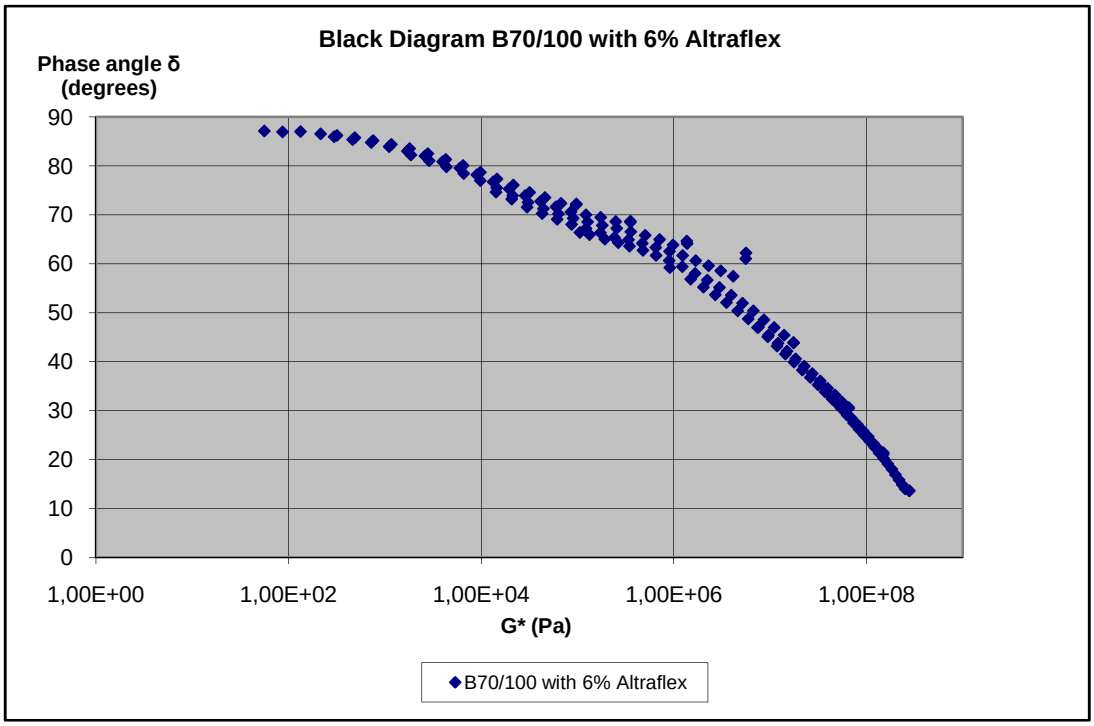


**Graph 4.36**: Black Diagram for B70/100 with 6% Altraflex 2006 aged

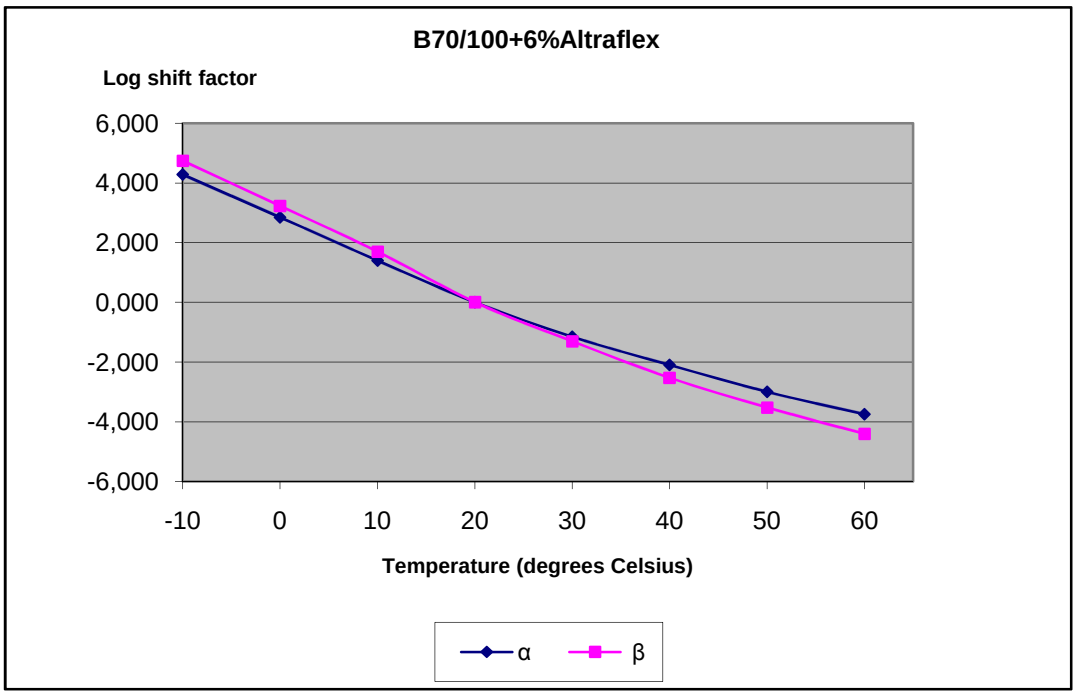


**Graph 4.37:** Dependency of the shift factors on temperature for B70/100 with 6% Altraflex 2006

### 4.6.3 Comparison of the rheological behavior of aged B70/100 and aged B70/100 with 6% Altraflex 2006

In order to be able to compare the behavior of the B70/100 aged and the B70/100 with 6% Altraflex 2006 aged, figures 4.38,4.39 and 4.40 were drawn.

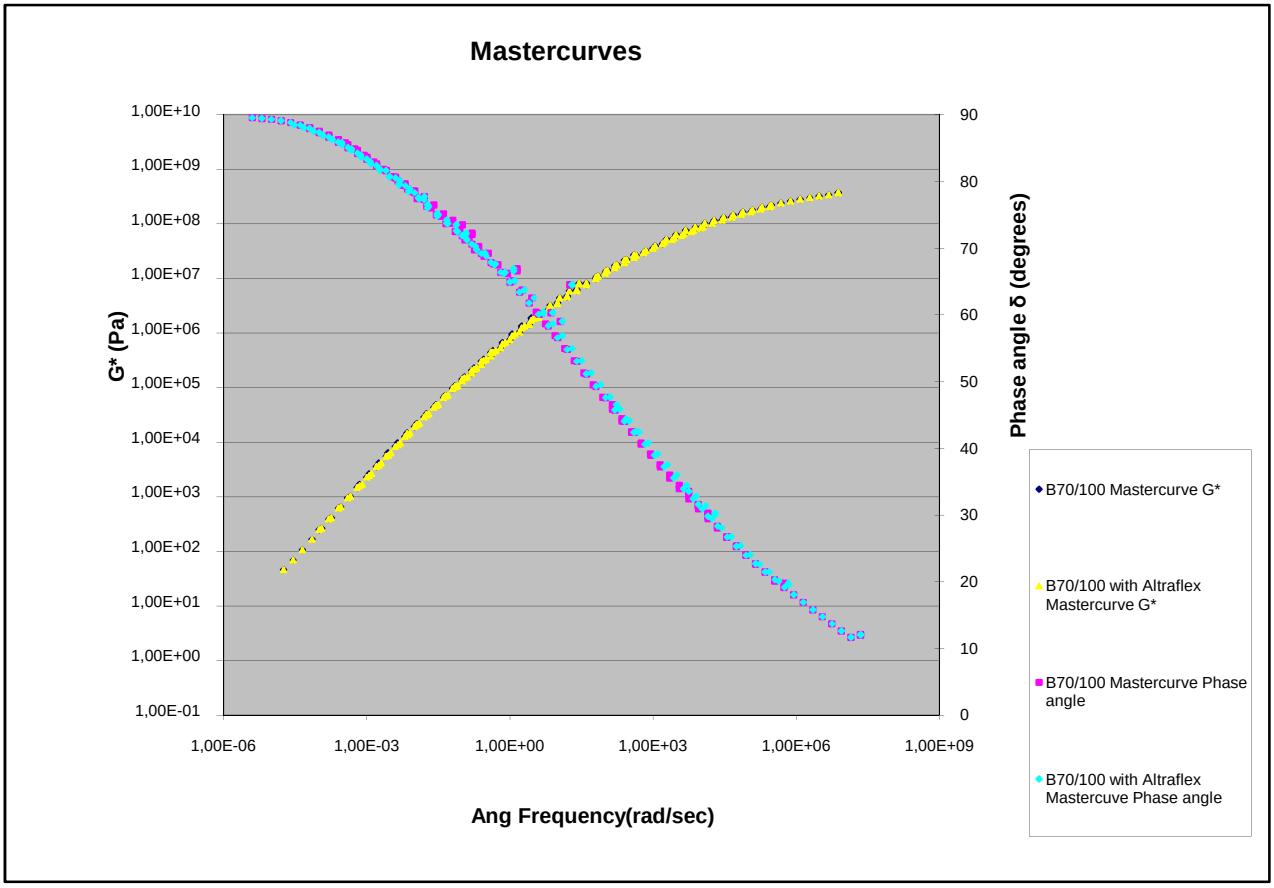


**Graph 4.38:** Mastercurves for G* and δ at $20^0$C for aged B70/100 and aged B70/100 with 6% Altraflex 2006

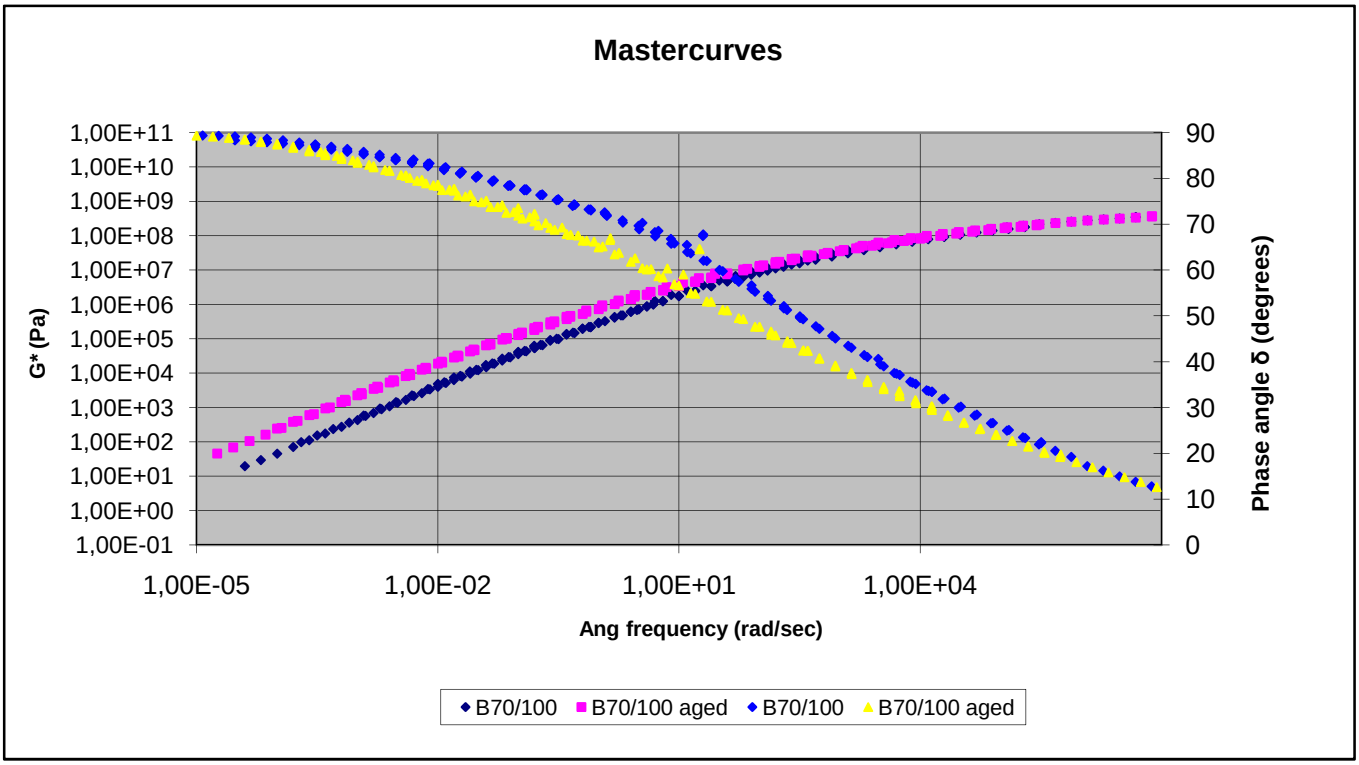


**Graph 4.39**: Mastercurves for G* and δ at 20$^0$C for unaged B70/100 and aged B70/100

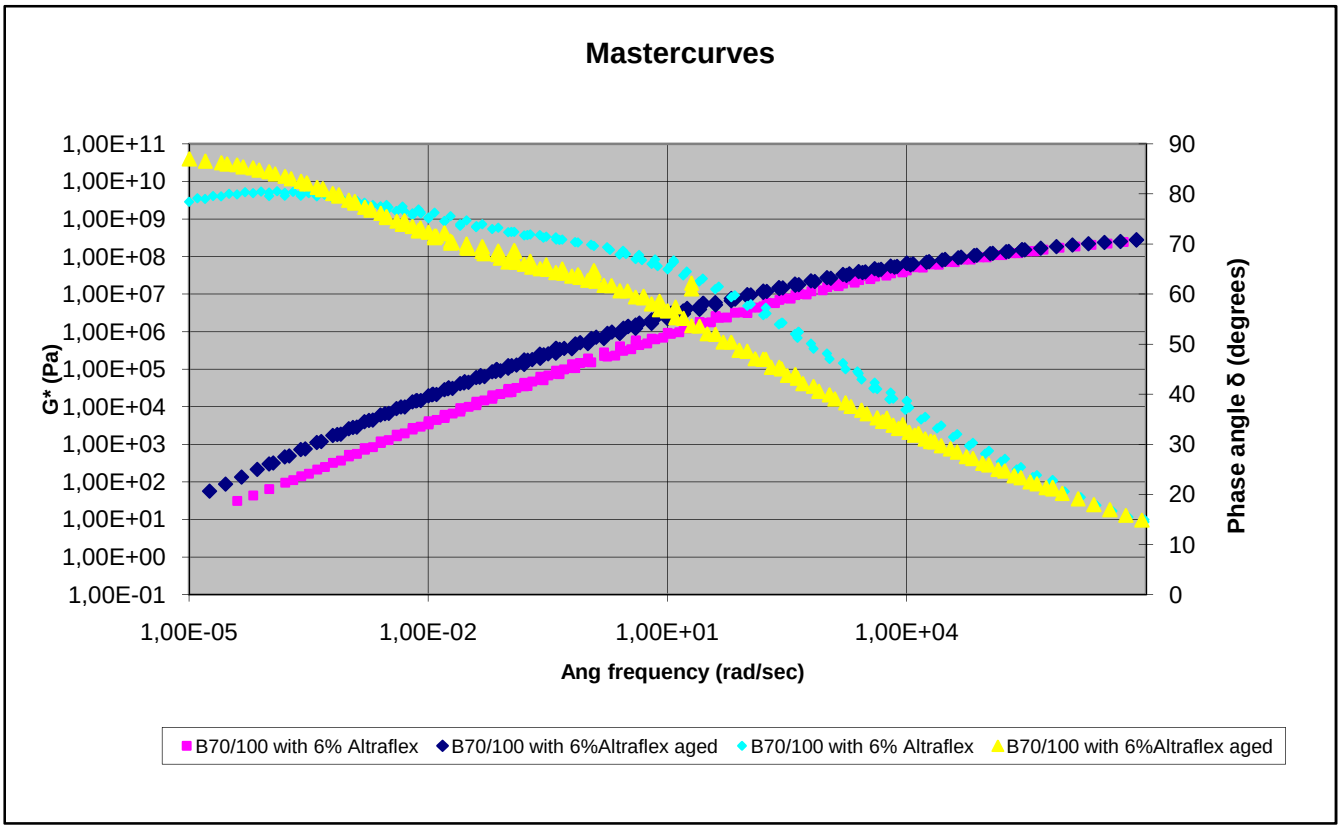


**Graph 4.40**: Mastercurves for G* and δ at 20$^0$C for unaged B70/100+6%Altraflex 2006 and aged B70/100+ 6%Altraflex 2006

In order to obtain a better indication of the differences between the materials, values of G* and δ are given for 0.1 Hz, 10 Hz and 100 Hz as well as the slope m of the G* curve are given in table 4.14a en table 4.14 b

| | B70/100 aged | | | B70/100+6% Altraflex 2006 aged | | |
|---|---|---|---|---|---|---|
| Frequency (Hz) | G* (Pa) | δ (degrees) | m | G* (Pa) | δ (degrees) | m |
| 0,1 | 5,30E+05 | 66,4 | 0,576 | 4,60E+05 | 64,3 | 0,3372 |
| 10 | 1,05E+07 | 49,3 | 0,721 | 1,90E+06 | 50,4 | 0,2788 |
| 100 | 2,95E+07 | 40,2 | 0,585 | 2,30E+07 | 42,1 | 0,6809 |

**Table 4.14a:** The values for G* and δ are given for the different frequencies.

| | B70/100 | | | B70/100+6% Altraflex 2006 | | |
|---|---|---|---|---|---|---|
| Frequency (Hz) | G* (Pa) | δ (degrees) | m | G* (Pa) | δ (degrees) | m |
| 0,1 | 1,95E+05 | 74,0 | 0,710 | 1,35E+05 | 70,1 | 0,7697 |
| 10 | 8,00E+06 | 55,4 | 0,903 | 5,00E+06 | 59,4 | 0,7990 |
| 100 | 2,70E+07 | 48,5 | 0,716 | 1,21E+07 | 50,1 | 0,5914 |

**Table 4.14b:** The values for G* and δ are given for the different frequencies.

From these tables it can be seen that the rheological properties of the aged material changes.

### 4.6.4 Aged Mortar B70/100 with Wigro 60K

The results of the DSR for Mortar B70/100 with Wigro 60K aged are presented in graph 4.41 till graph 4.45

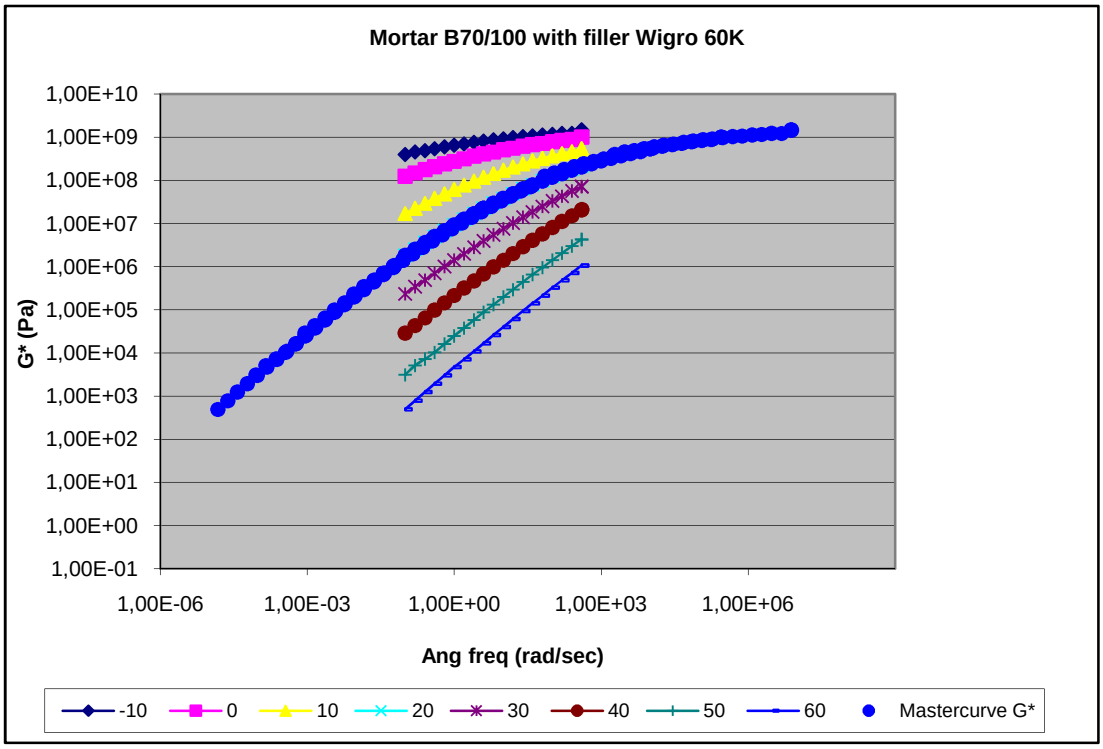


**Graph 4.41:** Mastercurve G* at 20$^0$C for Mortar B70/100 with Wigro 60K aged

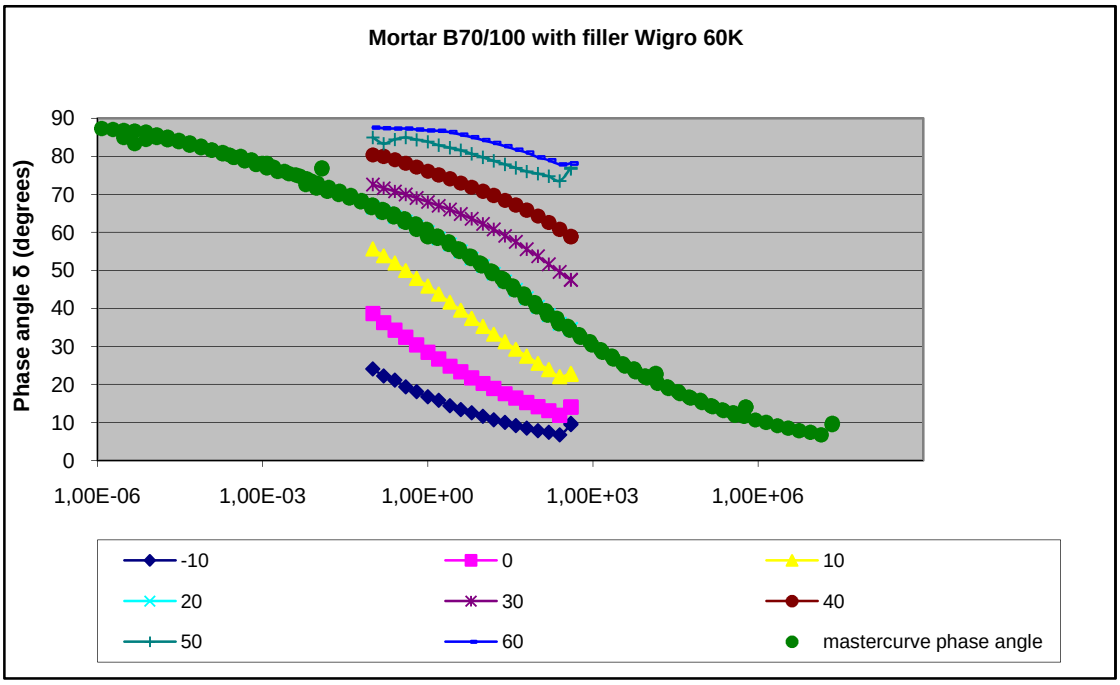


**Graph 4.42**: Mastercurve Phase angle δ at 20$^0$C for Mortar B70/100 with Wigro 60K aged

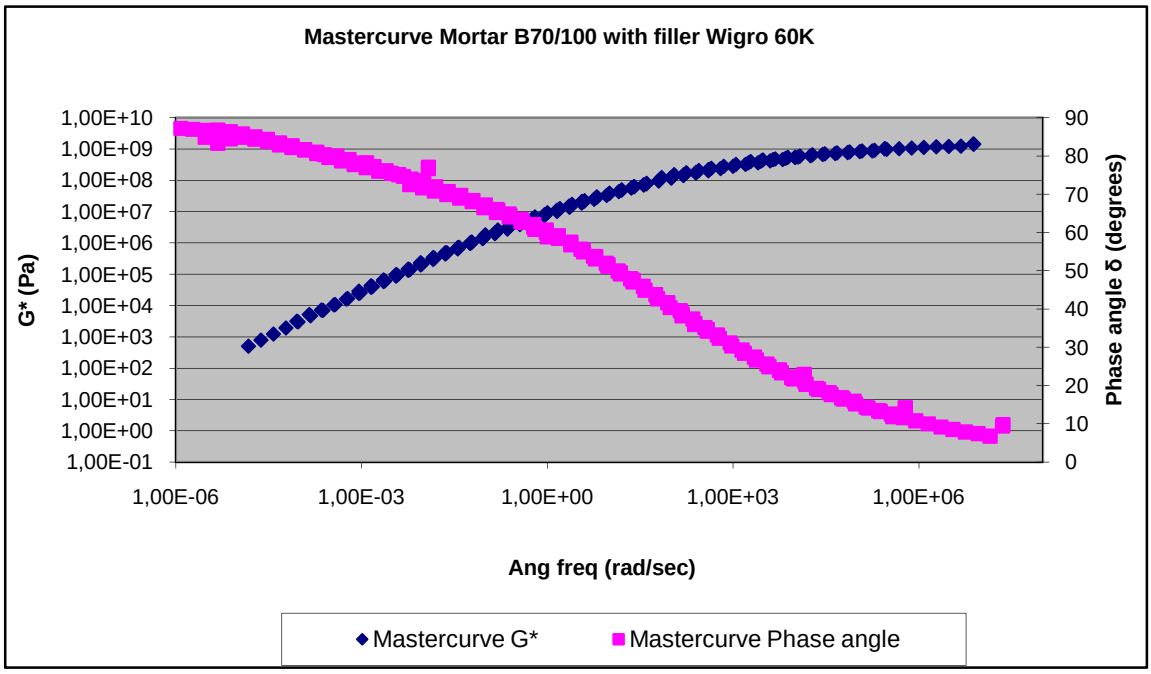


**Graph 4.43:** Mastercurves for G* and δ at 20$^0$C for Mortar B70/100 with Wigro 60K aged

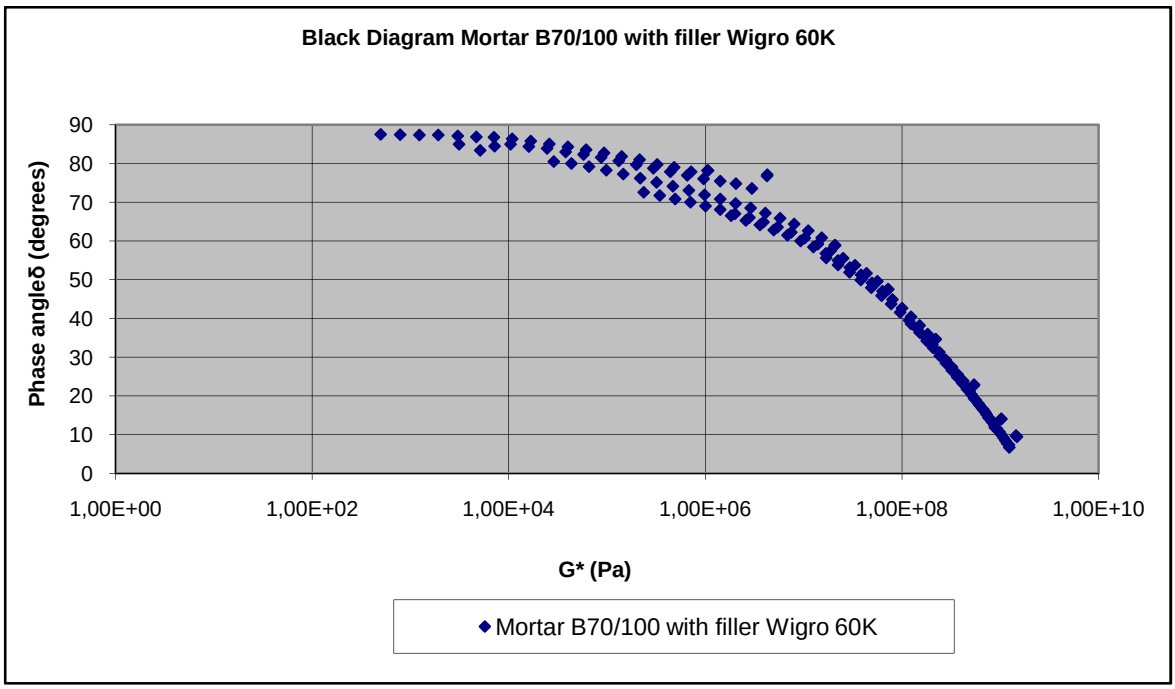


**Graph 4.44:** Black Diagram for Mortar B70/100 with Wigro 60K aged

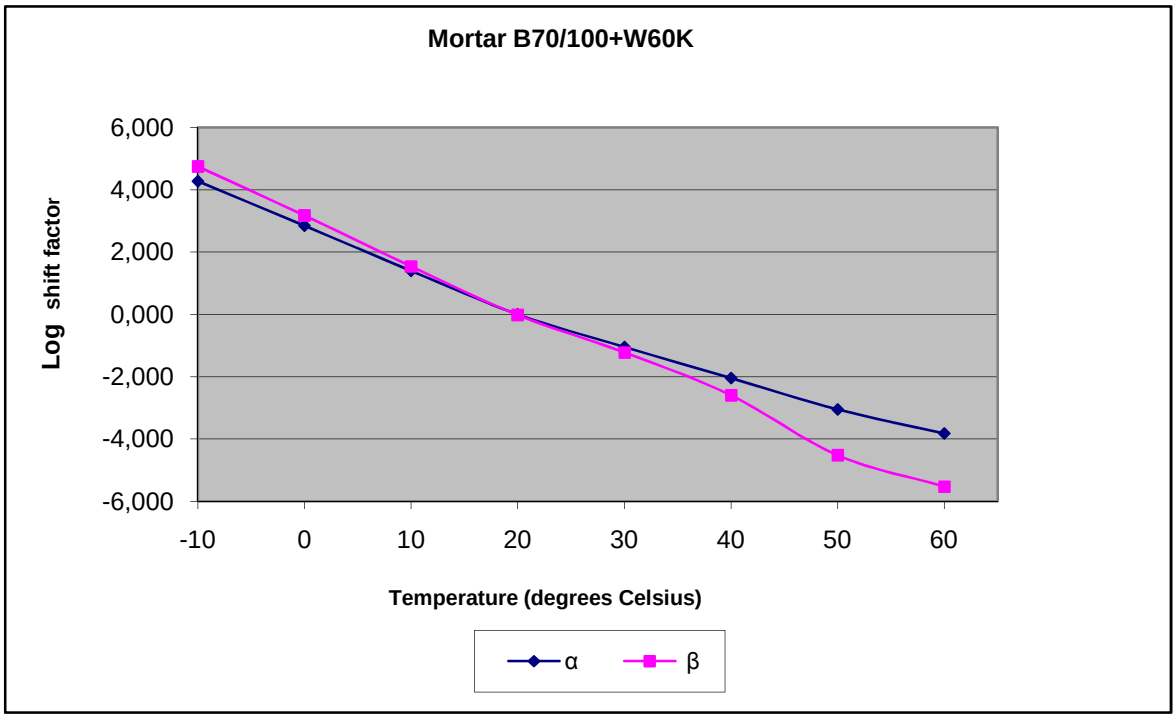


**Graph 4.45:** Dependency of the shift factors on temperature for Mortar B70/100 with Wigro 60K aged

### 4.6.5 Aged Mortar B70/100 with Wigro

The results of the DSR for Mortar B70/100 with Wigro aged are presented in graph 4.46 till graph 4.49.

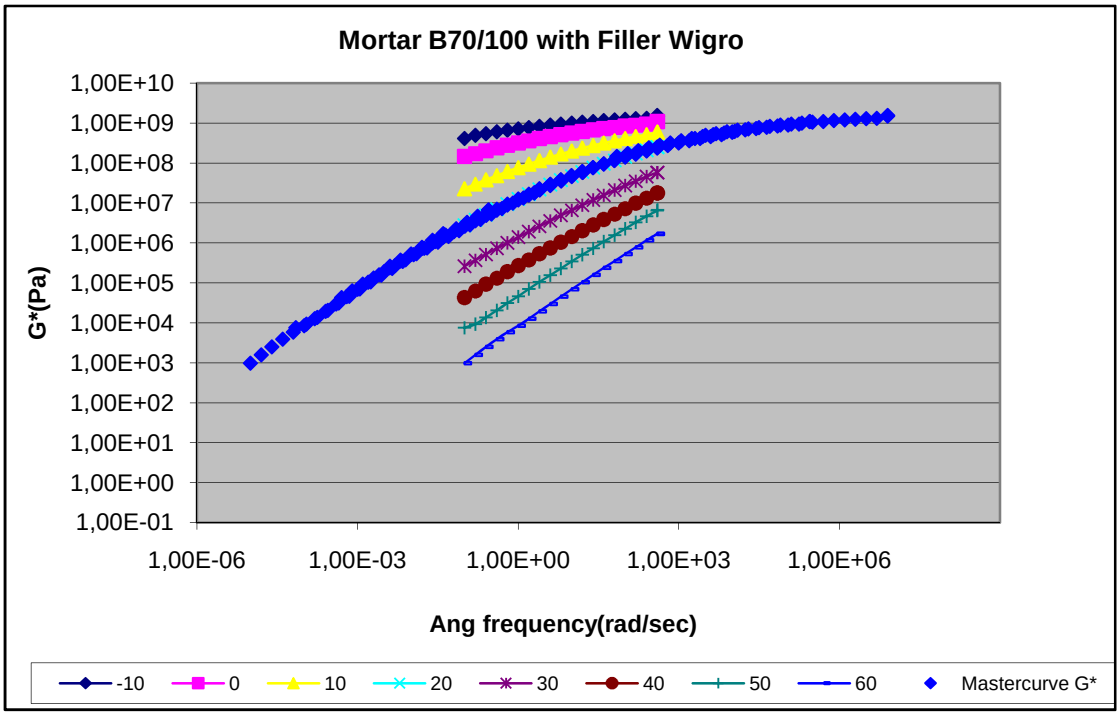


**Graph 4.46:** Mastercurve G* at 20$^0$C for Mortar B70/100 with Wigro aged

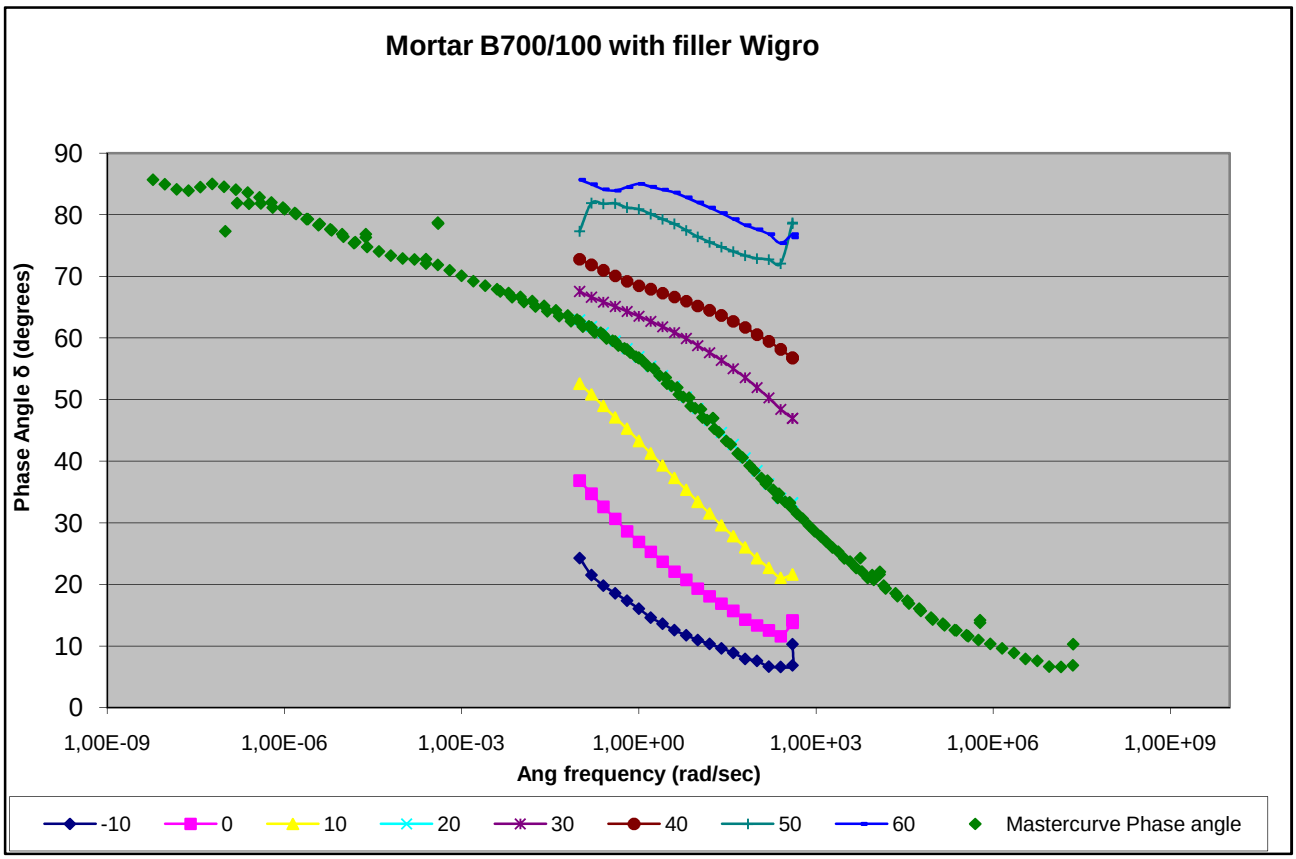


**Graph 4.47:** Mastercurve Phase angle δ at 20$^0$C for Mortar B70/100 with Wigro aged

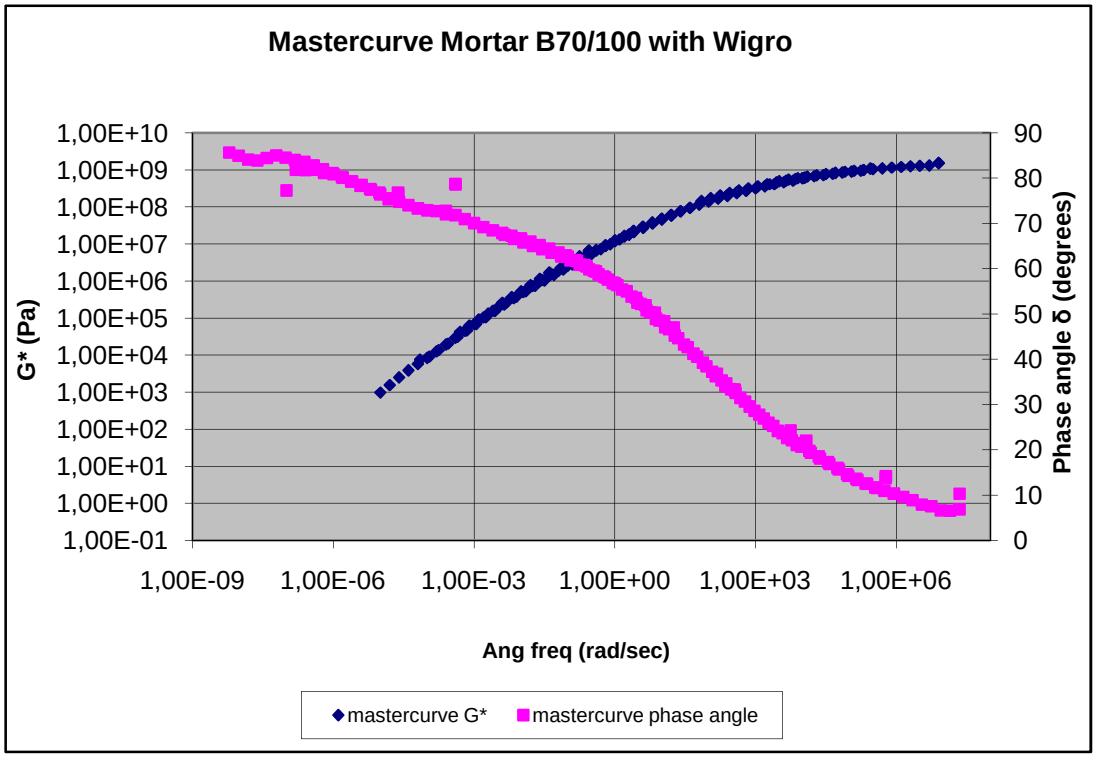


**Graph 4.48**: Mastercurves for G* and δ at 20$^0$C for Mortar B70/100 with Wigro aged

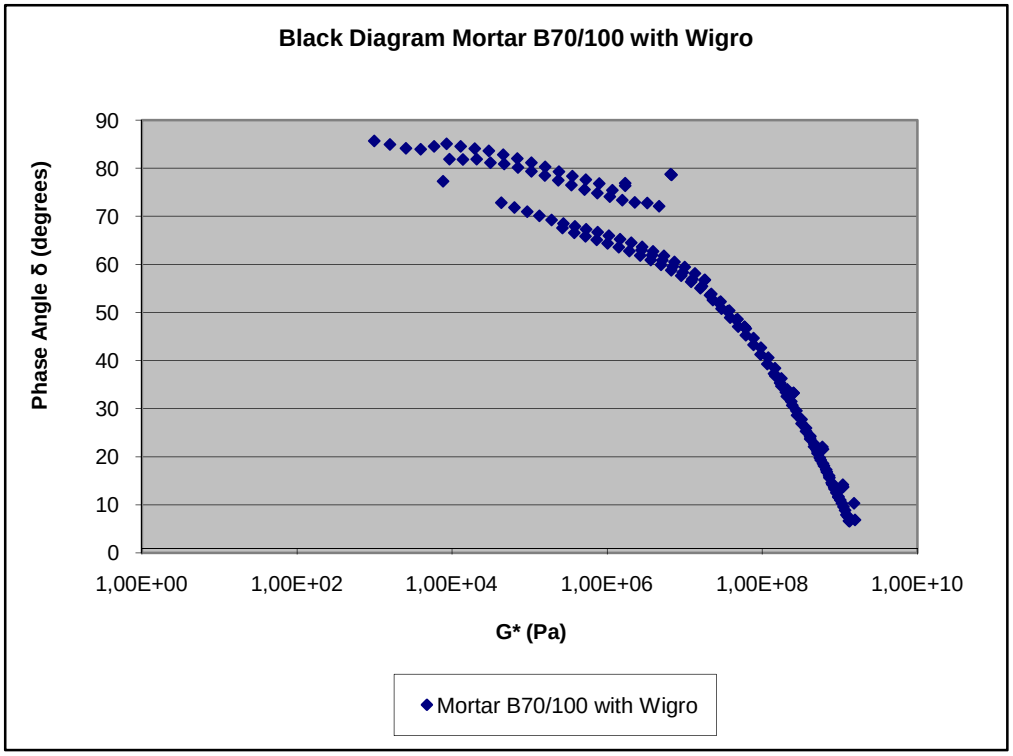


**Graph 4.49**: Black Diagram for Mortar B70/100 with Wigro aged

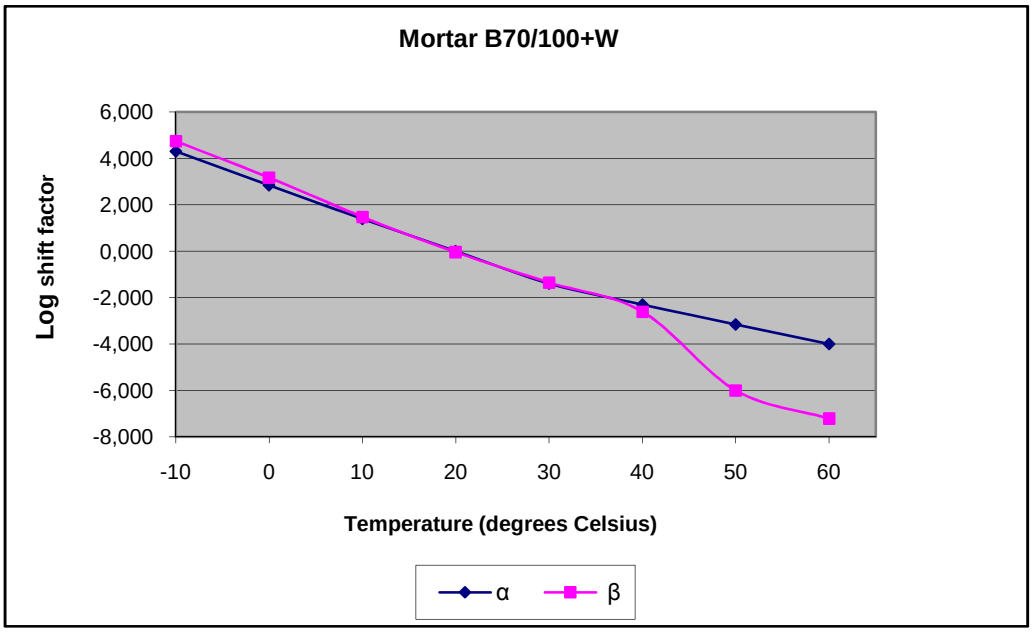


**Graph 4.50:** Dependency of the shift factors on temperature for Mortar B70/100 with Wigro aged

### 4.6.6 Aged Mortar B70/100 with Wigro 60K and Altraflex 2006

The results of the DSR for Mortar B70/100 with Wigro 60K and 6% Altraflex 2006 aged are presented in graph 4.51 till graph 4.54.

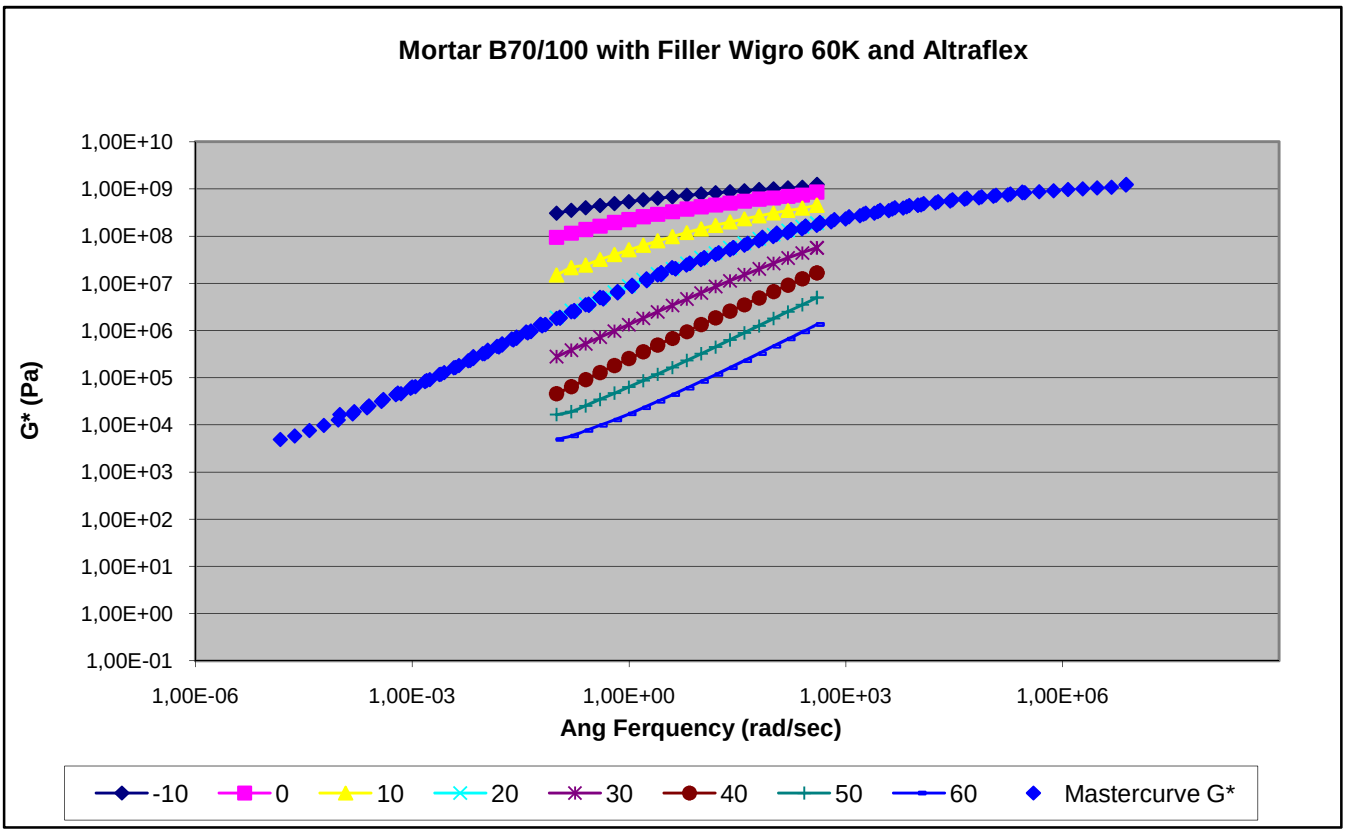


**Graph 4.51**: Mastercurve G* at 20$^0$C for Mortar B70/100 with Wigro 60K and 6% Altraflex 2006 aged

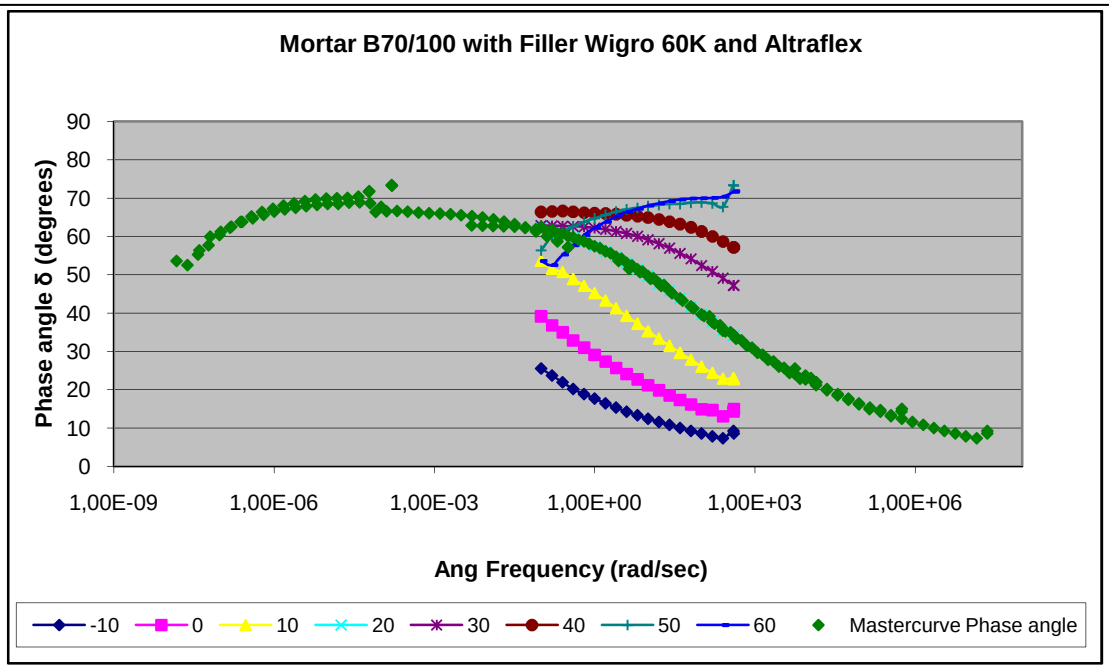


**Graph 4.52**: Mastercurve Phase angle δ at 20$^0$C for Mortar B70/100 with Wigro 60K and 6% Altraflex 2006 aged

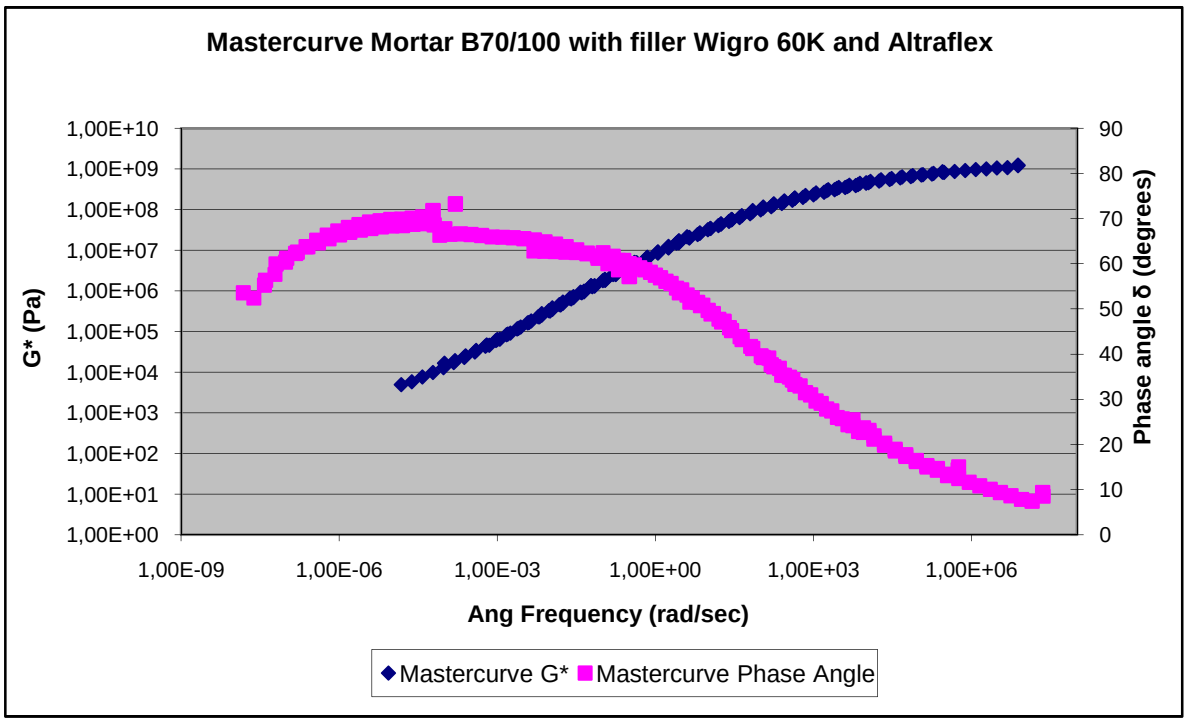


**Graph 4.53**: Mastercurves for G* and δ at 20$^0$C for Mortar B70/100 with Wigro 60K and 6% Altraflex 2006 aged

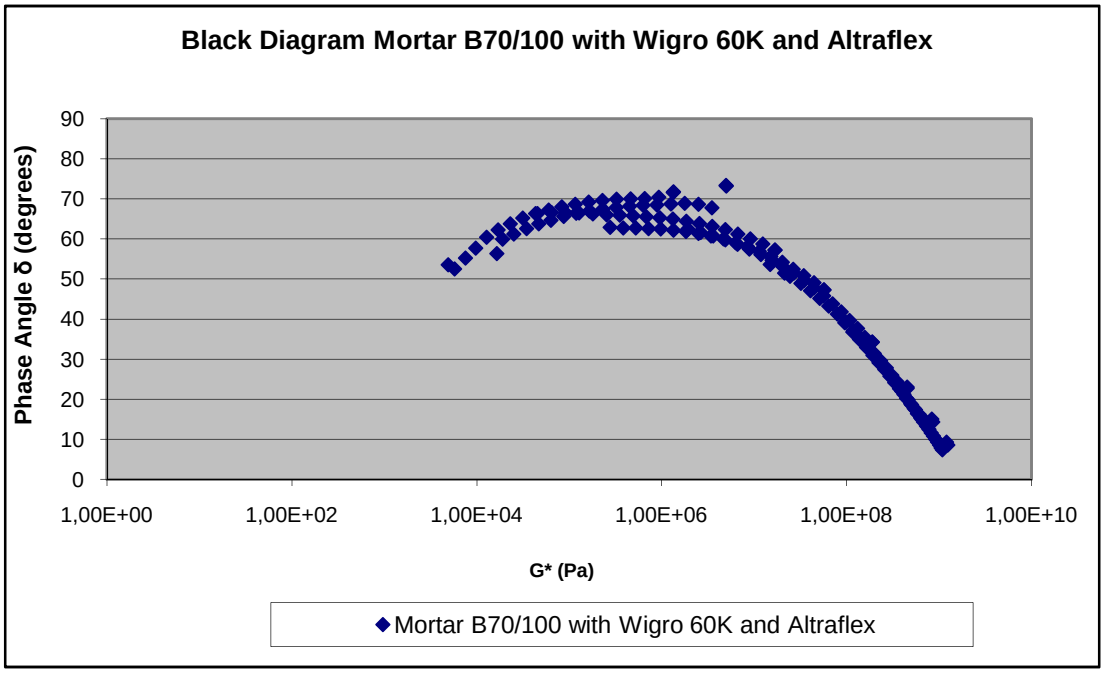


**Graph 4.54**: Black Diagram for Mortar B70/100 with Wigro 60K and 6% Altraflex 2006 aged

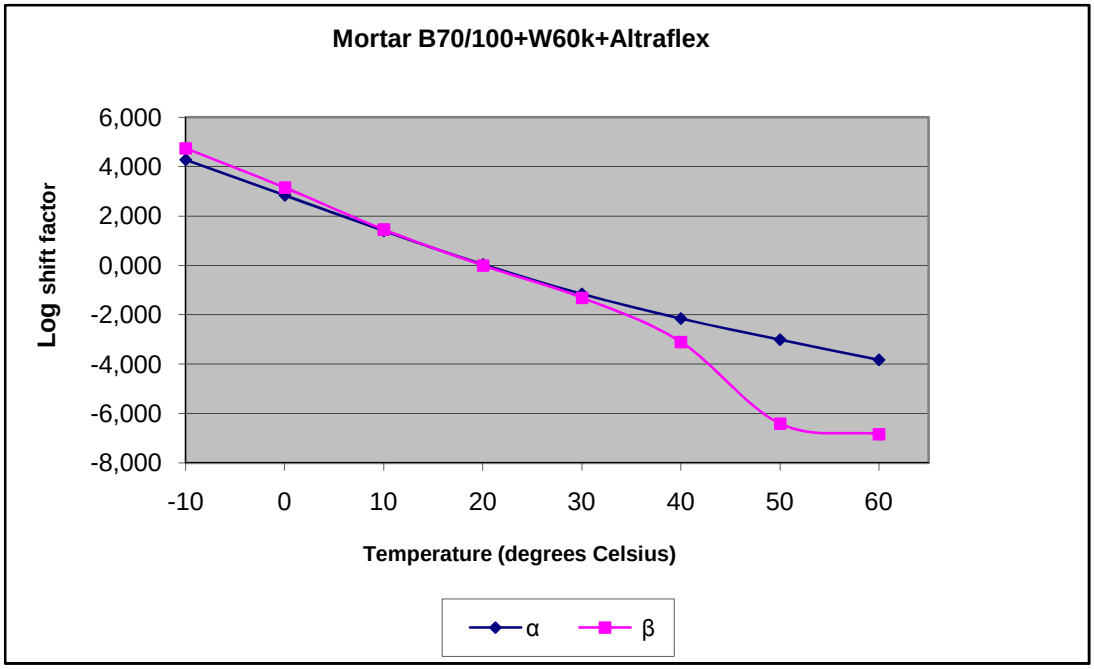


**Graph 4.55**: Dependency of the shift factors on temperature for Mortar B70/100 with Wigro 60K and 6% Altraflex 2006 aged

### 4.6.7 Aged Mortar B70/100 with Wigro and 6% Altraflex 2006

The results of the DSR for Mortar B70/100 with Wigro and 6% Altraflex 2006 aged are presented in graph 4.56 till graph 4.59.

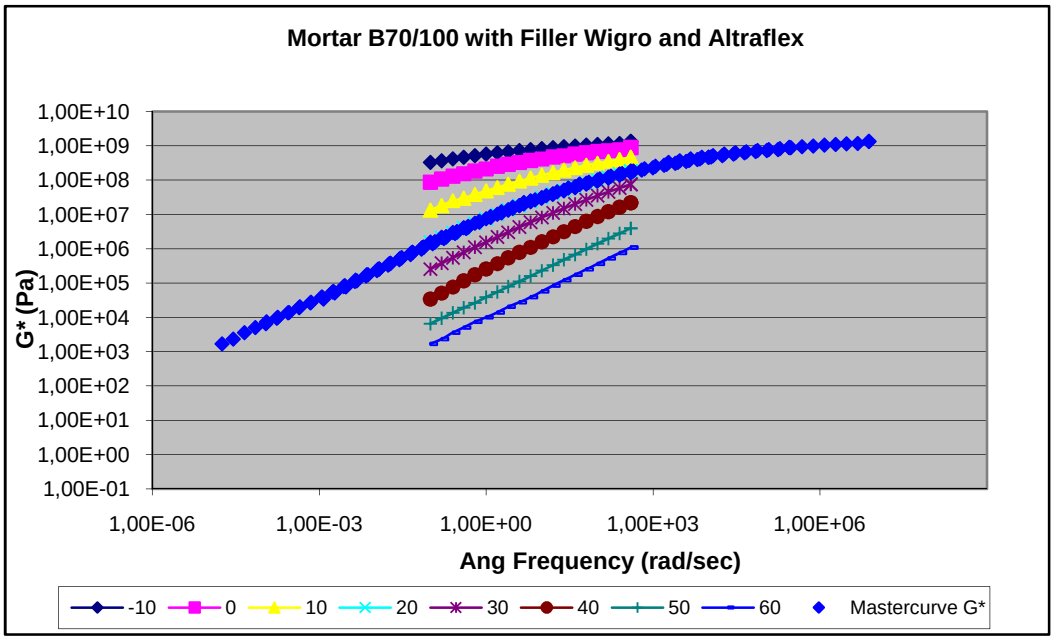


**Graph 4.56**: Mastercurve G* at 20$^0$C for Mortar B70/100 with Wigro and 6% Altraflex 2006 age.

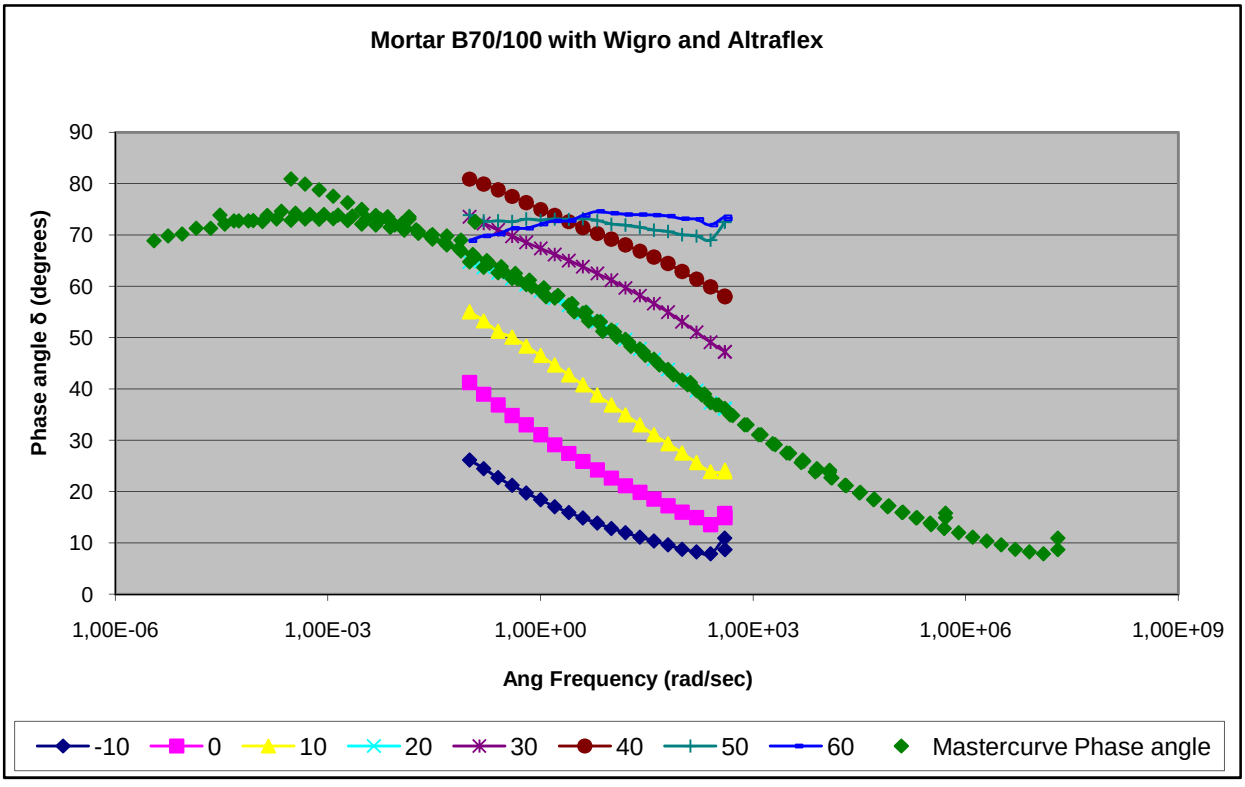


**Graph 4.57:** Mastercurve Phase angle δ at 20$^0$C for Mortar B70/100 with Wigro and 6% Altraflex 2006 aged

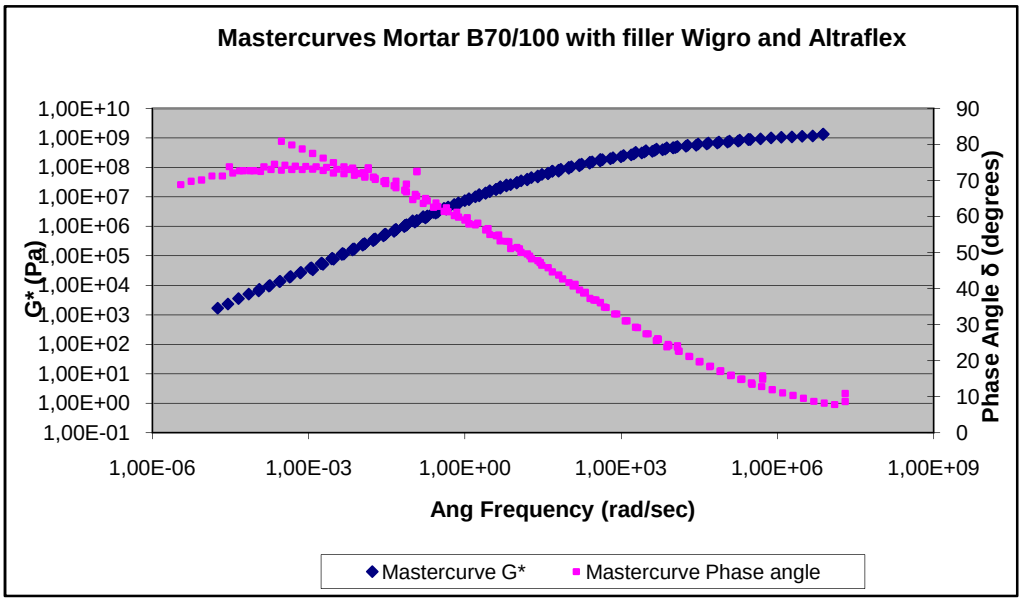


**Graph 4.58:** Mastercurves for G* and δ at 20$^0$C for Mortar B70/100 with Wigro and 6% Altraflex 2006 aged

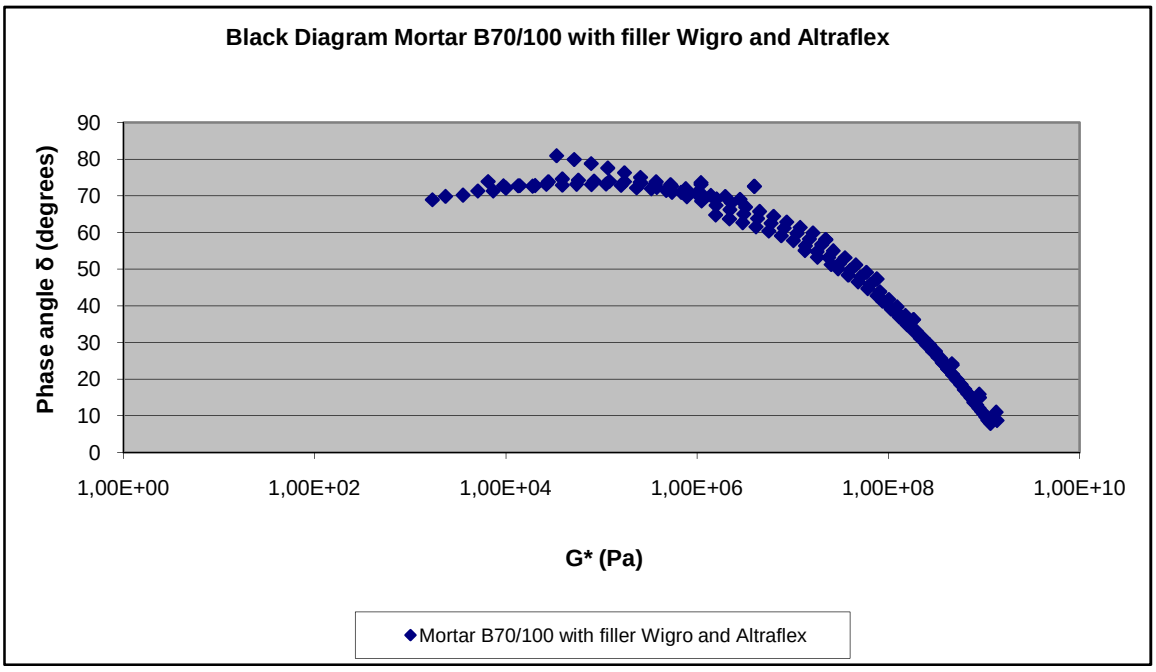


**Graph 4.59:** Black Diagram for Mortar B70/100 with Wigro and 6% Altraflex 2006 aged

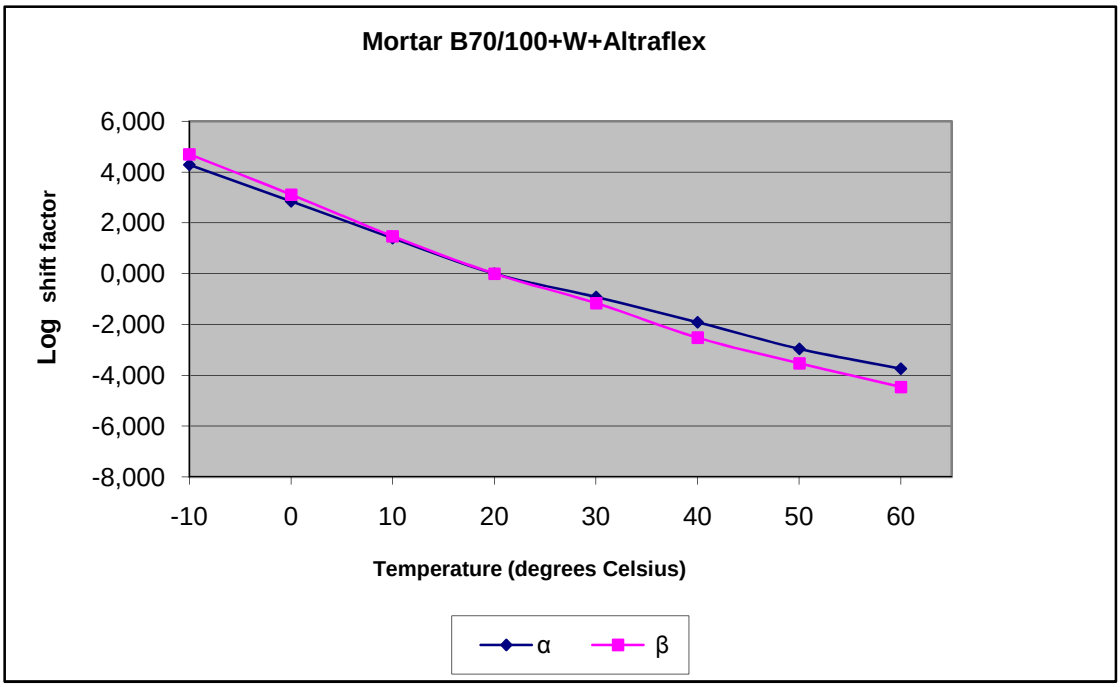


**Graph 4.60:** Dependency of the shift factors on temperature for Mortar B70/100 with Wigro and 6% Altraflex 2006 aged

### 4.6.8 Comparison of the rheological behavior of aged mortars

The results of the DSR for mortar 1 (B70/100 with Wigro 60K aged) and mortar 2 (B70/100 with Wigro aged) are presented in graph 4.61 and graph 4.62.

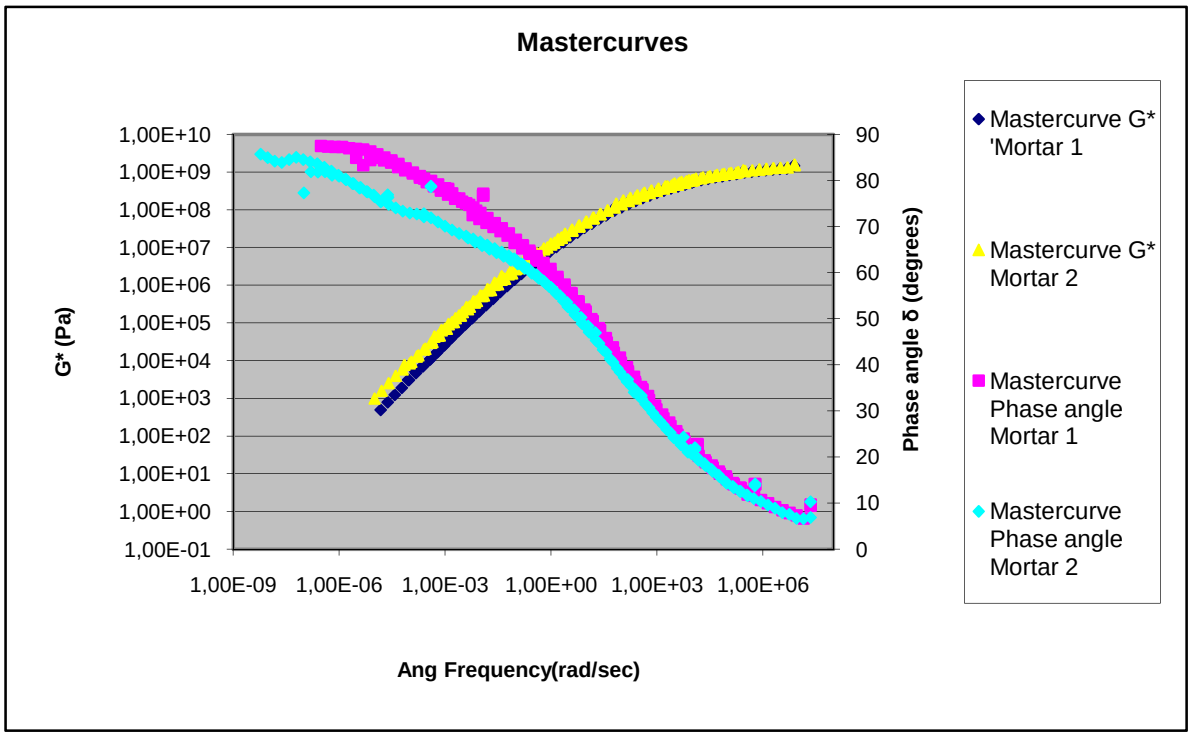


**Graph 4.61**: Mastercurves for G* and δ at 20$^0$C for Mortar B70/100 with Wigro 60K aged and Mortar B70/100 with Wigro aged

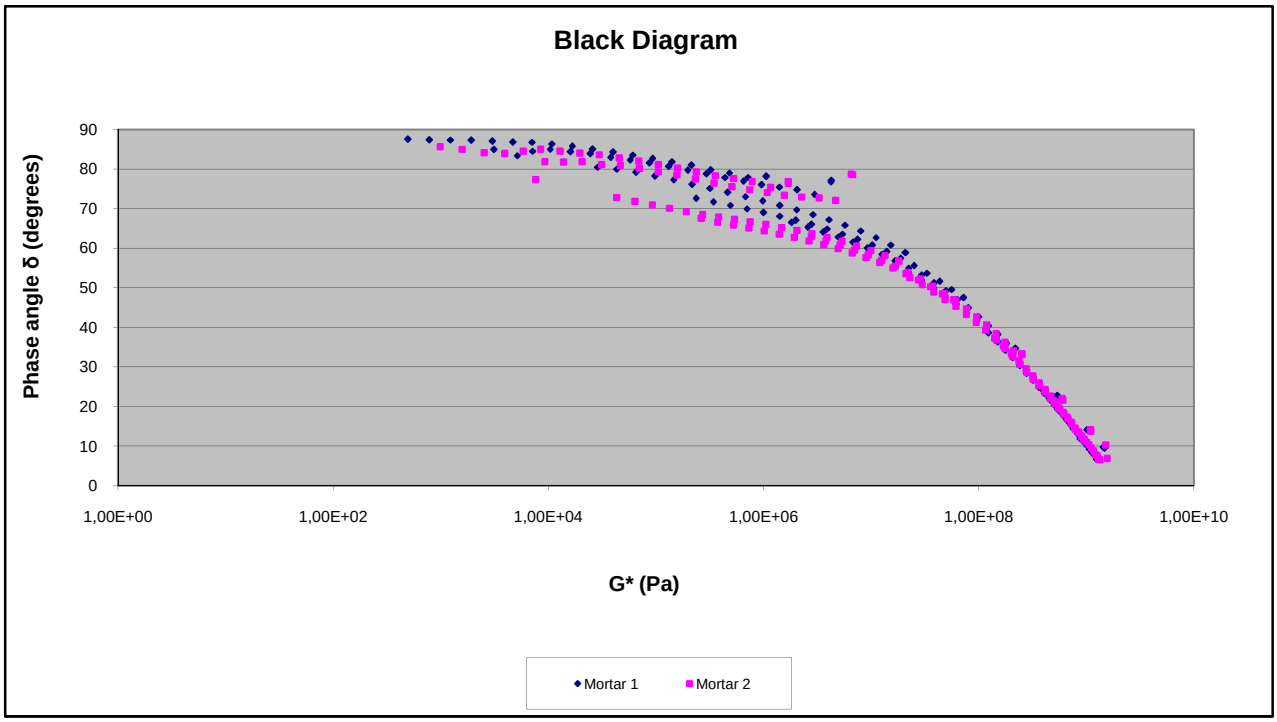


**Graph 4.62:** Black Diagram for Mortar B70/100 with Wigro 60K aged and Mortar B70/100 with Wigro aged

Mortar 1: B70/100 with Wigro 60K aged
Mortar 2: B70/100 with Wigro aged

The results of the DSR for mortar 3 (B70/100 with Wigro 60K and 6% Altraflex 2006 aged) and mortar 4 (B70/100 with Wigro and 6% Altraflex 2006 aged) are presented in graph 4.63 and graph 4.64

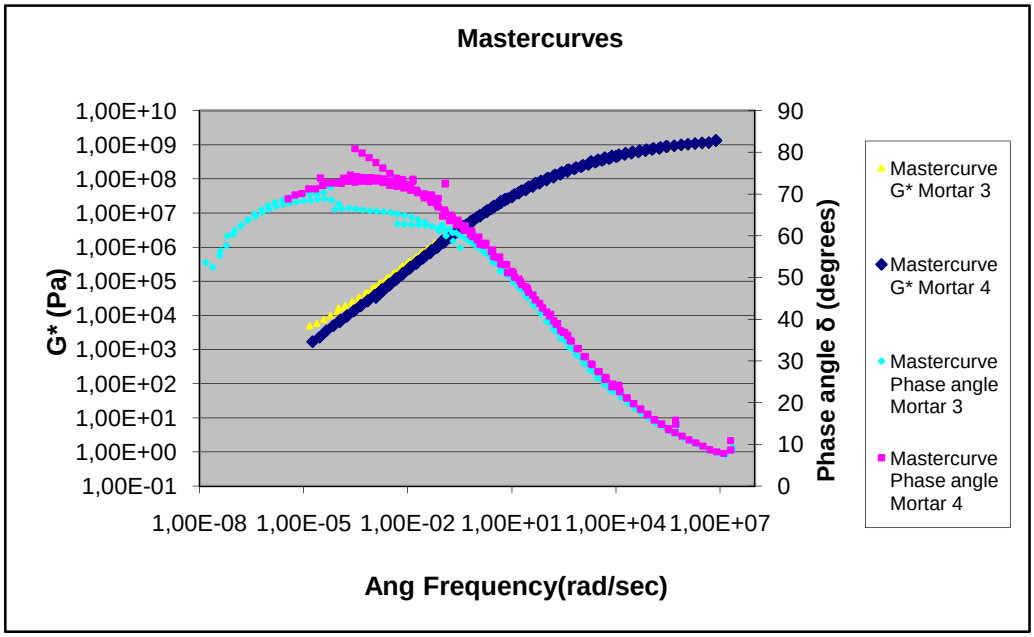


**Graph 4.63:** Mastercurves for G* and δ at 20$^0$C for Mortar B70/100 with Wigro 60K and 6% Altraflex 2006 aged and Mortar B70/100 with Wigro and 6% Altraflex 2006 aged

.

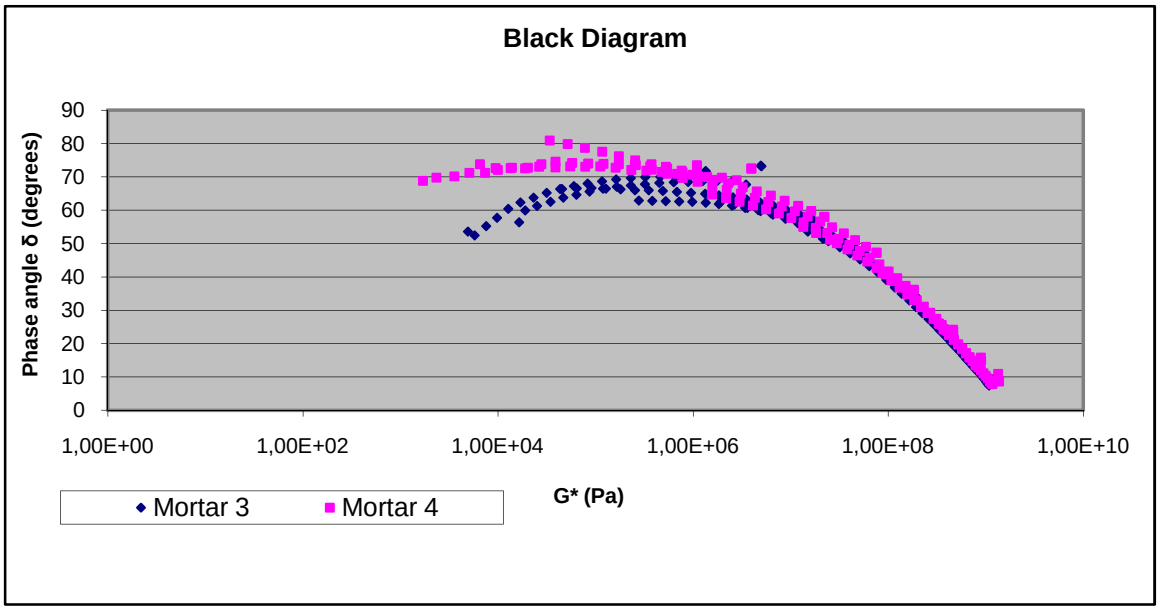


**Graph 4.64:** Black Diagram for G* and δ for Mortar B70/100 with Wigro 60K and 6% Altraflex 2006 aged and Mortar B70/100 with Wigro and 6% Altraflex 2006 aged.

Mortar 3: B70/100 with Wigro 60K and 6% Altraflex 2006 aged
Mortar 4: B70/100 with Wigro and 6% Altraflex 2006 aged

The results of the DSR for the four different aged mortars are presented in graph 4.65 and graph 4.66.

Mortar 1: B70/100 with Wigro 60K
Mortar 2: B70/100 with Wigro

Mortar 3: B70/100 with Wigro 60K and 6% Altraflex 2006
Mortar 4: B70/100 with Wigro and 6% Altraflex 2006

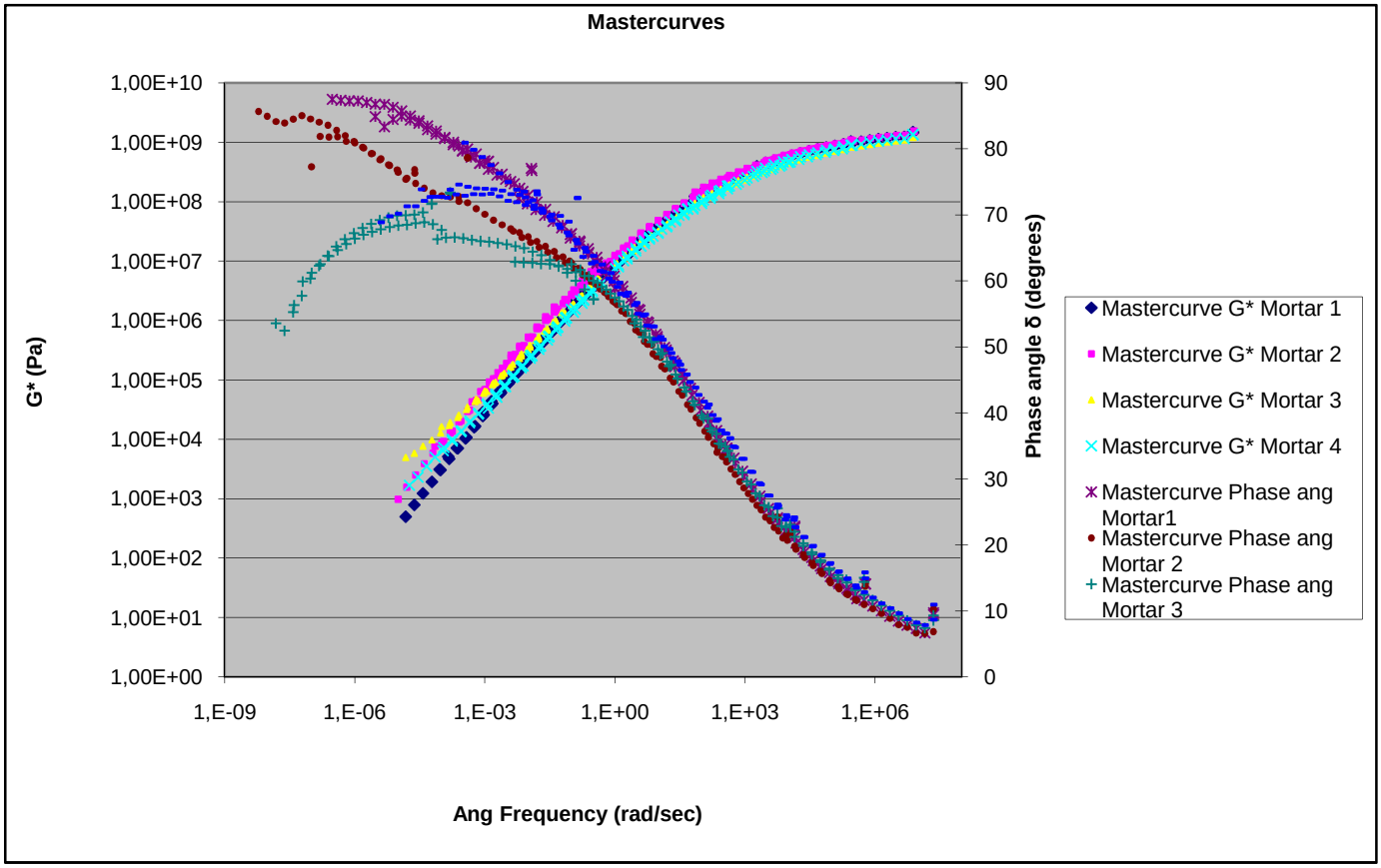


**Graph 4.65**: Mastercurves for G* and δ at 20$^0$C for all mortars

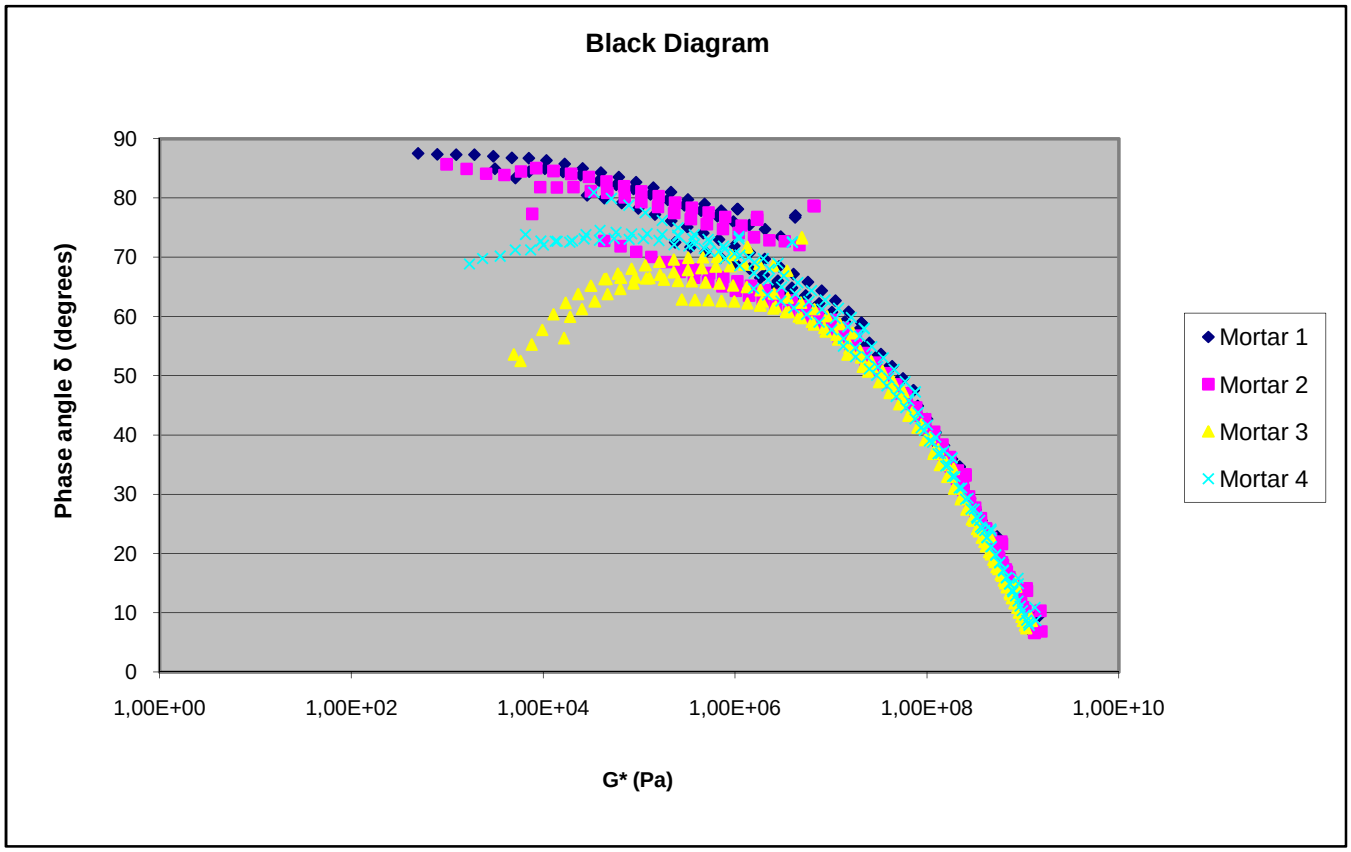


**Graph 4.66**: Black Diagram for all mortars

### 4.6.9 Conclusion

When we compare mortar 1 (B70/100 with Wigro 60K) with mortar 2 (B70/100 with Wigro) in graph 4.47 we see that at low angular frequencies the G* for mortar 1 is 500 Pa and the G* for mortar 2 is 1000 Pa (see table 4.14c). At high frequencies they both reach $2x10^9$ Pa. The lines do not differ much.
The phase angle δ of mortar 2 is less compared to mortar 1 during all the angular frequencies.
The lines differ much from each other. The difference may be the result of the effect of the fillers on the mortar.

When we compare mortar 3 (B70/100 with Wigro 60K and 6% Altraflex 2006) with mortar 4 (B70/100 with Wigro with 6% Altraflex 2006) in graph 4.49 we see that at low angular frequencies the G* for mortar 3 is 6000 Pa and the G* for mortar 4 is 2000 Pa (see table 4.14d). At high frequencies they both reach $2x10^9$ Pa, same for mortar 1 (B70/100 with Wigro 60K) and mortar 2 (B70/100 with Wigro). The lines do not differ much.

The phase angle of mortar 3 is less compared to mortar 4 during all the angular frequencies.
The lines do not differ much from each other.

In order to obtain a better indication of the differences between the materials, values of G* and δ are given for 0.1 Hz, 10 Hz and 100 Hz as well as the slope m of the G* curve are given in table 4.14c to table 4.14f:

| | **Mortar 1 aged** | | | **Mortar 2 aged** | | |
|---|---|---|---|---|---|---|
| Frequency (Hz) | G* (Pa) | δ (degrees) | m | G* (Pa) | δ (degrees) | m |
| 0,1 | 6,81E+06 | 62,2 | 0,467 | 9,50E+06 | 58,1 | 0,3223 |
| 10 | 3,30E+07 | 40,6 | 0,219 | 3,57E+07 | 39,5 | 0,2527 |
| 100 | 2,75E+08 | 30,3 | 0,570 | 2,75E+08 | 29,5 | 0,5697 |

**Table 4.14c:** Values for G* en δ at different frequencies for mortar 1 and mortar 2 at $20^0$C.

| | **Mortar 3 aged** | | | **Mortar 4 aged** | | |
|---|---|---|---|---|---|---|
| Frequency (Hz) | G* (Pa) | δ (degrees) | m | G* (Pa) | δ (degrees) | m |
| 0,1 | 6,10E+06 | 58,5 | 0,515 | 6,10E+06 | 60,34 | 0,515 |
| 10 | 8,11E+07 | 41,8 | 0,609 | 8,66E+07 | 43,82 | 0,638 |
| 100 | 1,96E+08 | 32,4 | 0,496 | 1,96E+08 | 33,10 | 0,496 |

**Table 4.14d:** Values for G* en δ at different frequencies for mortar 3 and mortar 4 at $20^0$C.

| | Mortar 1 aged | | | Mortar 3 aged | | |
|---|---|---|---|---|---|---|
| Frequency (Hz) | G* (Pa) | δ (degrees) | m | G* (Pa) | δ (degrees) | m |
| 0,1 | 6,81E+06 | 62,2 | 0,467 | 6,10E+06 | 58,5 | 0,515 |
| 10 | 3,30E+07 | 40,6 | 0,219 | 8,11E+07 | 41,8 | 0,609 |
| 100 | 2,75E+08 | 30,3 | 0,570 | 1,96E+08 | 32,4 | 0,496 |

**Table 4.14e:** Values for G* en δ at different frequencies for mortar 1 and mortar 3 at $20^0$C.

| | Mortar 2 aged | | | Mortar 4 aged | | |
|---|---|---|---|---|---|---|
| Frequency (Hz) | G* (Pa) | δ (degrees) | m | G* (Pa) | δ (degrees) | m |
| 0,1 | 9,50E+06 | 58,1 | 0,322 | 6,10E+06 | 60,34 | 0,515 |
| 10 | 3,57E+07 | 39,5 | 0,253 | 8,66E+07 | 43,82 | 0,638 |
| 100 | 2,75E+08 | 29,5 | 0,570 | 1,96E+08 | 33,10 | 0,496 |

**Table 4.14f:** Values for G* en δ at different frequencies for mortar 2 and mortar 4 at $20^0$C.

From these four tables we can conclude in the range considered (at $20^0$C ) that the G* is almost the same for all four cases. This is however not the same for the phase angle.
From table 4.14 c we see that mortar 2 has better rheological properties than mortar 1 at lower frequencies. In table 4.14 d we see that mortar 3 has smaller values for the phase angle at lower frequencies, compared to mortar 4.
From table 4.14e en table 4.14f we can say that mortar 3 has smaller values for the phase angle at lower frequencies, compared to mortar 1 and mortar 2 has smaller values for the phase angle at lower frequencies, compared to mortar 4.

Mortar 3 and mortar 4 show a strange behavior at $50^0$ C and $60^0$ C. This asks for critical look at the test results at these high temperatures.
The results of the black diagrams and the mastercurves of all the mortars will be presented in paragraph 4.6.10 without the temperatures of $50^0$ C and $60^0$ C.

### 4.6.10 Dynamic Shear Rheometer Tests on Aged material with limited temperature range

As suggested in 4.6.9 the DSR results are presented with a limited temperature range.
The characteristics of the results:
Temperature range: -10, 0, 10, 20, 30 and $40^0$ C
Frequency range: 0,1 – 400 rad/sec

#### 4.6.10.1 Mortar B70/100 with filler Wigro 60K

The results of the DSR for Mortar B70/100 with Wigro 60K aged are presented in graph 4.67 and graph 4.68.

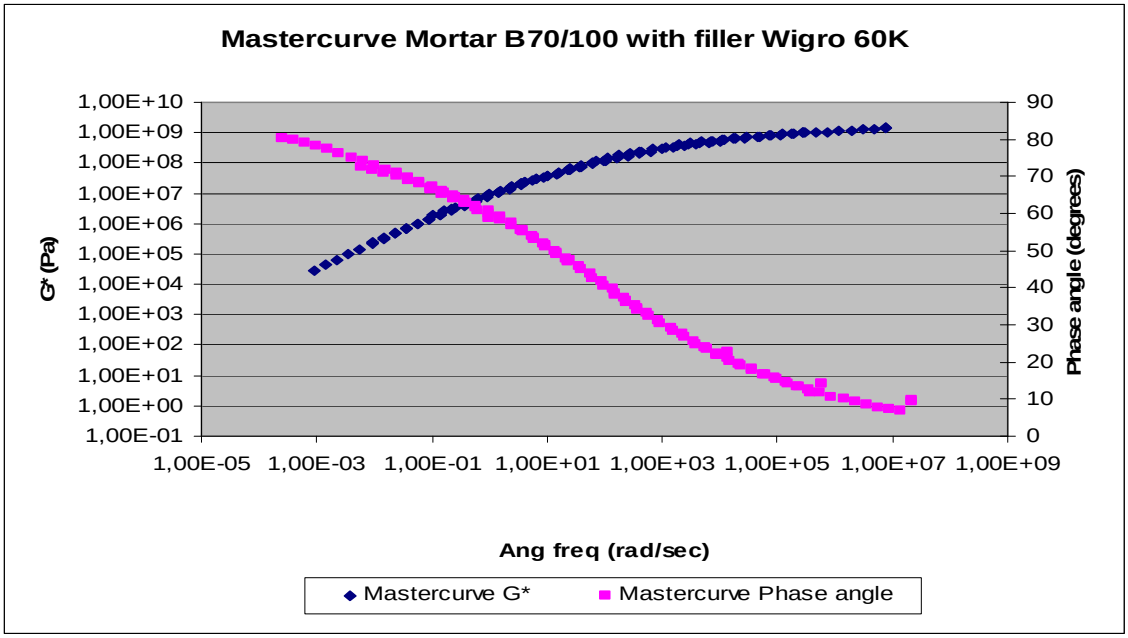


**Graph 4.67:** Mastercurves for G* and δ at 20$^0$C for Mortar B70/100 with Wigro 60K aged

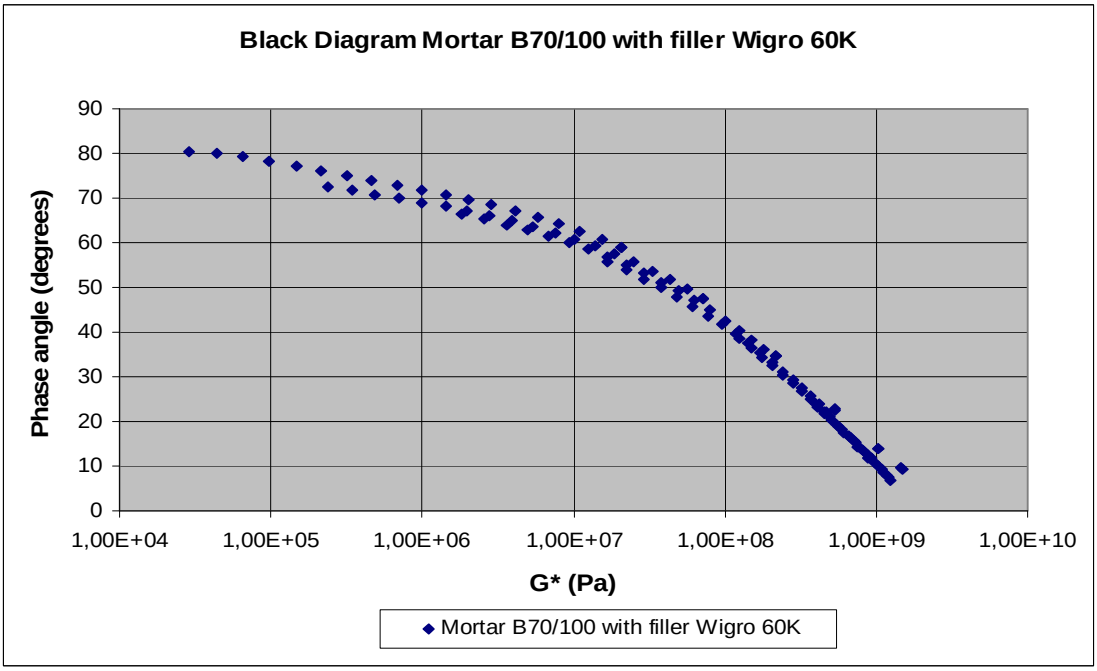


**Graph 4.68**: Black Diagram for Mortar B70/100 with Wigro 60K aged

### 4.6.10.2 Mortar B70/100 with filler Wigro

The results of the DSR for Mortar B70/100 with Wigro aged are presented in graph 4.69 and graph 4.70.

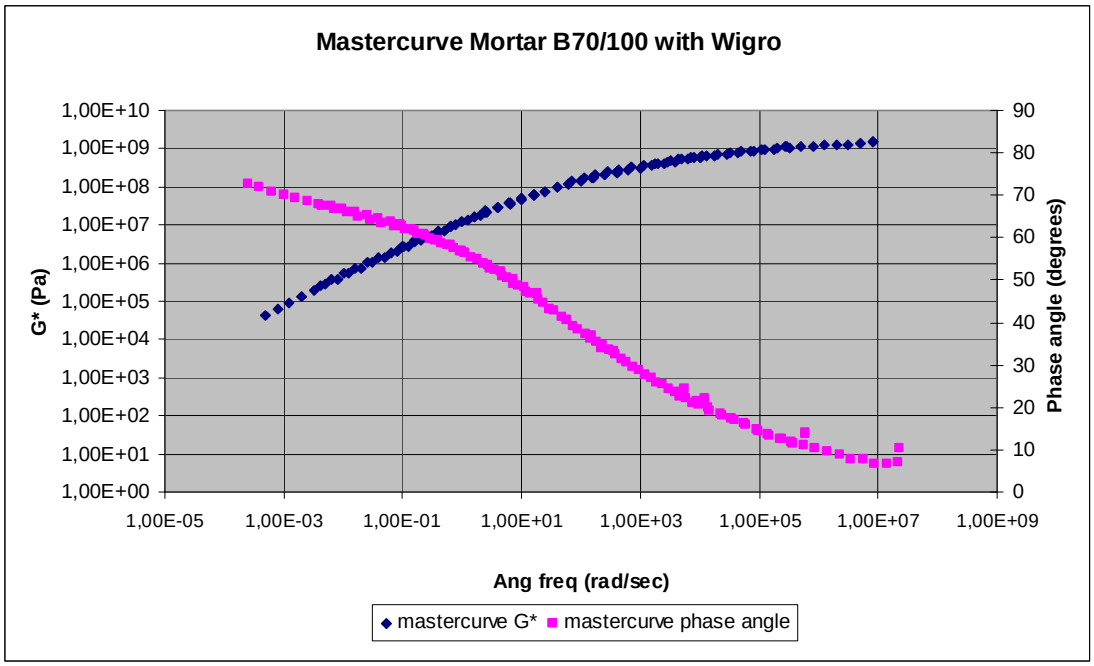


**Graph 4.69**: Mastercurves for G* and δ at 20$^0$C for Mortar B70/100 with Wigro aged

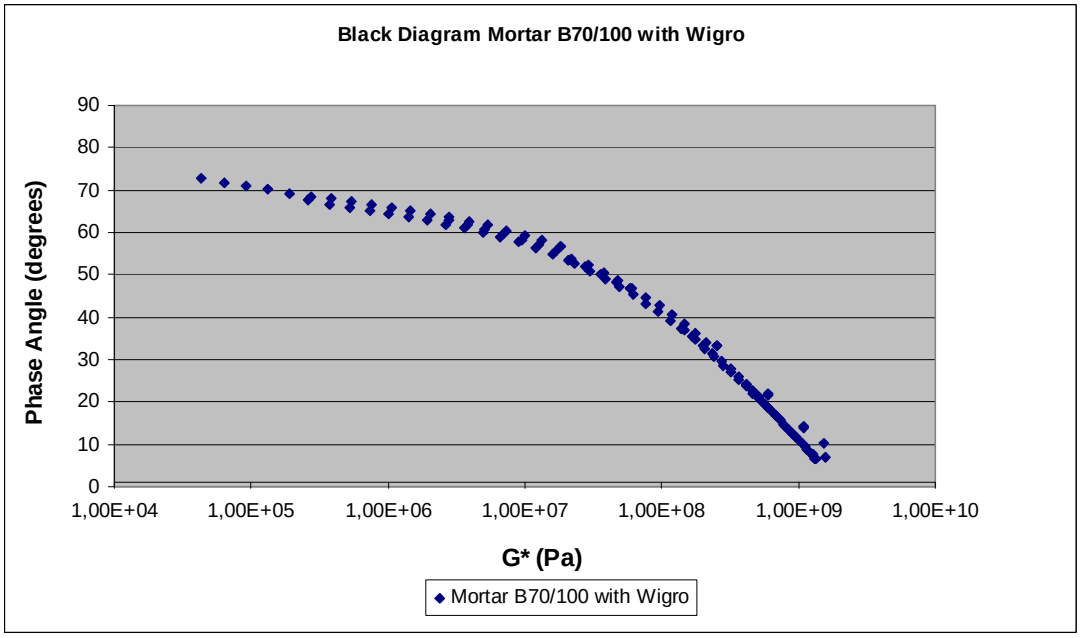


**Graph 4.70:** Black Diagram for Mortar B70/100 with Wigro aged

### 4.6.10.3 Mortar B70/100 with filler Wigro 60K and Altraflex 2006

The results of the DSR for Mortar B70/100 with Wigro 60K and Altraflex 2006 aged are presented in graph 4.71 and graph 4.72.

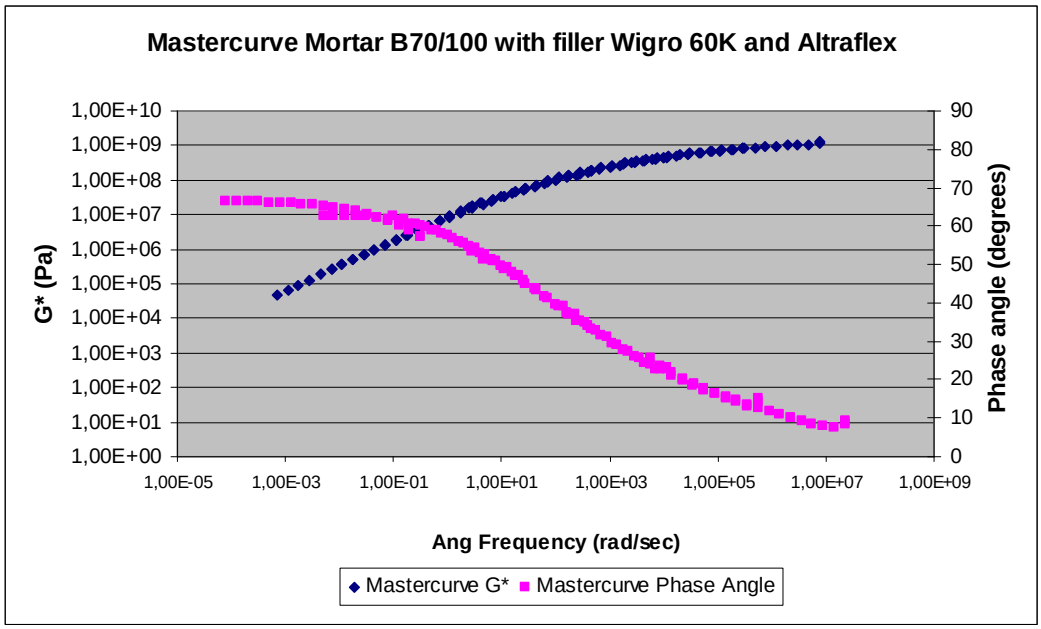


**Graph 4.71**: Mastercurves for G* and δ at 20$^0$C for Mortar B70/100 with Wigro 60K and Altraflex 2006 aged

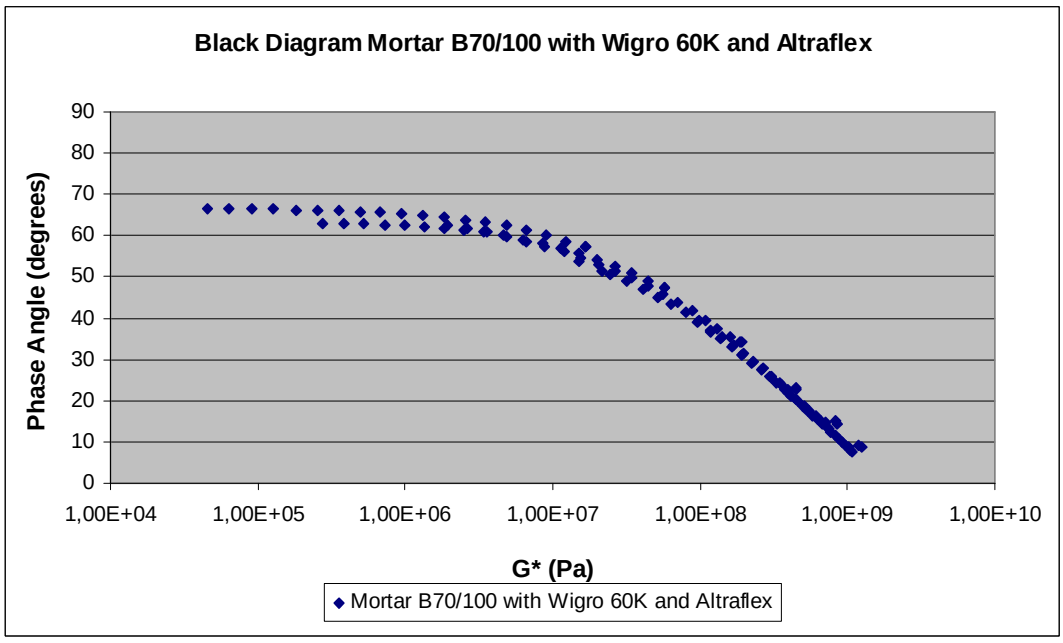


**Graph 4.72:** Black Diagram for Mortar B70/100 with Wigro 60K and Altraflex 2006 aged

#### 4.6.10.4 Mortar B70/100 with filler Wigro and Altraflex 2006

The results of the DSR for Mortar B70/100 with Wigro and 6% Altraflex 2006 aged are presented in graph 4.73 and graph 4.74.

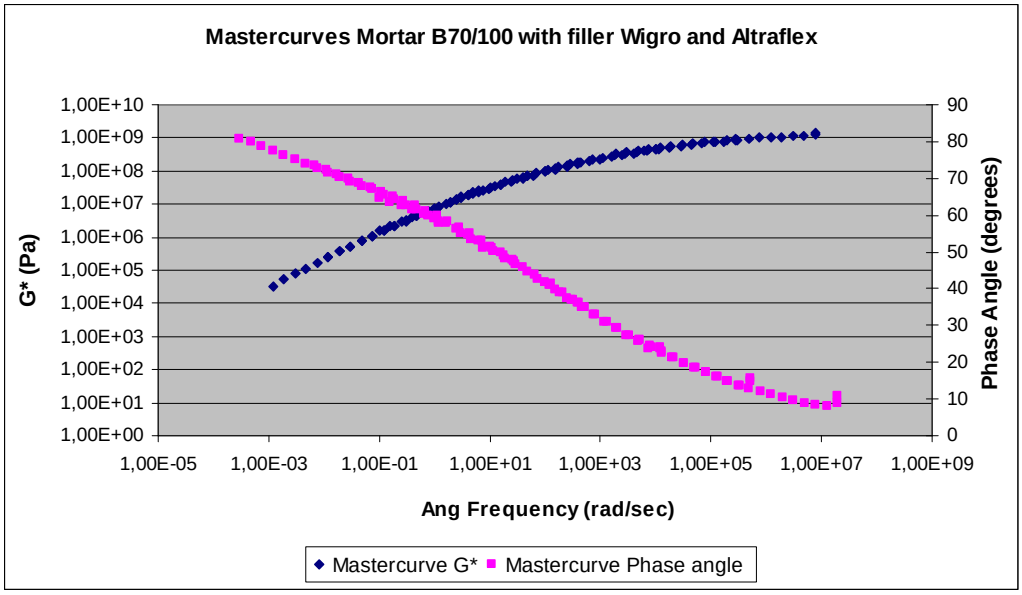


**Graph 4.73:** Mastercurves for G* and δ at 20$^0$C for Mortar B70/100 with Wigro and Altraflex 2006

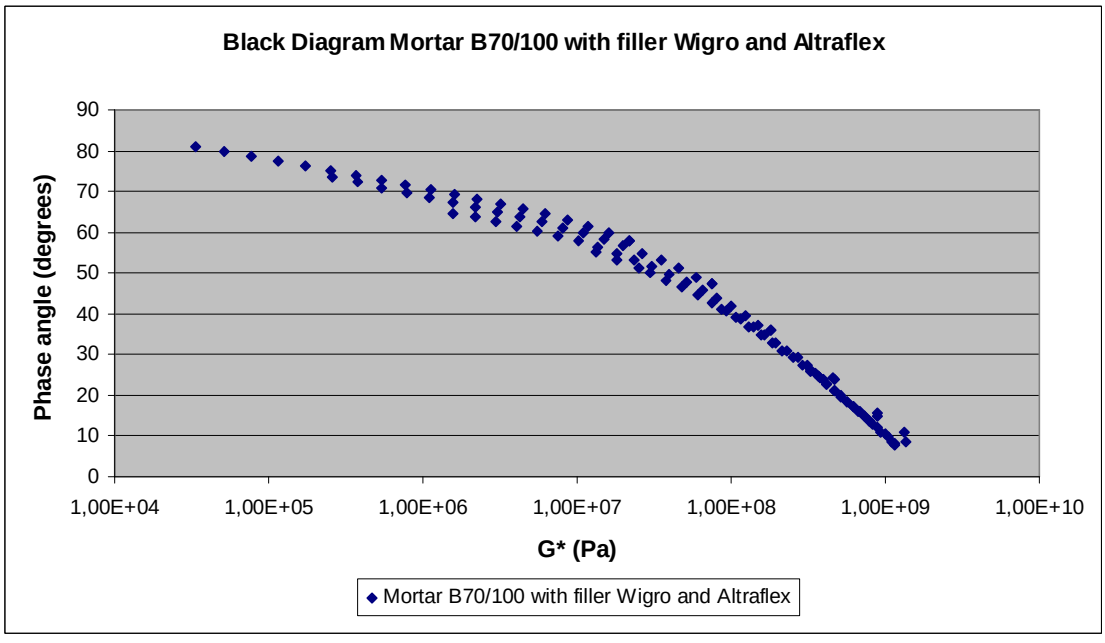


**Graph 4.74:** Black Diagram for Mortar B70/100 with Wigro and Altraflex 2006 aged

4.6.10.5 Comparison of the rheological behavior of aged mortars

The results of the DSR for the four different aged mortars are presented in graph 4.75 and graph 4.76.

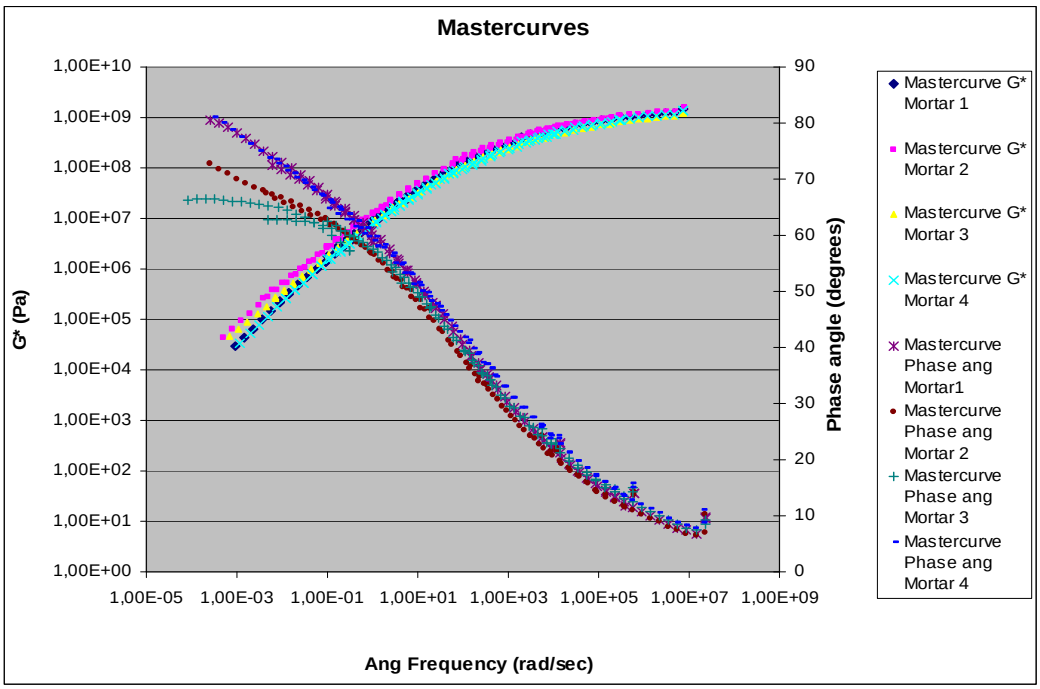


**Graph 4.75**: Mastercurves for G* and δ at 20$^0$C for all mortars

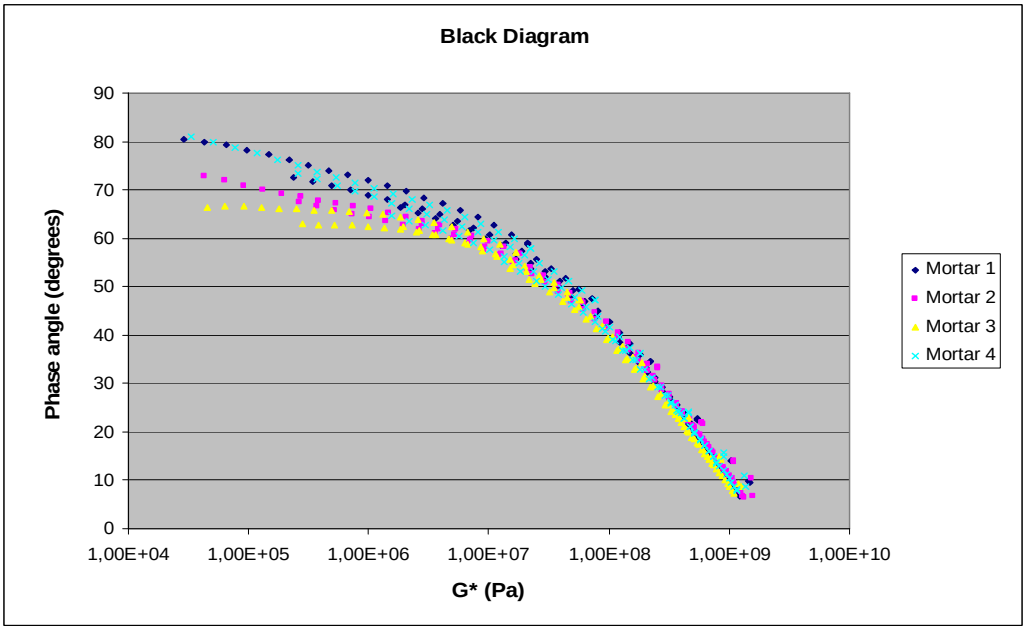


**Graph 4.76:** Black Diagram for all mortars

Mortar 1: B70/100 with Wigro 60K

Mortar 2: B70/100 with Wigro

Mortar 3: B70/100 with Wigro 60K and 6% Altraflex 2006
Mortar 4: B70/100 with Wigro and 6% Altraflex 2006

### 4.6.11 Conclusion

In paragraph 4.6.9 the effect of the fillers on the mortars is shown.
In graph 4.60 we see that the phase angle of mortar 1 ((B70/100 with Wigro 60K) and mortar 4 (B70/100 with Wigro with 6% Altraflex 2006) is almost the same, so is the graph for the G* (Pa).

At low angular frequencies mortar 3 (B70/100 with Wigro 60K and 6% Altraflex 2006) has the lowest phase angle followed by mortar 2 (B70/100 with Wigro) than mortar 1 (B70/100 with Wigro 60K) & mortar 4 (B70/100 with Wigro and 6% Altraflex 2006).
The effect of the filler on the mortar can play an important role, but has not been studied in this report.

## 4.7 Fatigue tests

The Fatigue tests are performed on the four different mortars with the Dynamic Shear Rheometer. The tests were done at $10^0$C and a frequency of 40 Hz. The specimen failure is measured at a constant torque.

### 4.7.1 Mortar B70/100 with Wigro 60K

The results of the fatigue test obtained on the B70/100 with Wigro 60K mortar are presented in the table 4.15a. Graph 4.77 gives a graphical representation of the data while graph 4.78 shows the fatigue data together with the regression line that was derived.
The $N_{Failure}$ is calculated with formula (5).

| Temp | Freq | Specimen radius | Torque | Max τ | Time | N failure |
|---|---|---|---|---|---|---|
| (degr C) | (Hz) | (mm) | (Nmm) | (Mpa) | (sec) | |
| | | | | | | |
| 10 | 40 | 3 | 20 | 0,471809 | 28203,0 | 1128120 |
| 10 | 40 | 3 | 25 | 0,589762 | 29164,0 | 1166560 |
| 10 | 40 | 3 | 30 | 0,707714 | 12510,0 | 500400 |
| 10 | 40 | 3 | 35 | 0,825666 | 3300,0 | 132000 |
| 10 | 40 | 3 | 40 | 0,943619 | 3659,3 | 146370 |
| 10 | 40 | 3 | 45 | 1,061571 | 450,3 | 18012 |
| 10 | 40 | 3 | 50 | 1,179523 | 214,4 | 8576 |

**Table 4.15a:** Mortar B70/100 with Wigro 60K

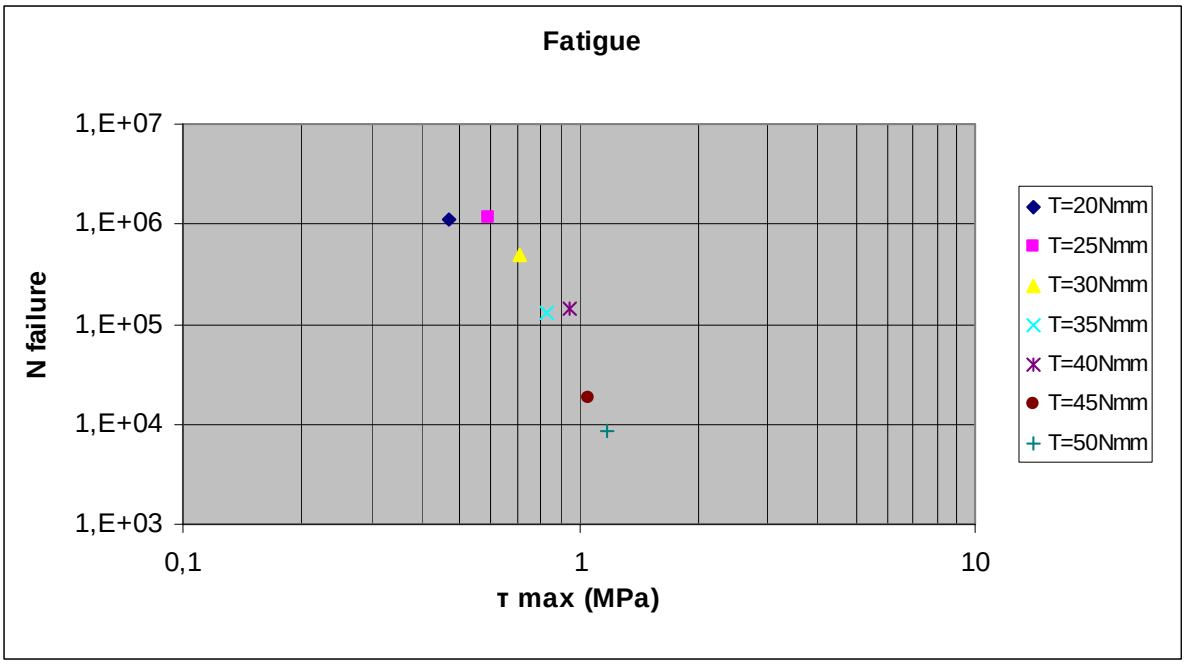


**Graph 4.77:** Fatigue Mortar B70/100 with Wigro 60K

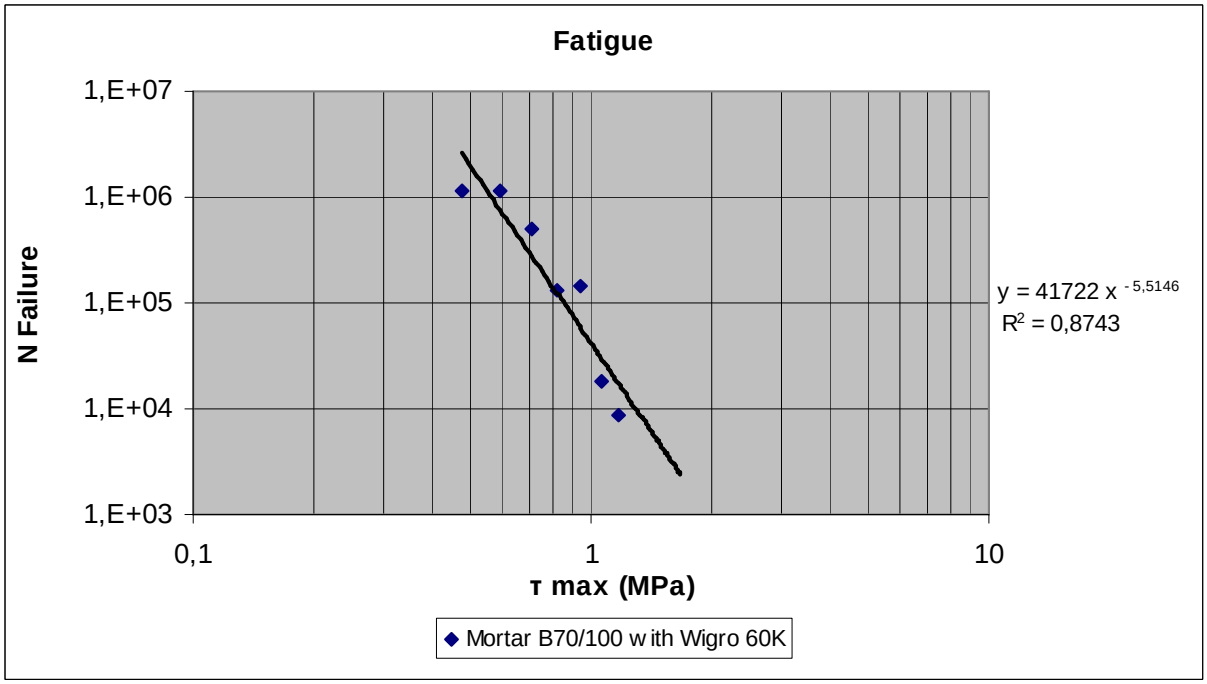


**Graph 4.78**: Fatigue Mortar B70/100 with Wigro 60K

### 4.7.2 Mortar B70/100 with Wigro

The results of the fatigue test obtained on the B70/100 with Wigro mortar are presented in the table 4.15b. Graph 4.79 gives a graphical representation of the data while graph 4.80 shows the fatigue data together with the regression line that was derived. The $N_{Failure}$ is calculated with formula (5).

| Temp | Freq | Specimen radius | Torque | Max τ | Time | N failure |
|---|---|---|---|---|---|---|
| (degr C) | (Hz) | (mm) | (Nmm) | (Mpa) | (sec) | |
| | | | | | | |
| 10 | 40 | 3 | 30 | 0,707714 | 31197,0 | 1247880 |
| 10 | 40 | 3 | 35 | 0,825666 | 5034,0 | 201360 |
| 10 | 40 | 3 | 40 | 0,943619 | 3180 | 127200 |
| 10 | 40 | 3 | 50 | 1,179523 | 381,5 | 15260 |
| 10 | 40 | 3 | 55 | 1,297476 | 530,3 | 21212 |
| 10 | 40 | 3 | 60 | 1,415428 | 224,4 | 8976 |

**Table 4.15b**: Mortar B70/100 with Wigro

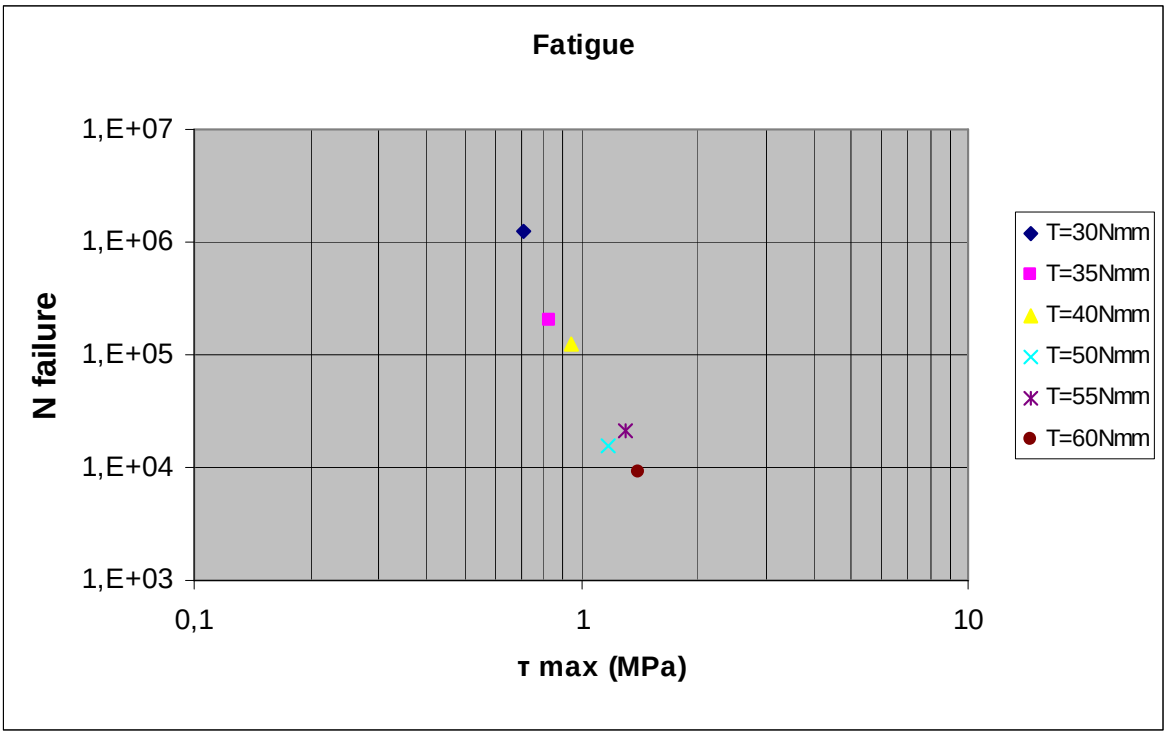


**Graph 4.79**: Fatigue Mortar B70/100 with Wigro

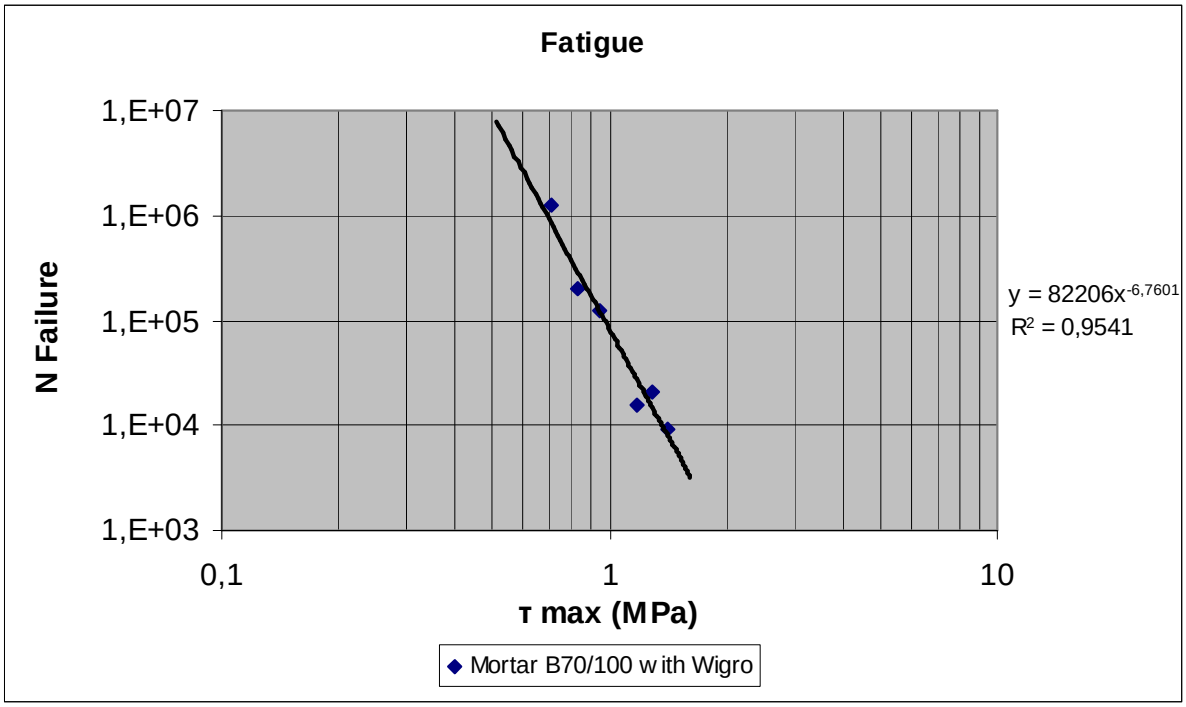


**Graph 4.80**: Fatigue Mortar B70/100 with Wigro

### 4.7.3 Mortar B70/100 with Wigro 60K and Altraflex 2006

The results of the fatigue test obtained on the B70/100 with Wigro 60K and Altraflex 2006 mortar are presented in the table 4.16. Graph 4.81 gives a graphical representation of the data while graph 4.82 shows the fatigue data together with the regression line that was derived. The $N_{Failure}$ is calculated with formula (5).

| **Temp** | **Freq** | **Specimen radius** | **Torque** | **Max τ** | **Time** | **N failure** |
|---|---|---|---|---|---|---|
| (degr C) | (Hz) | (mm) | (Nmm) | (Mpa) | (sec) | |
| | | | | | | |
| 10 | 40 | 3 | 20 | 0,471809 | 97233,0 | 3889320 |
| 10 | 40 | 3 | 22,5 | 0,530786 | 87754,0 | 3510160 |
| 10 | 40 | 3 | 25 | 0,589762 | 26285,0 | 1051400 |
| 10 | 40 | 3 | 30 | 0,707714 | 8680,0 | 347200 |
| 10 | 40 | 3 | 35 | 0,825666 | 3560,0 | 142400 |
| 10 | 40 | 3 | 40 | 0,943619 | 1090,0 | 43600 |
| 10 | 40 | 3 | 50 | 1,179523 | 540,3 | 21612 |
| 10 | 40 | 3 | 60 | 1,415428 | 430,6 | 17224 |

**Table 4.16:** Mortar B70/100 with Wigro 60K and Altraflex 2006

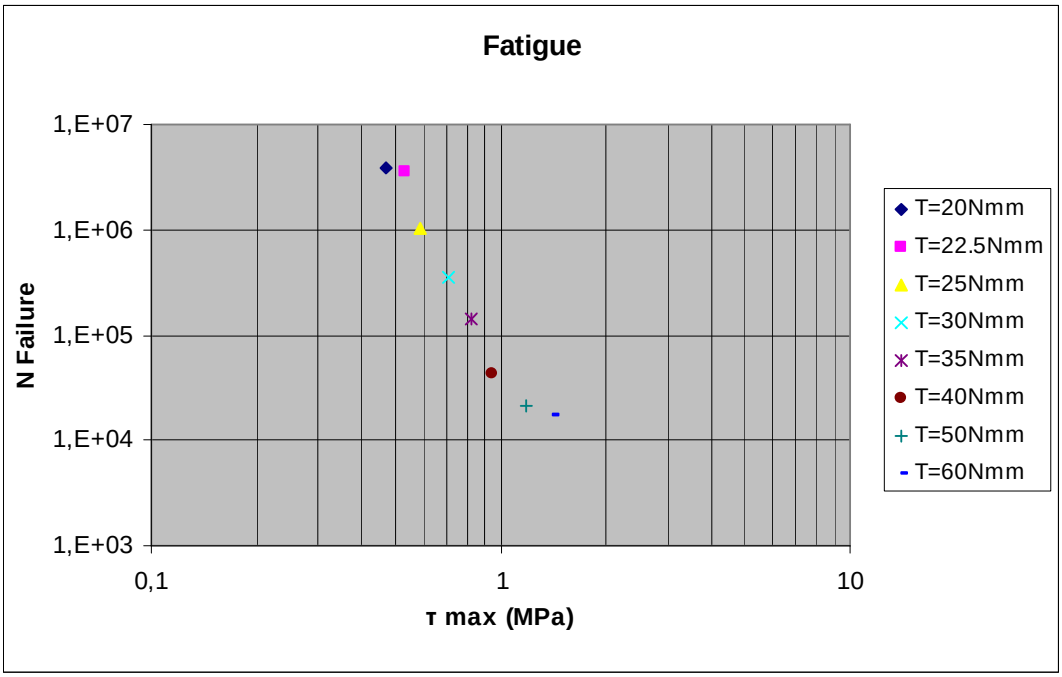


**Graph 4.81**: Fatigue Mortar B70/100 with Wigro 60K and Altraflex 2006

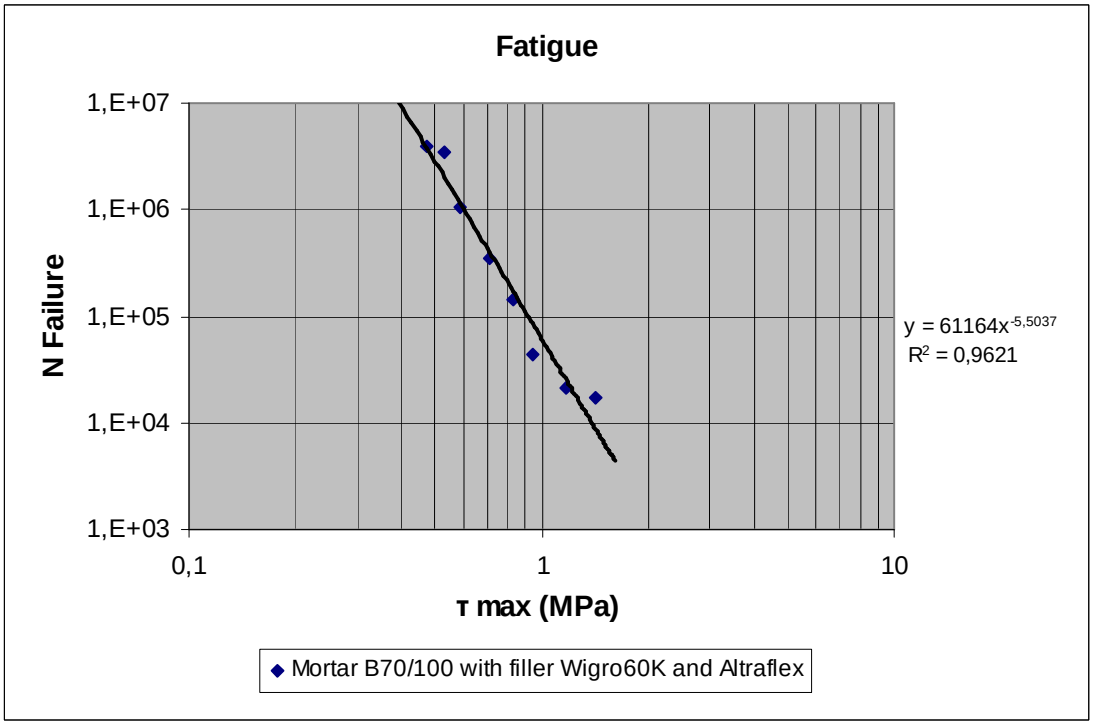


**Graph 4.82**: Fatigue Mortar B70/100 with Wigro 60K and Altraflex 2006

### 4.7.4 Mortar B70/100 with Wigro and Altraflex 2006

The results of the fatigue test obtained on the B70/100 with Wigro and Altraflex 2006 mortar are presented in the table 4.17. Graph 4.83 gives a graphical representation of the data while graph 4.84 shows the fatigue data together with the regression line that was derived. The $N_{Failure}$ is calculated with formula (5).

| **Temp** | **Freq** | **Specimen radius** | **Torque** | **Max τ** | **Time** | **N failure** |
|---|---|---|---|---|---|---|
| (degr C) | (Hz) | (mm) | (Nmm) | (Mpa) | (sec) | |
| | | | | | | |
| 10 | 40 | 3 | 30 | 0,70771408 | 5215,0 | 208600 |
| 10 | 40 | 3 | 32,5 | 0,76669026 | 6649,0 | 265960 |
| 10 | 40 | 3 | 35 | 0,82566643 | 1410,0 | 56400 |
| 10 | 40 | 3 | 40 | 0,94361878 | 630,3 | 25212 |
| 10 | 40 | 3 | 50 | 1,17952347 | 370,8 | 14832 |
| 10 | 40 | 3 | 60 | 1,41542817 | 58,2 | 2327 |

**Table 4.17**: Mortar B70/100 with Wigro and Altraflex 2006

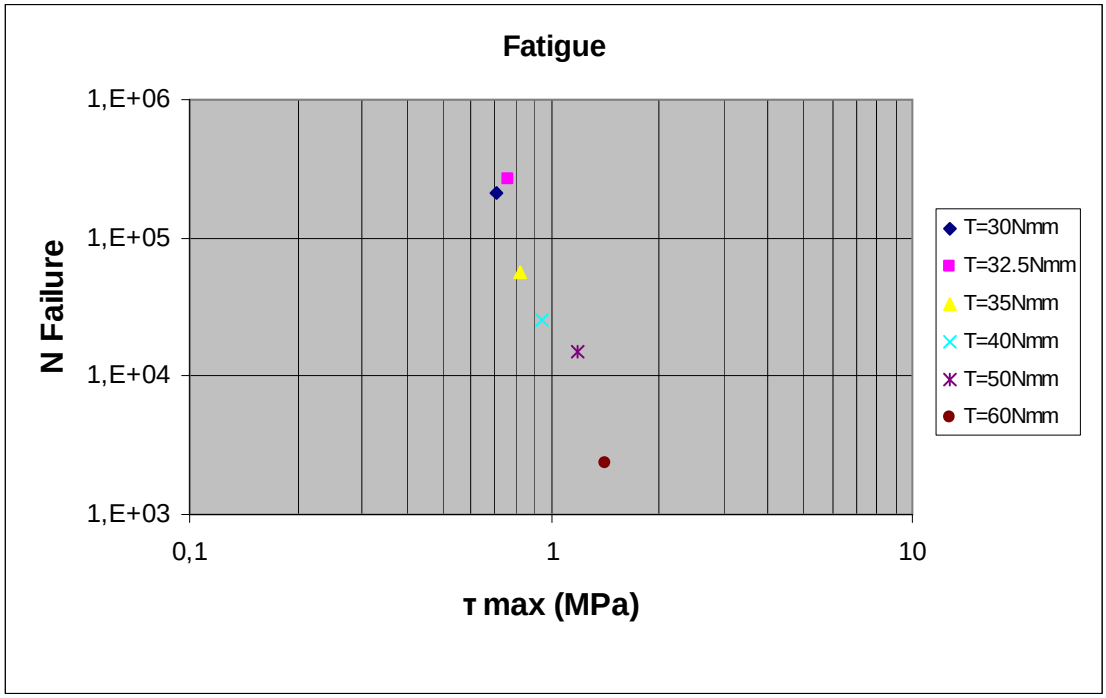


**Graph 4.83:** Fatigue Mortar B70/100 with Wigro and Altraflex 2006

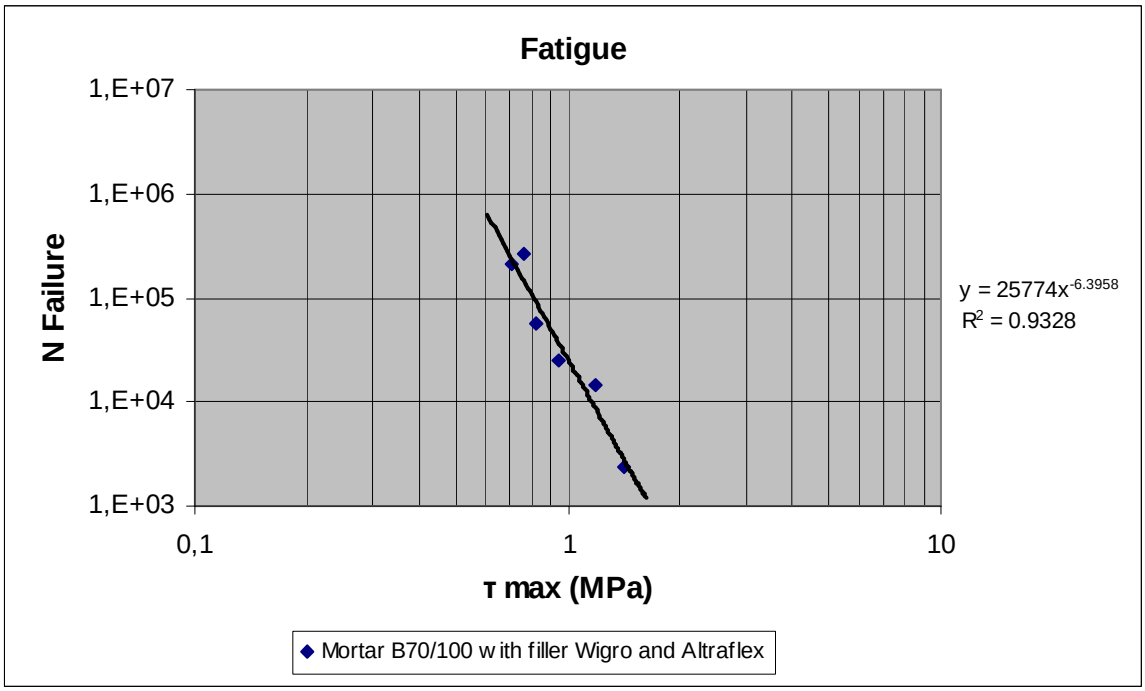


**Graph 4.84**: Fatigue Mortar B70/100 with Wigro and Altraflex 2006

### 4.7.5 Evaluating results

When we put all the results together we get:

| Mortar | function | $R^2$ |
|---|---|---|
| B70/100 with Wigro 60K | $y = 41422\,x^{-5.5146}$ | 0,8743 |
| B70/100 with Wigro | $y = 82206\,x^{-6.7601}$ | 0,9541 |
| B70/100 with Wigro 60K and Altraflex 2006 | $y = 61164\,x^{-5.5037}$ | 0,9621 |
| B70/100 with Wigro and Altraflex 2006 | $y = 25774\,x^{-6.3958}$ | 0,9328 |

**Table 4.18:** Fatigue results

The results of $\tau_{max}$ are given between 0.4 MPa and 2.0 MPa and $N_{failure}$ between $10^3$ and $10^7$

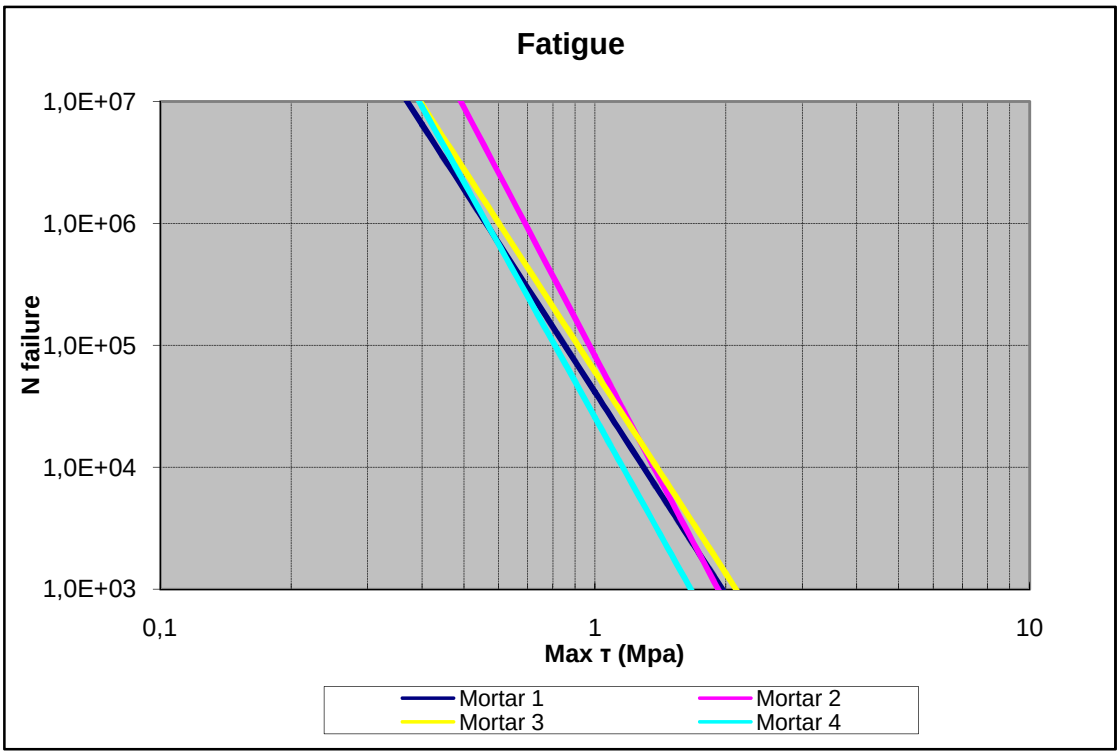


**Graph 4.85**: Fatigue results

Mortar 1: B70/100 with Wigro 60K
Mortar 2: B70/100 with Wigro
Mortar 3: B70/100 with Wigro 60K and 6% Altraflex 2006
Mortar 4: B70/100 with Wigro and 6% Altraflex 2006

The results of $\tau_{max}$ are given between 0.4 MPa and 2.0 MPa and $N_{failure}$ are given in table 4.19

| | N failure | | | |
|---|---|---|---|---|
| $\tau_{max\ (MPa)}$ | Mortar 1 | Mortar 2 | Mortar 3 | Mortar 4 |
| 0.4 | 6.5E+06 | 4.0E+07 | 9.5E+06 | 9.0E+06 |
| 1 | 4.1E+04 | 8.2E+04 | 6.1E+04 | 2.6E+04 |
| 2 | 9.1E+02 | 7.6E+02 | 1.3E+03 | 3.1E+02 |

**Table 4.19**: The results of $\tau_{max}$ are given between 0.4 MPa and 2.0 MPa

### 4.7.6 Discussion

The dissipated energy (W) is calculated for all the mortars at the different torque levels. With formula (6) we calculated the W (J/m$^3$) per cycle (see Appendix 2 for the graphs of the different mortars). If complete area is the $W_{FAT}$. In graph 4.86 the result for mortar 1 is presented. With the relation obtained from this graph the $A_F$ and z are determined. With this information the ψ can be calculated with formula (8), followed by the calculation of $\sigma$ and β and than comparing $\frac{1}{\beta} = \frac{x}{m}$ .The m is the slope of the G* curve at $10^0$ C and 40 Hz.

The results are presented in the tables below the graphs.

The results of mortar 1 can be seen in graph 4.86 and table 4.20:

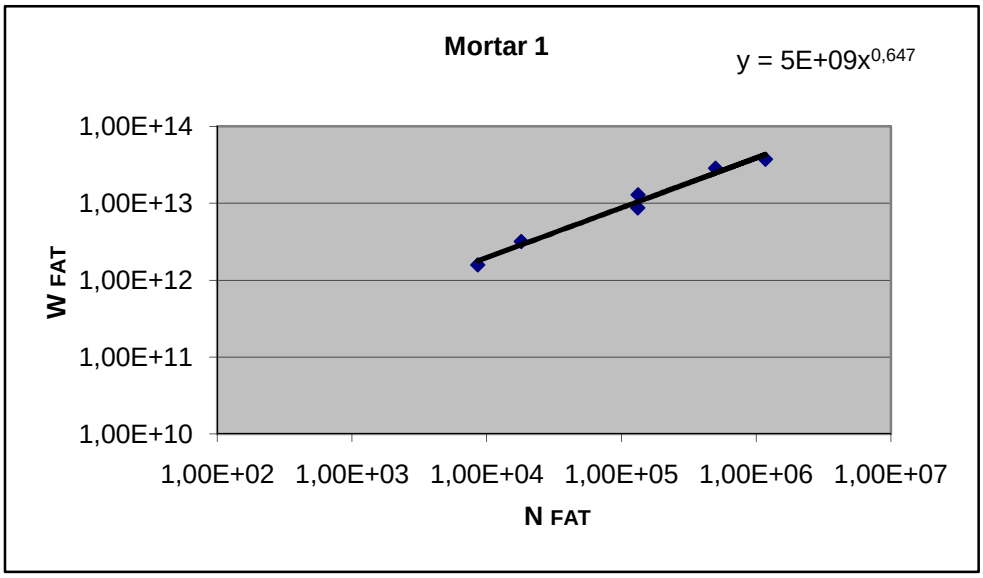


**Graph 4.86:** Dissipated energy for mortar 1

| Torque | Wi | Ni | G sin(delta) | Nf | Wf | Af | z | ψ | α | β | 1/β | m | x |
|---|---|---|---|---|---|---|---|---|---|---|---|---|---|
| (Nmm) | (J/m3) | ( - ) | Pa | ( - ) | (J/m3) | | | | | | | | |
| 50 | 8,30E+07 | 372 | 1,66E+08 | 8,58E+03 | 1,57E+12 | 5,00E+09 | 0,6477 | 0,45 | 2,09 | -0,176 | -5,68 | -0,360 | 2,0 |
| 45 | 8,11E+07 | 373 | 1,38E+08 | 1,80E+04 | 3,17E+12 | 5,00E+09 | 0,6477 | 0,46 | 2,31 | -0,176 | -5,68 | -0,360 | 2,0 |
| 40 | 4,71E+07 | 372 | 1,71E+08 | 1,33E+05 | 1,28E+13 | 5,00E+09 | 0,6477 | 0,49 | 2,13 | -0,176 | -5,68 | -0,360 | 2,0 |
| 35 | 3,18E+07 | 369 | 1,79E+08 | 1,32E+05 | 8,64E+12 | 5,00E+09 | 0,6477 | 0,49 | 2,08 | -0,176 | -5,68 | -0,360 | 2,0 |
| 30 | 3,44E+07 | 372 | 1,32E+08 | 5,00E+05 | 2,84E+13 | 5,00E+09 | 0,6477 | 0,61 | 2,70 | -0,176 | -5,68 | -0,360 | 2,0 |
| 25 | 1,92E+07 | 371 | 1,48E+08 | 1,17E+06 | 3,70E+13 | 5,00E+09 | 0,6477 | 0,61 | 2,56 | -0,176 | -5,68 | -0,360 | 2,0 |
| 20 | 1,24E+04 | 762 | 1,69E+08 | 1,13E+06 | 1,90E+10 | 5,00E+09 | 0,6477 | 0,74 | 2,64 | -0,176 | -5,68 | -0,360 | 2,0 |

**Table 4.20:** Dissipated energy for mortar 1

The results of mortar 2 can be seen in graph 4.87 and table 4.21:

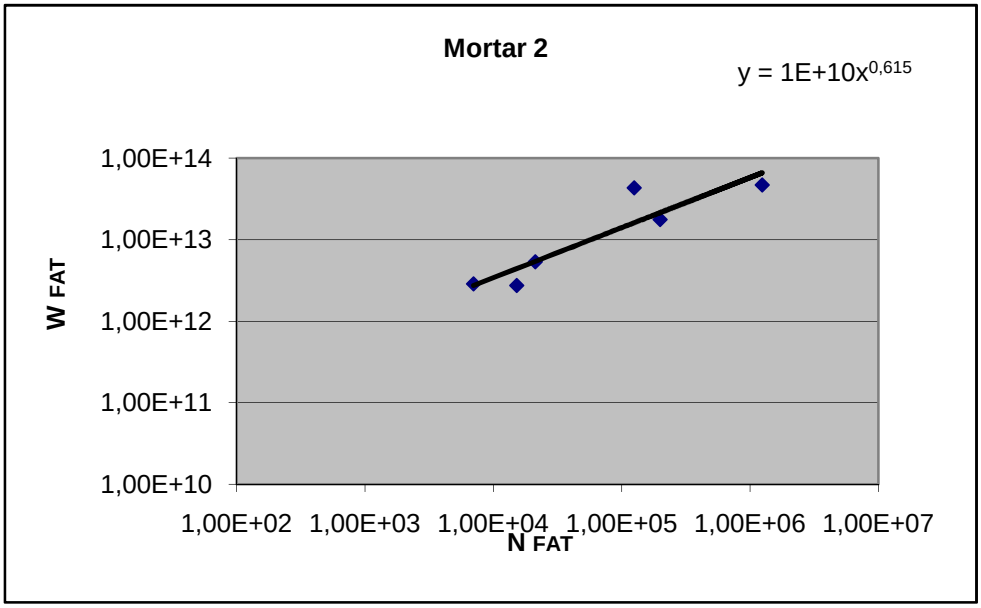


**Graph 4.87:** Dissipated energy for mortar 2.

| Torque | Wi | Ni | G sin(delta) | Nf | Wf | Af | z | ψ | α | β | 1/β | m | x |
|---|---|---|---|---|---|---|---|---|---|---|---|---|---|
| (Nmm) | (J/m3) | ( - ) | Pa | ( - ) | (J/m3) | | | | | | | | |
| 60 | 1,24E+08 | 373,20 | 1,68E+08 | 7,02E+03 | 2,87E+12 | 1,00E+10 | 0,631 | 0,30 | 2,40 | -0,185 | -5,42 | -0,511 | 2,8 |
| 55 | 8,71E+07 | 371,80 | 1,92E+08 | 2,12E+04 | 5,33E+12 | 1,00E+10 | 0,631 | 0,35 | 2,40 | -0,185 | -5,42 | -0,511 | 2,8 |
| 50 | 8,17E+07 | 371,84 | 1,73E+08 | 1,53E+04 | 2,75E+12 | 1,00E+10 | 0,631 | 0,45 | 2,89 | -0,185 | -5,42 | -0,511 | 2,8 |
| 40 | 4,96E+07 | 369,36 | 1,76E+08 | 1,25E+05 | 4,33E+13 | 1,00E+10 | 0,631 | 0,14 | 1,61 | -0,185 | -5,42 | -0,511 | 2,8 |
| 35 | 4,43E+07 | 373,72 | 1,56E+08 | 1,99E+05 | 1,76E+13 | 1,00E+10 | 0,631 | 0,50 | 3,20 | -0,185 | -5,42 | -0,511 | 2,8 |
| 30 | 2,40E+07 | 371,24 | 1,77E+08 | 1,24E+06 | 4,68E+13 | 1,00E+10 | 0,631 | 0,64 | 3,39 | -0,185 | -5,42 | -0,511 | 2,8 |

**Table 4.21:** Dissipated energy for mortar 2

The results of mortar 3 can be seen in graph 4.88 and table 4.22:

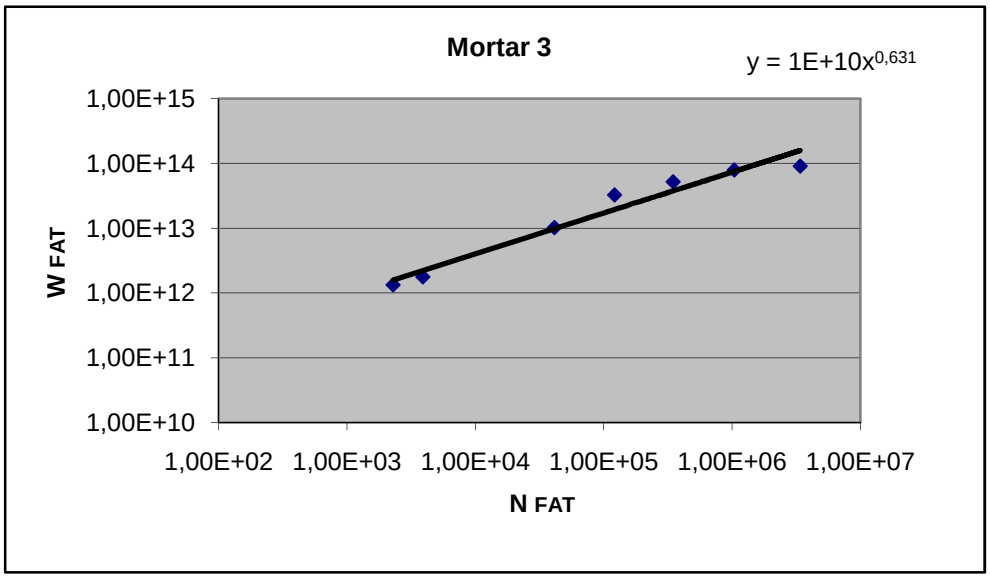


**Graph 4.88:** Dissipated energy for mortar 3.

| Torque | Wi | Ni | G sin(delta) | Nf | Wf | Af | z | ψ | α | β | 1/β | m | x |
|---|---|---|---|---|---|---|---|---|---|---|---|---|---|
| (Nmm) | (J/m3) | ( - ) | Pa | ( - ) | (J/m3) | | | | | | | | |
| 60 | 2,91E+08 | 373,12 | 1,15E+08 | 2,28E+03 | 1,33E+12 | 1,00E+10 | 0,6154 | 0,50 | 3,71 | -0,192 | -5,20 | -0,421 | 2,2 |
| 50 | 1,86E+08 | 372,48 | 1,15E+08 | 3,88E+03 | 1,77E+12 | 1,00E+10 | 0,6154 | 0,41 | 3,36 | -0,192 | -5,20 | -0,421 | 2,2 |
| 40 | 7,70E+07 | 370,00 | 1,38E+08 | 4,12E+04 | 1,02E+13 | 1,00E+10 | 0,6154 | 0,31 | 2,68 | -0,192 | -5,20 | -0,421 | 2,2 |
| 30 | 4,59E+07 | 371,84 | 1,23E+08 | 3,47E+05 | 5,22E+13 | 1,00E+10 | 0,6154 | 0,31 | 2,81 | -0,192 | -5,20 | -0,421 | 2,2 |
| 35 | 6,74E+07 | 373,10 | 1,24E+08 | 1,21E+05 | 3,27E+13 | 1,00E+10 | 0,6154 | 0,25 | 2,53 | -0,192 | -5,20 | -0,421 | 2,2 |
| 25 | 3,07E+07 | 369,40 | 1,24E+08 | 1,04E+06 | 7,94E+13 | 1,00E+10 | 0,6154 | 0,40 | 3,21 | -0,192 | -5,20 | -0,421 | 2,2 |
| 20 | 1,68E+07 | 371,28 | 1,29E+08 | 3,38E+06 | 9,04E+13 | 1,00E+10 | 0,6154 | 0,63 | 3,94 | -0,192 | -5,20 | -0,421 | 2,2 |

**Table 4.22:** Dissipated energy for mortar 3

The results of mortar 4 can be seen in graph 4.89 and table 4.23:

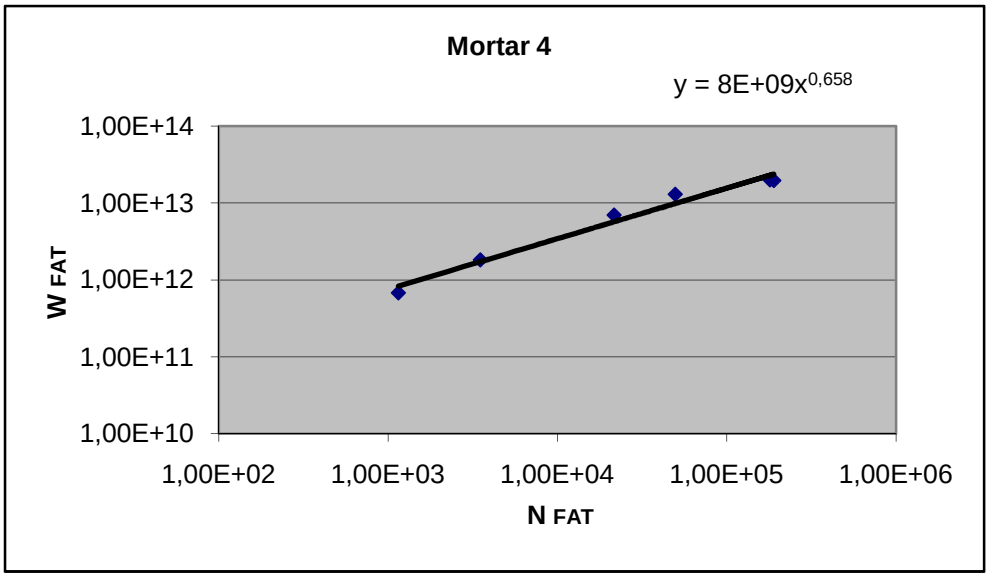


**Graph 4.89:** Dissipated energy for mortar 4.

| Torque | Wi | Ni | G sin(delta) | Nf | Wf | Af | z | ψ | α | β | 1/β | m | x |
|---|---|---|---|---|---|---|---|---|---|---|---|---|---|
| (Nmm) | (J/m3) | ( - ) | Pa | ( - ) | (J/m3) | | | | | | | | |
| 60 | 6,77E+08 | 370,00 | 7,12E+07 | 1,15E+03 | 6,78E+11 | 8,00E+09 | 0,6582 | 1,15 | 6,41 | -0,171 | -5,85 | -0,520 | 3,0 |
| 50 | 2,46E+08 | 370,60 | 1,01E+08 | 3,50E+03 | 1,81E+12 | 8,00E+09 | 0,6582 | 0,48 | 3,47 | -0,171 | -5,85 | -0,520 | 3,0 |
| 40 | 8,99E+07 | 375,00 | 1,36E+08 | 2,16E+04 | 6,95E+12 | 8,00E+09 | 0,6582 | 0,28 | 2,29 | -0,171 | -5,85 | -0,520 | 3,0 |
| 35 | 7,14E+07 | 372,52 | 1,28E+08 | 4,96E+04 | 1,29E+13 | 8,00E+09 | 0,6582 | 0,27 | 2,34 | -0,171 | -5,85 | -0,520 | 3,0 |
| 32,5 | 4,77E+07 | 371 | 1,46E+08 | 1,80E+05 | 2,00E+13 | 8,00E+09 | 0,6582 | 0,43 | 2,74 | -0,171 | -5,85 | -0,520 | 3,0 |
| 30 | 4,45E+07 | 371 | 1,42E+08 | 1,89E+05 | 1,96E+13 | 8,00E+09 | 0,6582 | 0,43 | 2,78 | -0,171 | -5,85 | -0,520 | 3,0 |

**Table 4.23:** Dissipated energy for mortar 4

From the results from the dissipated energy we can see that the lower the torque level the higher the total amount of dissipated energy and on the other hand the higher the torque level the lower the amount of dissipated energy. In the case of determining Nf with the dissipated energy mortar 4 obtains the lowest Nf, which is also the case with the fatigue analysis in graph 4.85 and table 4.19 and mortar 1 obtains the highest Nf.
From table 4.19 we see that at low shear stresses mortar 2 gives the highest Nf and at high shear stresses mortar 3 gives the highest Nf.

### 4.7.7 Conclusion

No clear differences in fatigue behavior between the different mortars can be observed from graph 4.70. This implies that it cannot yet be concluded that adding Altraflex 2006 results into a better fatigue performance.

# 5 DISCUSSION OF ALL THE RESULTS OBTAINED

In the first phase the rheological properties of Altraflex 2006 modified bitumen were investigated.

It is observed that the penetration measurement at $25^0$C increases, as the level of modification gets higher in contrast to penetration measurements done at $40^0$C where it decreases when the level of modification gets higher.
In case 6% of Altraflex 2006 is added to a harder bitumen the penetration is lower compared with adding 6% of Altraflex 2006 into a softer bitumen where it becomes higher at $25^0$C.
When the penetration tests are done at 40 degrees Celsius the penetration gets lower by adding 12% Altraflex 2006 compared to adding 6% Altraflex 2006 to the base bitumen.
Usually the penetration gets higher by adding SBS polymers to the bitumen.

For the penetration tests performed at 25 degrees Celsius the penetration eventually gets higher with larger mixing times for both 6% and 12% Altraflex 2006 added to the base bitumen (B70/100). Contradictory is the case of penetration tests performed at 40 degrees Celsius the penetration gets lower with larger mixing times for both 6% and 12% Altraflex 2006 added to the base bitumen (B70/100).
The mixing time together with the amount of Altraflex 2006 added and the type of bitumen used, have a significant influence on the penetration value.

In general we can say that adding Altraflex 2006 to B70/100 results into higher ring and ball temperatures.
An increased mixing time leads to an increased ring and ball temperature in case we add 6% Altraflex 2006 concentration to the bitumen. In the case of adding 12% Altraflex 2006 concentration to the bitumen the ring and ball temperature first reaches avey high maximum and then decreases a little bit but is much higher than all the other softening points.
The ring and ball temperature decreases when adding 6% Altraflex 2006 concentration to a harder bitumen (B40/60), which is in contrast in the case of a softer bitumen (B70/100), where it increases. In general SBS increases the ring and ball temperature.
The ring and ball temperature seems to be dependent on the amount of Altraflex 2006 added, the mixing time and the type of bitumen used.

PI may normally only be used for unmodified bitumen, but for discussion comparison is made.
Normally the value of PI ranges from around -3 for highly temperature susceptible bitumens to around +7 for highly blown low-temperature susceptible bitumens.
The B70/100 with 6% Altraflex 2006 concentration seem to reduce temperature susceptible, and B70/100 with 12% Altraflex 2006 concentration, shows to be low temperature susceptible. B40/60 with 6% Altraflex 2006 concentration also shows lower temperature susceptibility compared to B40/60.

At microscopic level, the yellow spores which characterize the polymers in the bitumen increases in number as the content of polymer is increased. From the distribution of these

spots we can conclude that the polymer is evenly distributed in the base bitumen in the case of 6% concentration, however for the 12% concentration an uneven pattern starts to develop. To get a well-dispersed structure in the base bitumen seems to be dependent on the amount of Altraflex 2006 added and the mixing time. Still the interpretation of the results is a tricky one.

When we compare the base bitumen with the Altraflex 2006 modified bitumen the complex shear modulus (G*) does not differ a lot. In the low frequency range (< 1Hz) both Altraflex 2006 mixtures have a lower phase angle than the base bitumen indicating that these materials have a higher elastic and less viscous behavior than the base bitumen. In the higher frequency range (> $10^3$ Hz) this is just the other way around.
Based on the high PI values for the B70/100 + 12% Altraflex 2006 samples, it was expected that the G* mastercurve of that material would be much flatter i.e. implying a less temperature (frequency) dependency of G*. This however was not observed.

In the second phase the rheological properties of Altraflex 2006 binders and Altraflex 2006 modified mortars were investigated.

Aged bitumen (B70/100) shows different rheological properties (higher stifnesses and lower phase angle at same (T,f) than unaged bitumen (B70/100) at practical frequencies (between $10^{-2}$ Hz and $10^2$ Hz).

Aged modified bitumen (B70/100 with 6% Altraflex 2006) shows different rheological properties than unaged modified bitumen (B70/100 with 6% Altraflex 2006) at practical frequencies (between $10^{-2}$ Hz and $10^2$ Hz).

The addition of 6% Altraflex 2006 to the bitumen (aged) seems to have no significant effect on the complex shear modulus (G*) and the phase angle δ, at practical frequencies (between $10^{-2}$ Hz and $10^2$ Hz).

The complex shear modulus G* of aged mortar 1 (B70/100 with Wigro 60K) and mortar 2 (B70/100 with Wigro) has no significant distinction.
In the case of the phase angle δ, for mortar 2 (B70/100 with Wigro) the phase angle δ is lower at lower frequencies compared to mortar 1(B70/100 with Wigro 60K), indicating that mortar 2 has higher elastic and less viscous behavior than mortar 1. The difference may be the result of the effect of the fillers on the mortar.

The complex shear modulus G* of aged mortar 3 (B70/100 with Wigro 60K and 6% Altraflex 2006) and mortar 4 (B70/100 with Wigro and Altraflex 2006) shows no significant difference.
In the case of the phase angle δ, for mortar 3 (B70/100 with Wigro 60K and 6% Altraflex 2006) the phase angle δ is lower at lower frequencies compared to mortar 4 (B70/100 with Wigro and 6% Altraflex 2006), indicating that mortar 3 has higher elastic and less viscous behavior than mortar 4.

There is no clear difference in fatigue behavior between the different mortars.

In phase one of this research however only two percentages of Altraflex 2006 are used and investigated and in phase two only one percentage of Altraflex 2006 is used.

# 6 CONCLUSIONS

All the conclusions must be considered to be only based on the modification available at the moment: Altraflex 2006. Also choises were made on mixing, ageing, etc. that could have influenced the results.
The mixing time together with the amount of Altraflex 2006 added and the type of bitumen used, have a significant influence on the penetration value
The ring and ball temperature seems to be dependent on the amount of Altraflex 2006 added, the mixing time and the type of bitumen used.

B70/100 with 12% Altraflex 2006 concentration appears to be low temperature susceptible.

To get a well-dispersed structure in the base bitumen seems to be dependent on the amount of Altraflex 2006 added and the mixing time. Interpretation of the pictures is not easy.

6% Altraflex 2006 addition in the bitumen did not show significant effect on the complex shear modulus (G*) at practical frequencies (between $10^{-2}$ Hz and $10^{2}$ Hz).

Ageing results in different rheological properties for base bitumen (B70/100) and modified bitumen (B70/100 with 6% Altraflex 2006) at practical frequencies (between $10^{-2}$ Hz and $10^{2}$ Hz).

The addition of 6% Altraflex 2006 to the bitumen (aged) did not show significant effect on the complex shear modulus (G*) and the phase angle δ, at practical frequencies (between $10^{-2}$ Hz and $10^{2}$ Hz).

From the DSR tests (to determine the complex shear modulus (G*) and the phase angle δ) it cannot be concluded that the addition of Altraflex 2006 results into an improved performance. However it must be mentioned that the DSR results for 12% Altraflex 2006 are strange compared to other SBS modified bitumen results.

From the fatigue tests it cannot thus far be concluded that adding Altraflex 2006 has a better effect on fatigue.

# 7 RECOMMENDATIONS

The shape and size of the Altraflex 2006 grains could be re-analyzed so the mixing time can be reduced. Smaller particles for instance can lead to more rapidly dissolving of the Altraflex 2006 into the bitumen and results in a reduced mixing time to obtain a suitable dispersion.

The actual contribution of Altraflex 2006 can be seen by comparing results from tests performed with pure SBS.

There could be investigated what the effect of the ageing process (in the PAV and also overall ageing) has on Altraflex 2006. SBS in itself is sensitive to oxidation and Altraflex 2006 includes additives to reduse this sensitivity. From the research it is not clear and more research is needed.

Tests can be performed with other percentages of Altraflex 2006 for better understanding of the rheological behaviour of Altraflex 2006 modified binders and Altraflex 2006 modified mortars.

There can also be research in the performance of harder bitumens with higher percentages of Altraflex 2006.

The effect of fillers in the mortars could also be studied further.

## REFERENCES

1. John Read; David Whiteoak
   The Shell Bitumen Handbook
   Fifth Edition
   London -2003

2. Charles Hendriks
   Materials for Road and Hydraulic Constructions
   Netherlands -2004

3. Molenaar A.A.A.
   Road Materials Part 3: Asphaltic Materials
   Lecture notes CT4850; Faculty of Civil Engineering, Delft University of Technology - September 2005

4. Report 7-07-170-4
   Lifetime Optimization Tool – Sample preparation and laboratory testing for the LOT Research Program
   Faculty of Civil Engineering, Delft University of Technology

5. Molenaar A.A.A.
   Structural Design of Pavements
   Part 3: Design of Flexible Pavements
   Lecture notes CT4860; Faculty of Civil Engineering, Delft University of Technology - January 2006

6. Molenaar A.A.A.
   Design of Flexible Pavements
   Faculty of Civil Engineering, Delft University of Technology - March 2007

7. Asfalt in de wegen - en waterbouw
   Vereniging tot Bevordering van Werken in Asfalt
   Breukelen, november 2000

8. NEN-EN 1426
   Bitumen and bituminous binders
   Determination of needle penetration

9. NEN-EN 1427
   Bitumen and bituminous binders
   Determination of softening point - Ring and ball method

10. NEN-EN 13632
Visualization of the polymer dispersion in polymer modified bitumen.

11. NEN-EN 1427
Bitumen and bituminous binders
Determination of complex shear modulus and phase angle
Dynamic Shear Rheometer (DSR)

12. NEN-EN 14769
Bitumen and bituminous binders
Accelerated long-term ageing conditioning by a Pressurised Aging Vessel (PAV)

13. NEN-EN 14023
Bitumen and bituminous binders
Framework specification for polymer modified bitumens

14. ASTM D6521
Accelerated Aging of Asphalt Binder using a Pressurised Aging Vessel (PAV)

15. ASTM D7175
Bitumen and bituminous binders
Determining the rheological properties of asphalt binder using a Dynamic Shear Rheometer (DSR)

16. ASTM D5
Penetration of Bituminous Materials

17. ASTM D36
Softening Point of Bitumen (Ring-and-Ball Apparatus)

18. Freddy L. Roberts; Prithvi S. Kandhal; E. Ray Brown;Dah-Yinn Lee; Thomas W. Kennedy
Hot mix Asphalt Materials
Mixture Design and Construction, second edition 1996
NAPA Education Foundation, Linham, Maryland

19. E.J. Scholten
Durability of thin noise reducing surface courses
M.Sc. Thesis - Faculty of Civil Engineering, Delft University of Technology- May 2003

20. E.T.Hagos
Characterisation of Polymer Modified Bitumen

M.Sc. Thesis - IHE Delft - March 2002

21. Young R.J. & Lovell P.A.
Introduction to Polymers
Second edition, London, 1991

# Appendix 1

Shell bitumen data test Chart

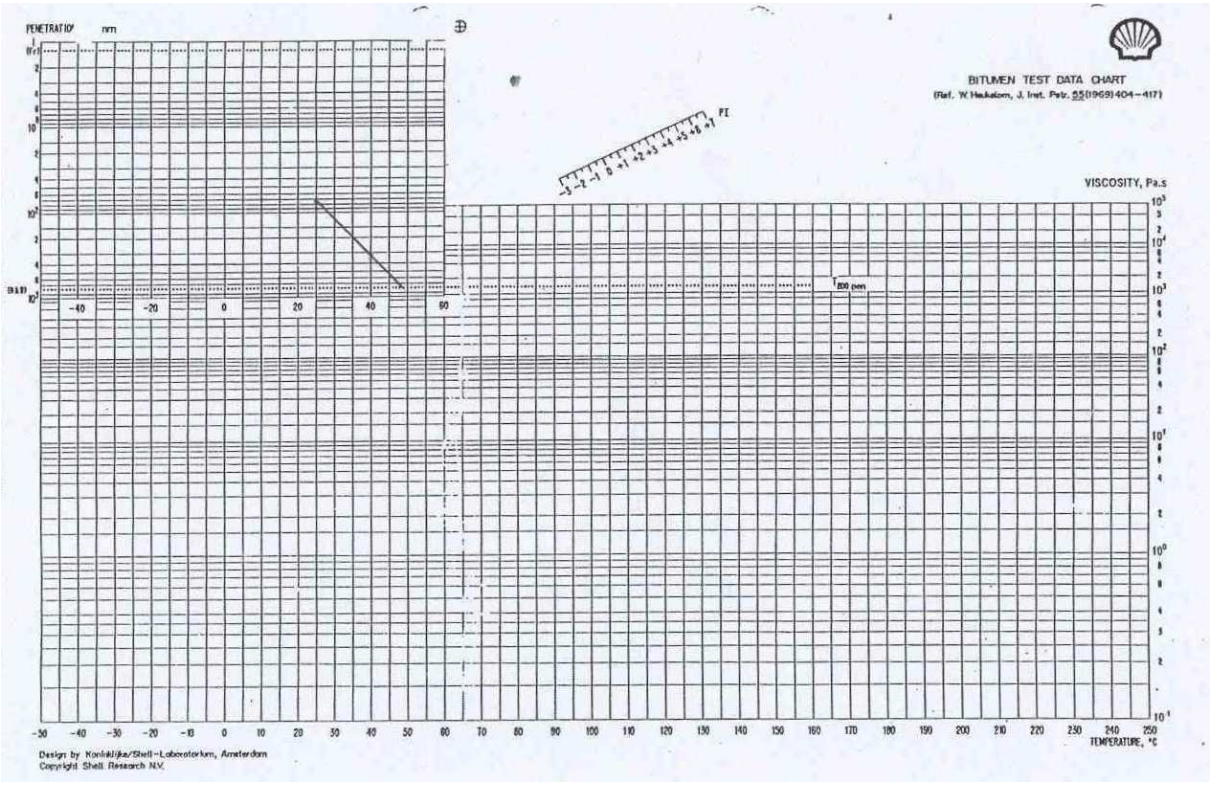


**Figure 1.1:** Shell bitumen test data chart for B70/100

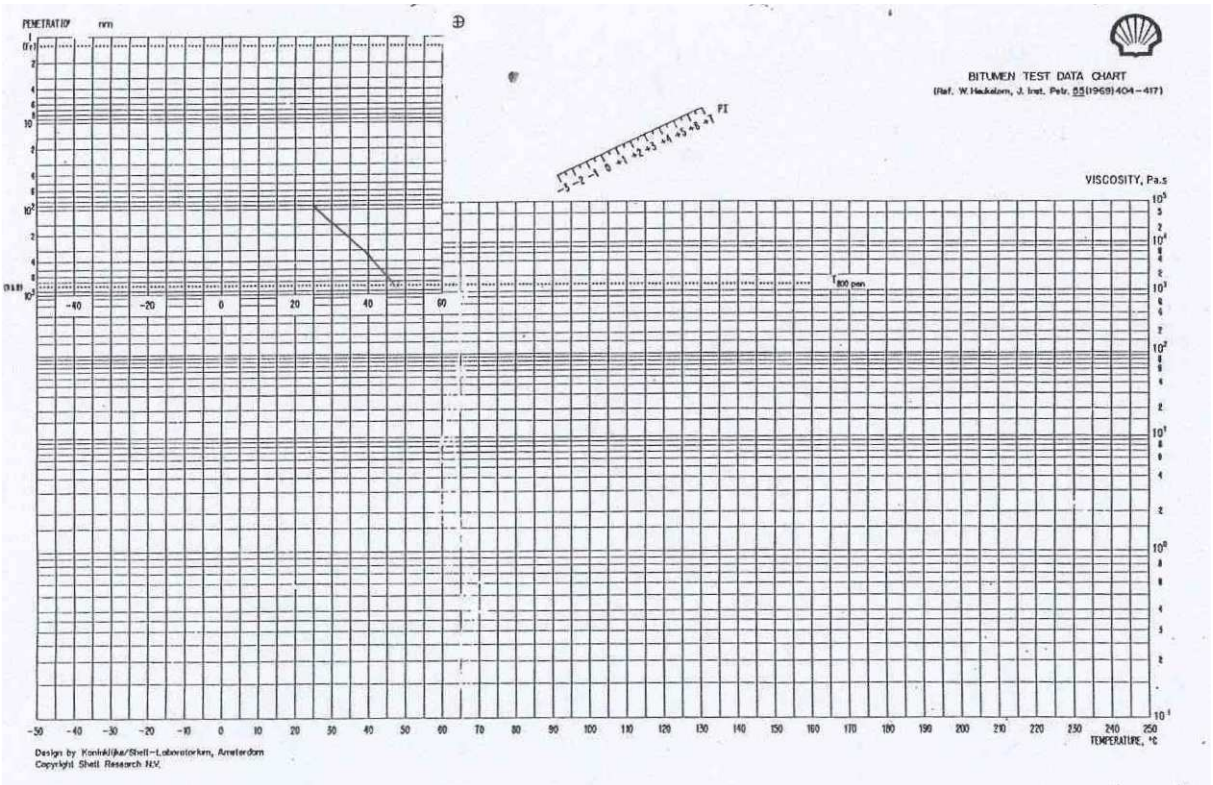


**Figure 1.2:** Shell bitumen test data chart for B70/100 with 6% Altraflex

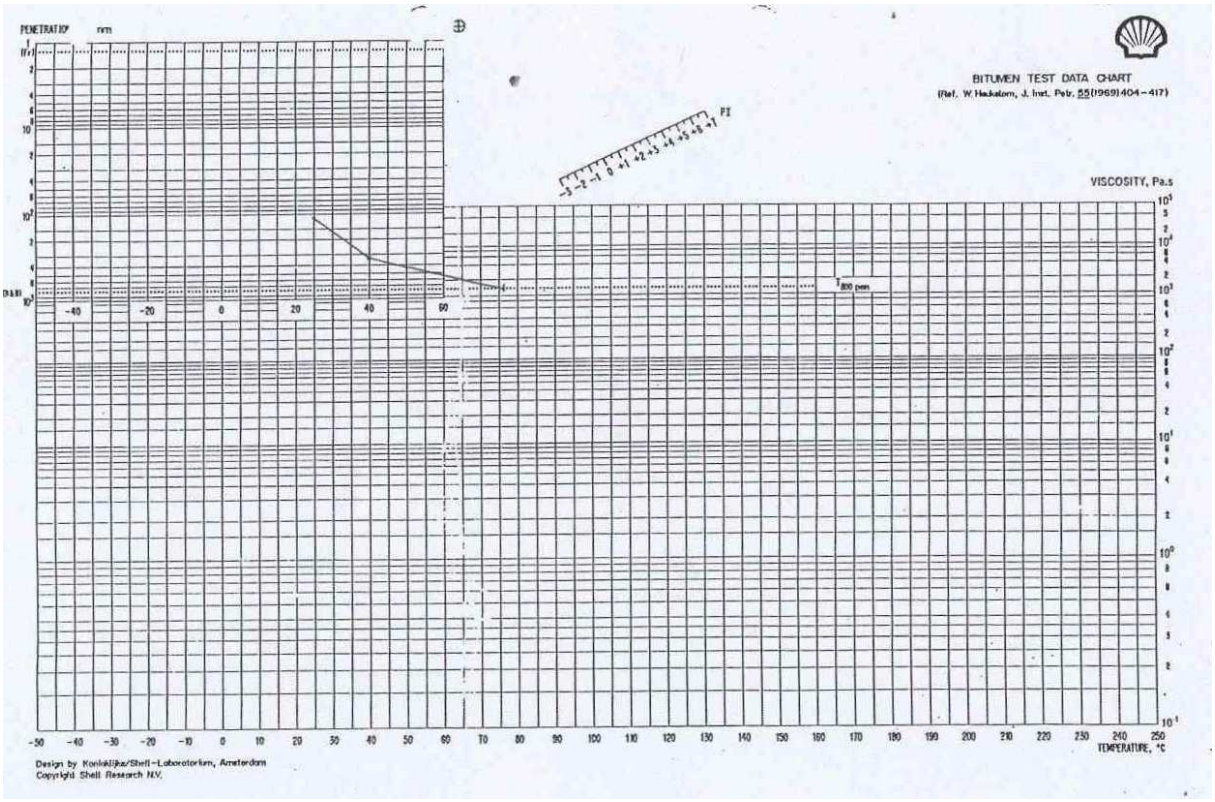


**Figure 1.3:** Shell bitumen test data chart for B70/100 with 12% Altraflex

# Appendix 2

## Mortar1

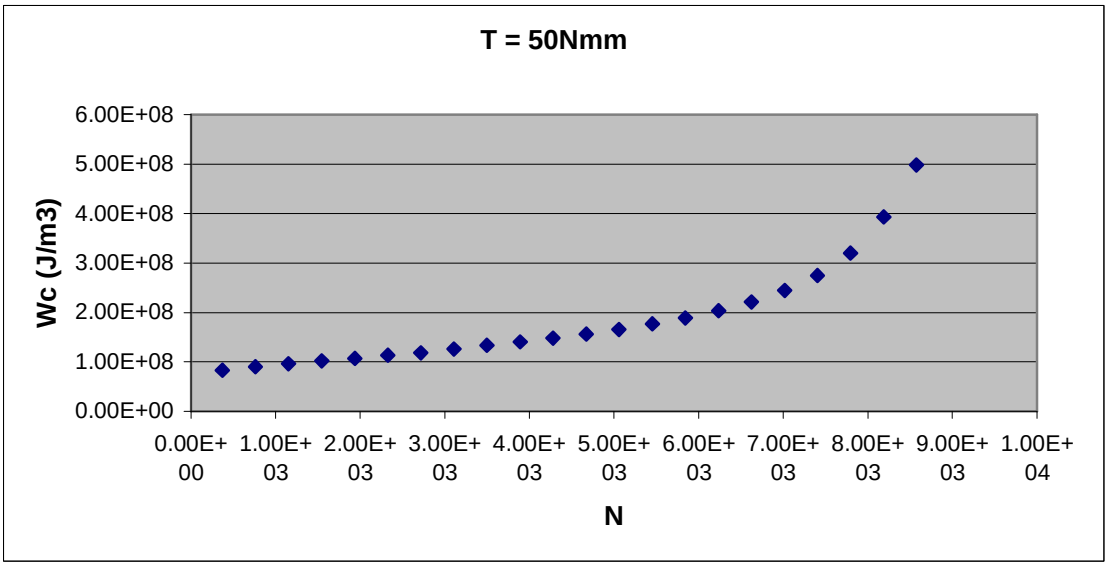


**Graph A2.1:** Dissipated energy for mortar 1, T = 50 Nmm

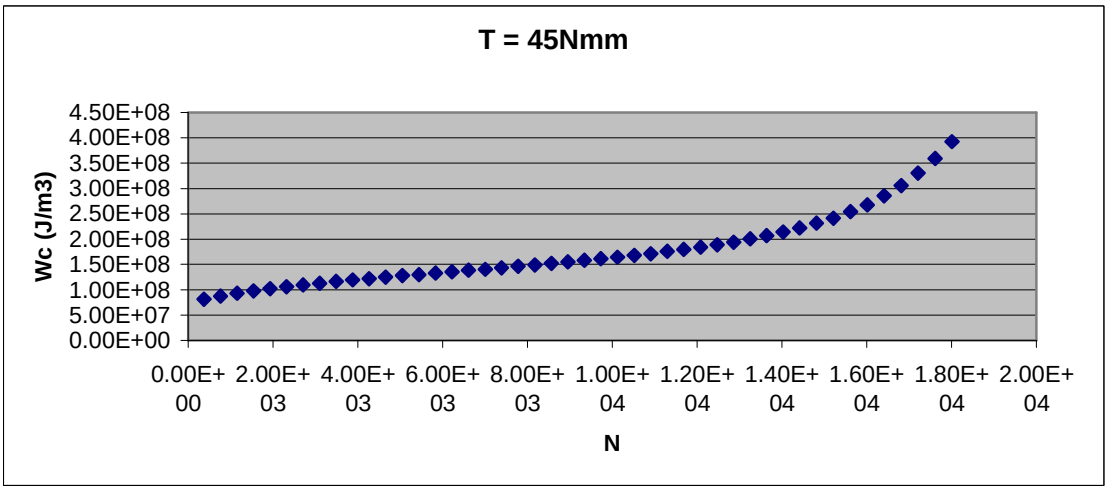


**Graph A2.2:** Dissipated energy for mortar, T = 45 Nmm

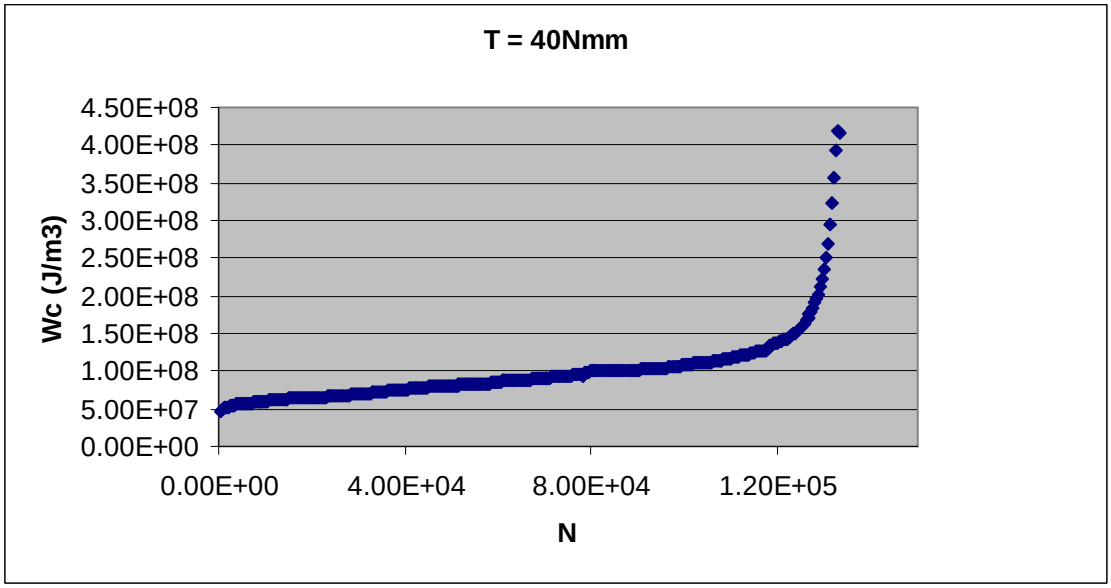


**Graph A2.3:** Dissipated energy for mortar 1 , T = 40 Nmm

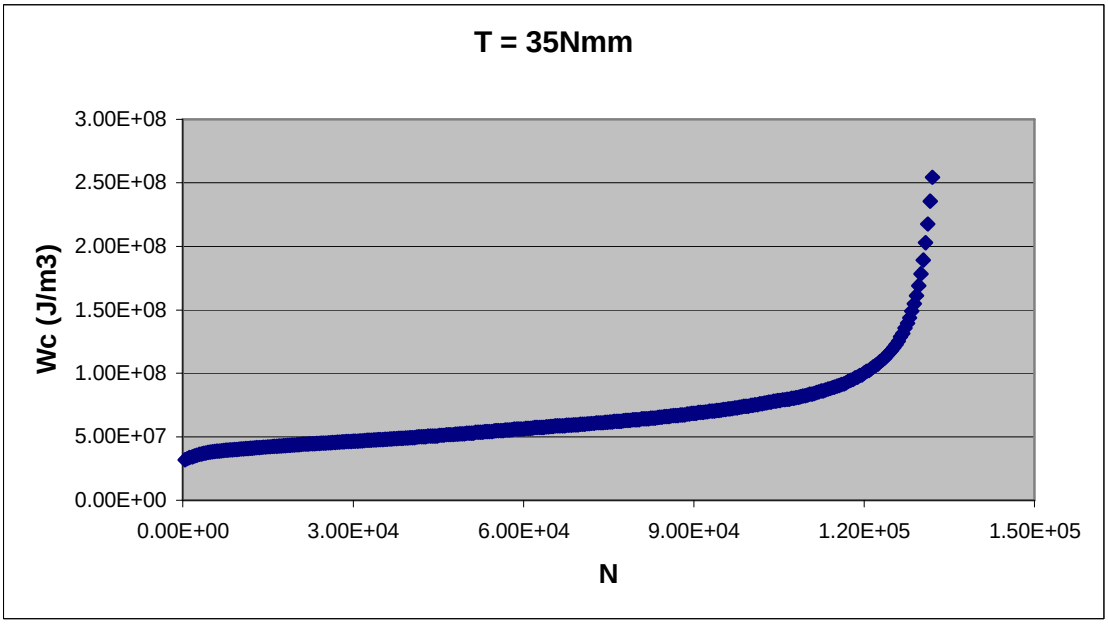


**Graph A2.4:** Dissipated energy for mortar 1, T = 35 Nmm

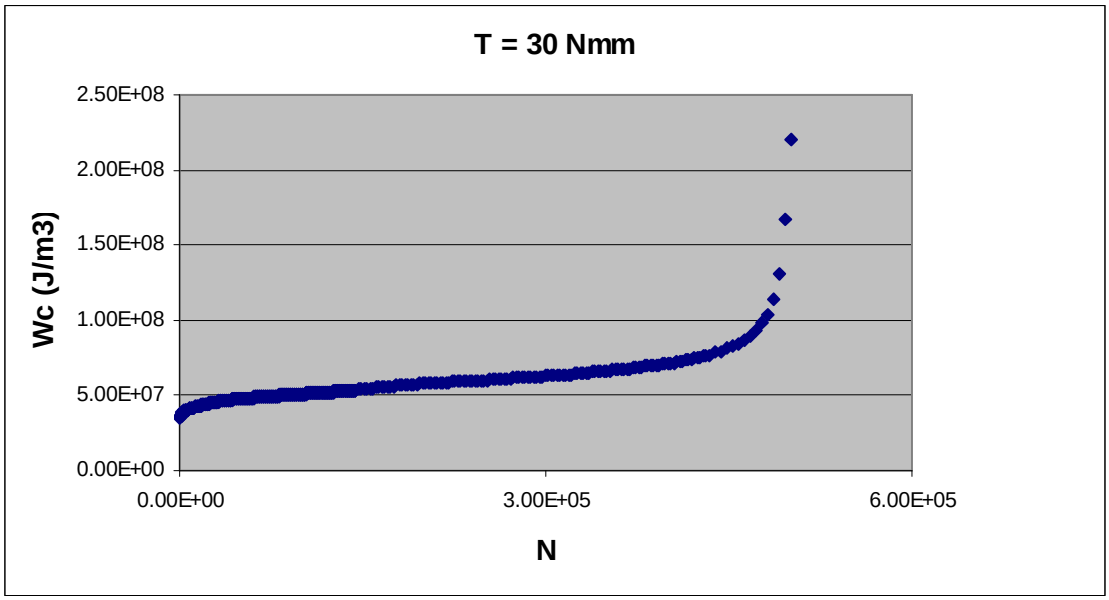


**Graph A2.5:** Dissipated energy for mortar 1, T = 30 Nmm

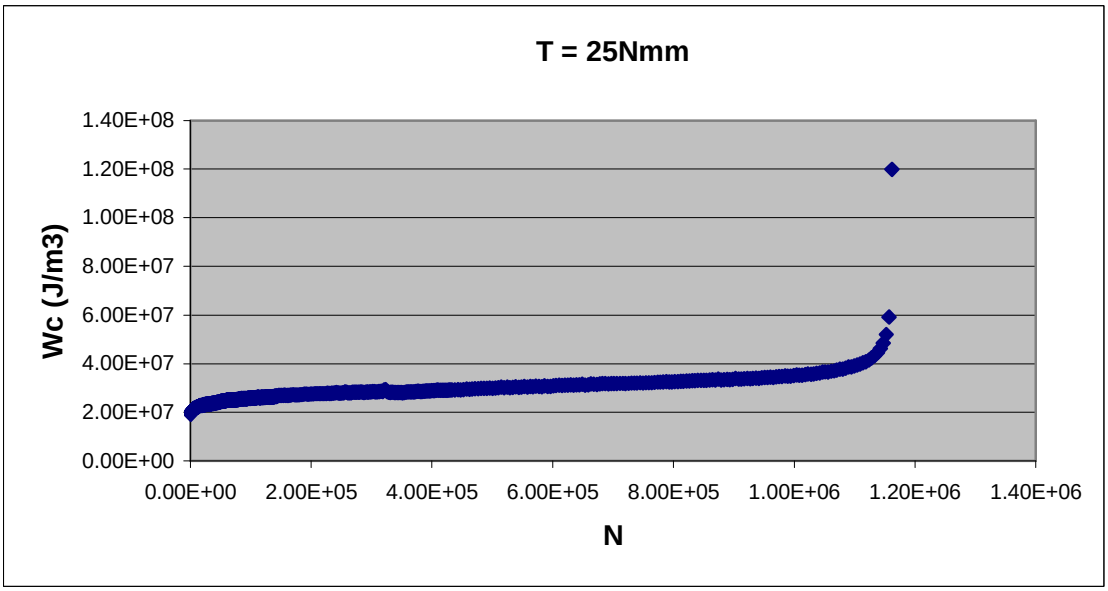


**Graph A2.6:** Dissipated energy for mortar 1, T = 25 Nmm

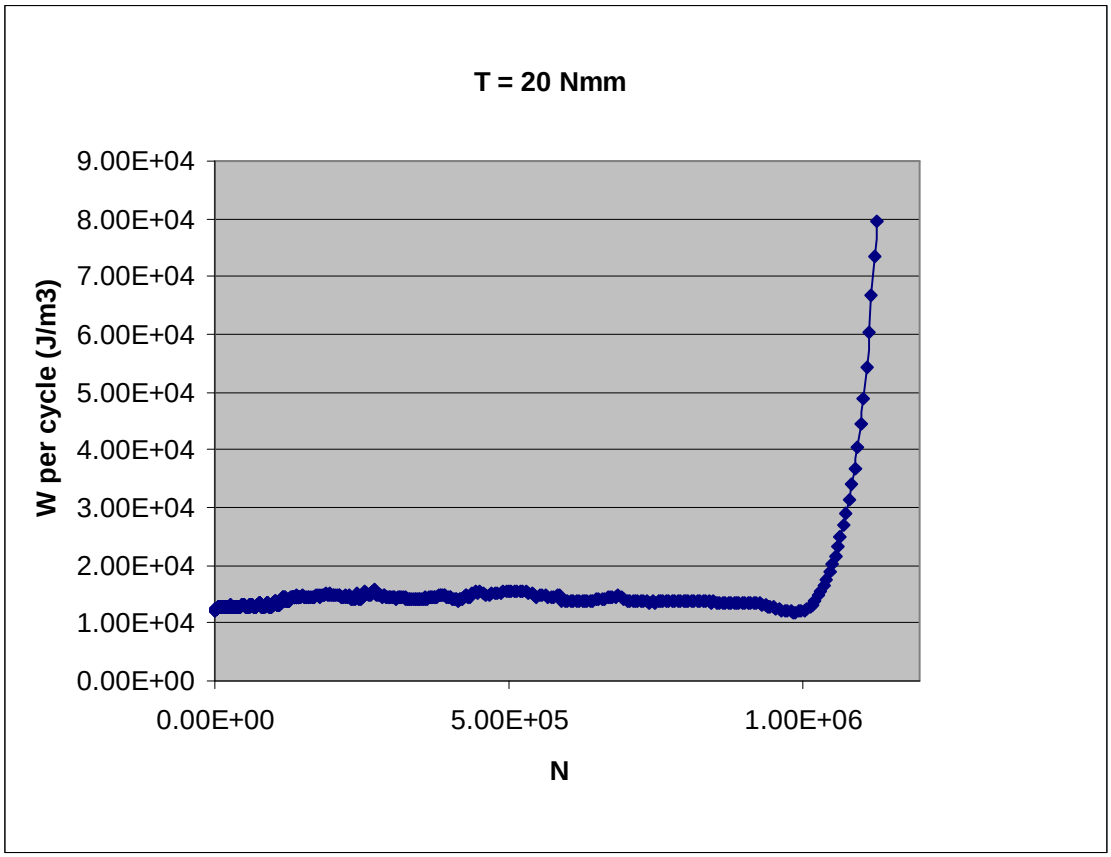


**Graph A2.6:** Dissipated energy for mortar 1, T = 20 Nmm

## Mortar 2

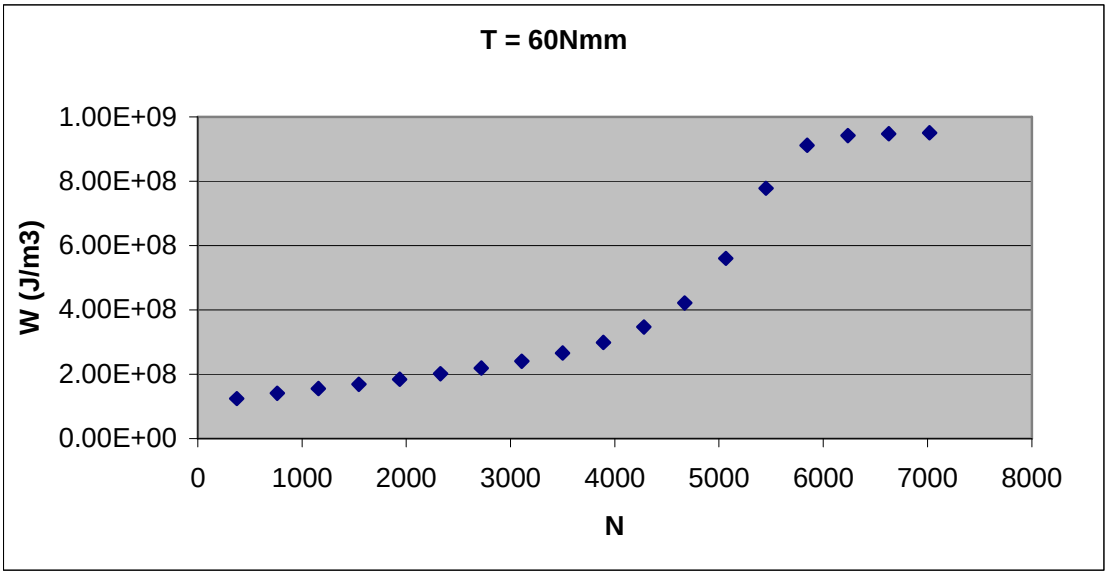


**Graph A2.7:** Dissipated energy for mortar 2, T = 60 Nmm

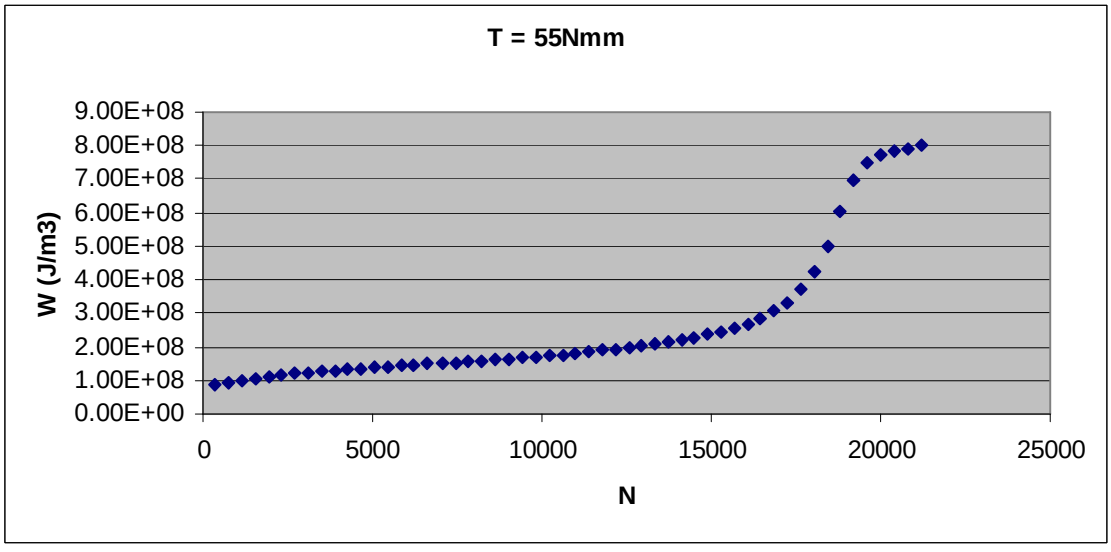


**Graph A2.7:** Dissipated energy for mortar 2, T = 55 Nmm

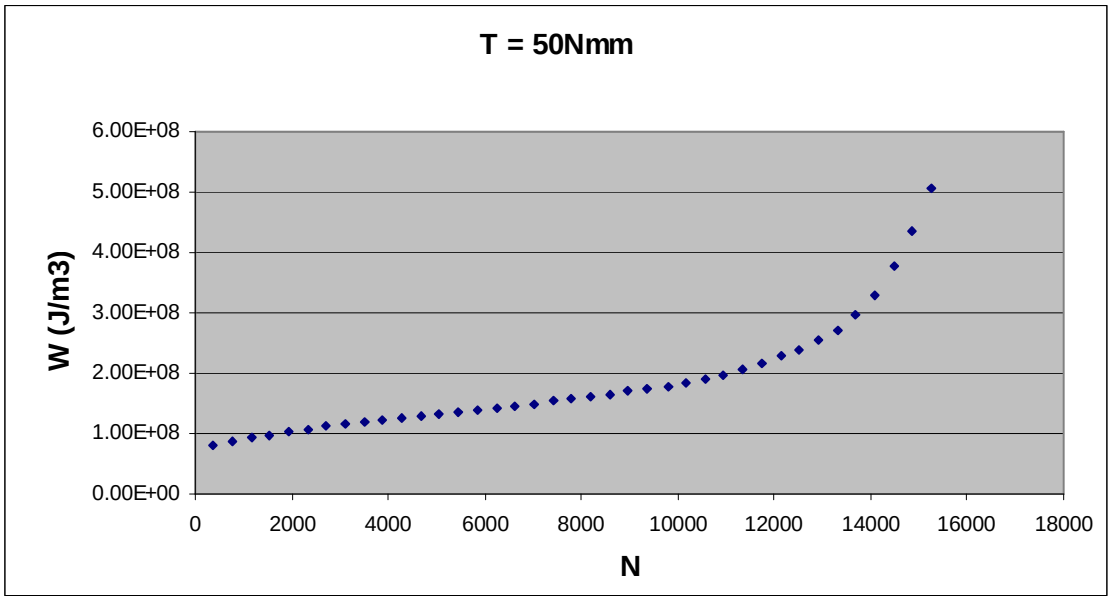


**Graph A2.7:** Dissipated energy for mortar 2, T = 50 Nmm

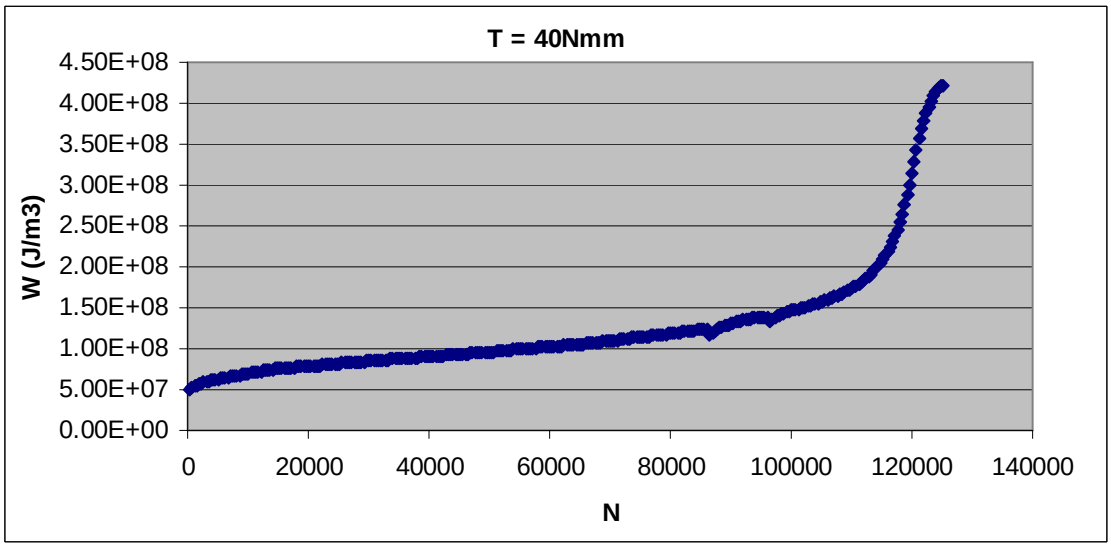


**Graph A2.8:** Dissipated energy for mortar 2, T = 40 Nmm

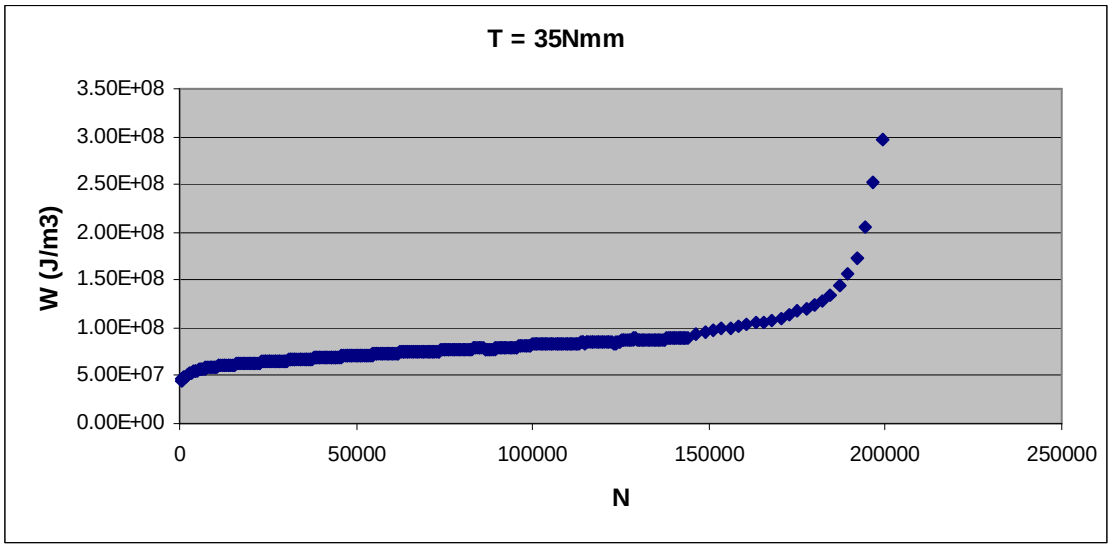


**Graph A2.9:** Dissipated energy for mortar 2, T = 35 Nmm

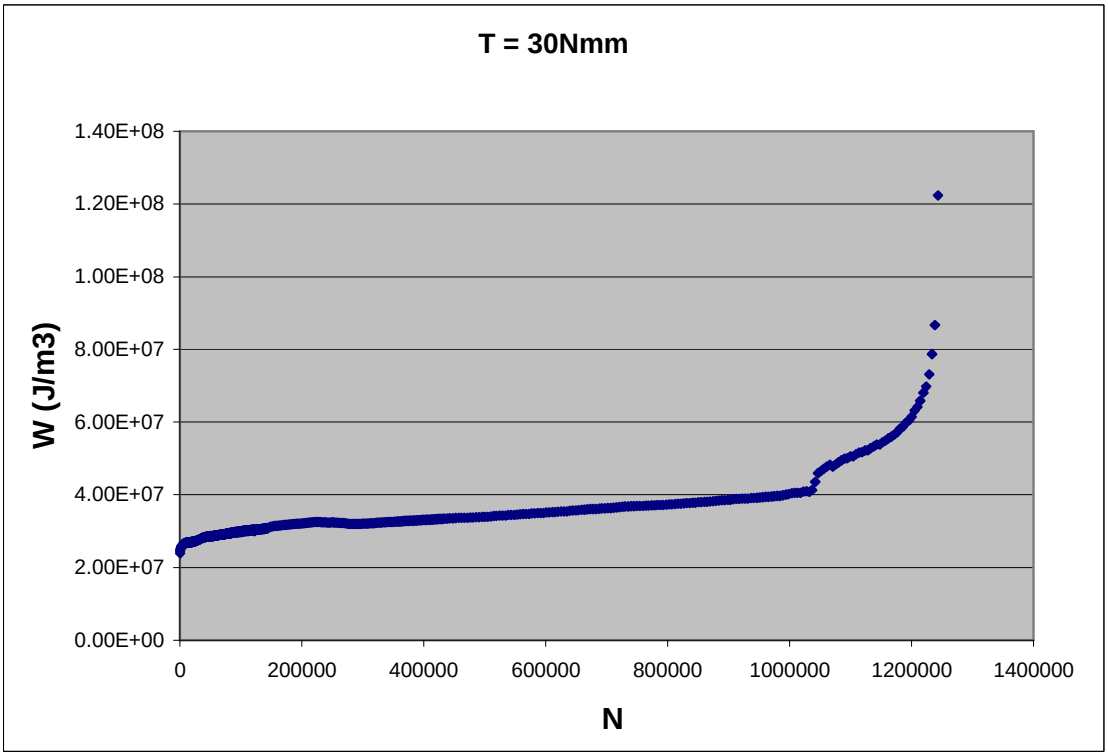


**Graph A2.10:** Dissipated energy for mortar 2, T = 30 Nmm

# Mortar 3

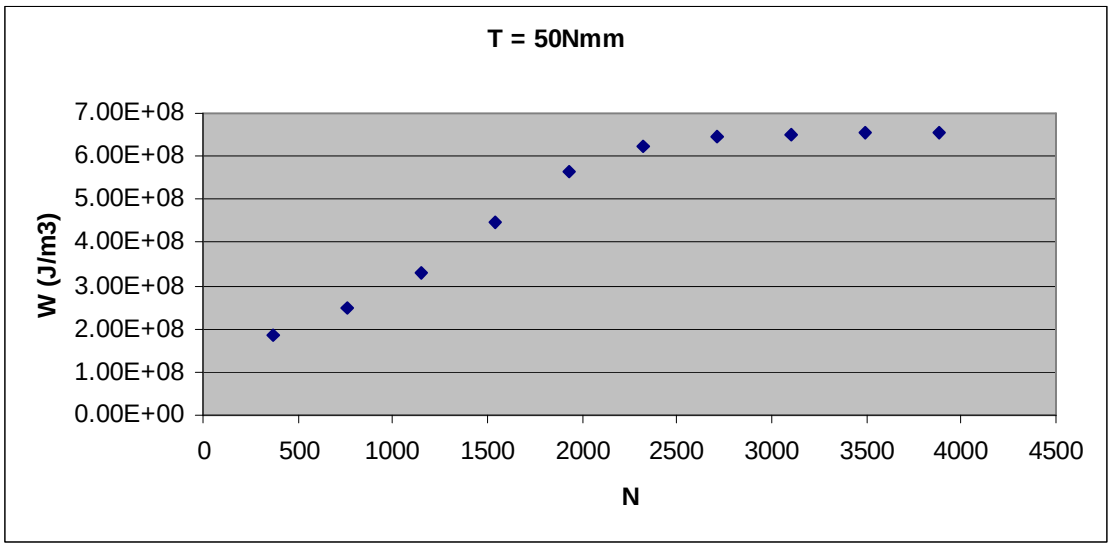


**Graph A2.11:** Dissipated energy for mortar 3, T = 50 Nmm

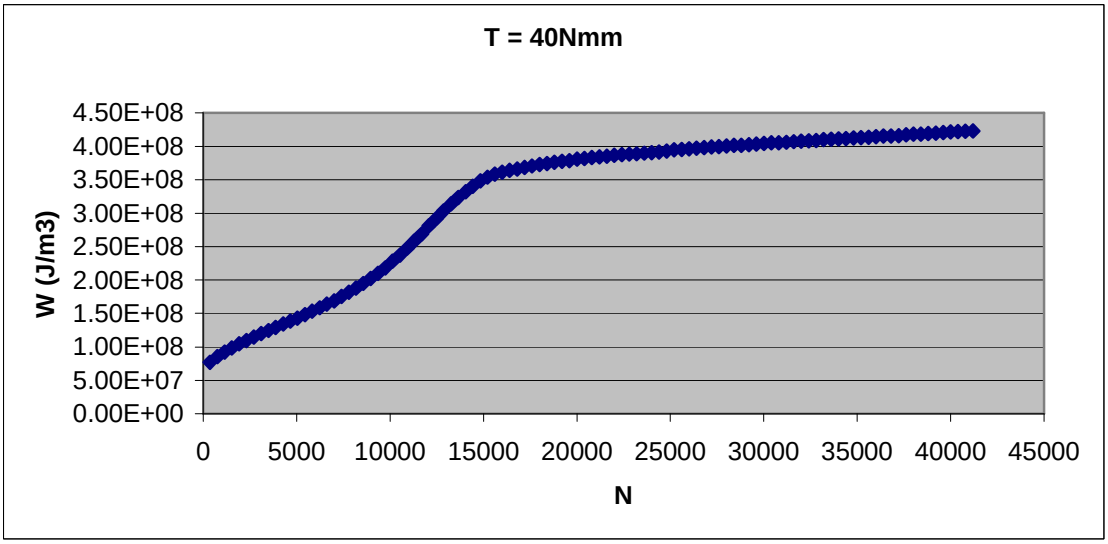


**Graph A2.12:** Dissipated energy for mortar 3, T = 40 Nmm

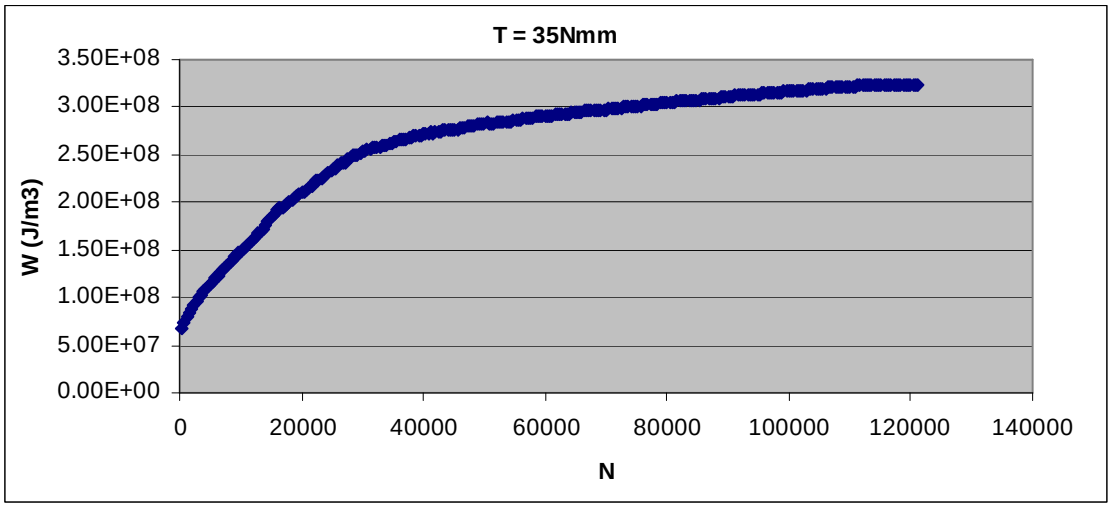


**Graph A2.12:** Dissipated energy for mortar 3, T = 35 Nmm

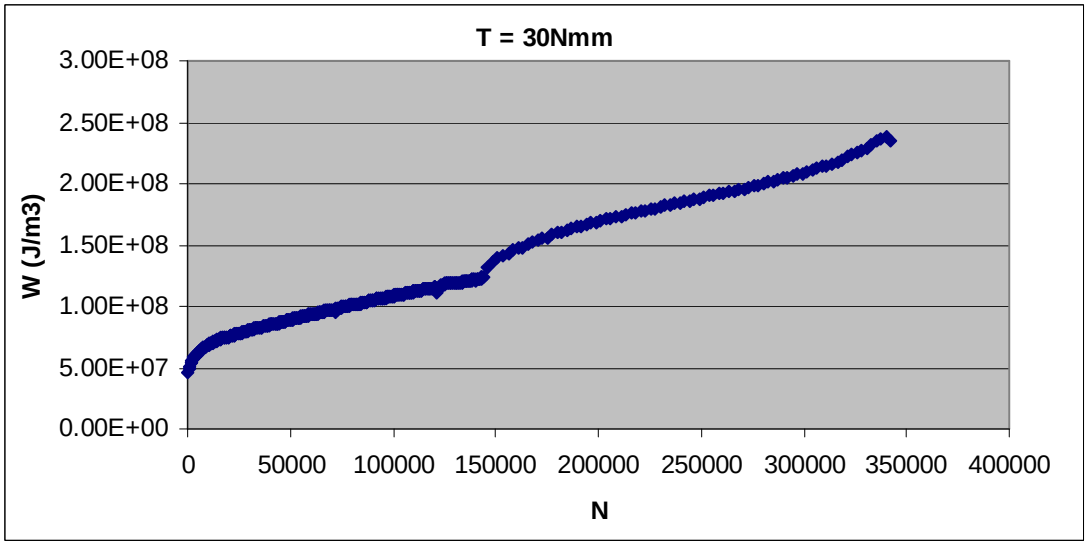


**Graph A2.13:** Dissipated energy for mortar 3, T = 30 Nmm

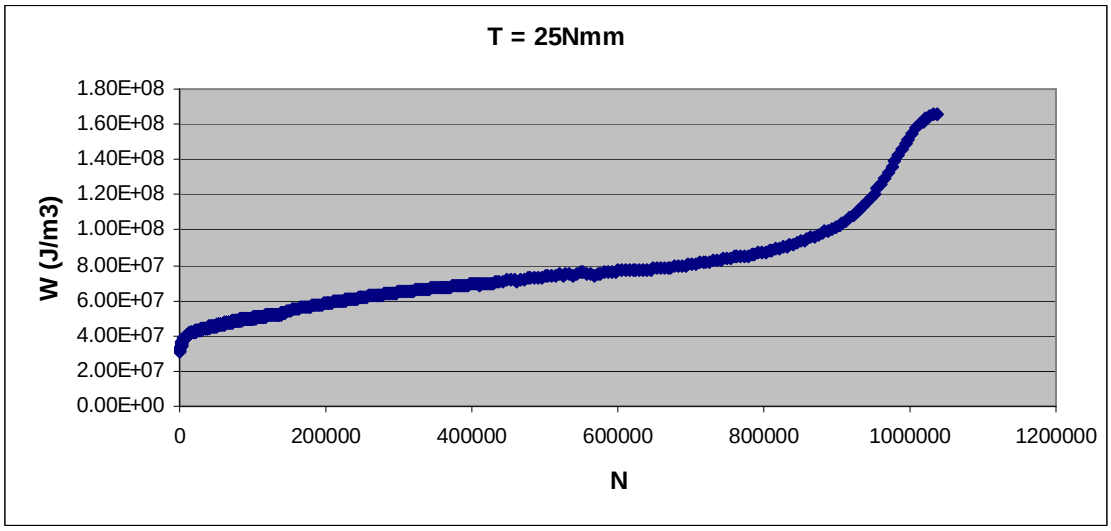


**Graph A2.14:** Dissipated energy for mortar 3, T = 25 Nmm

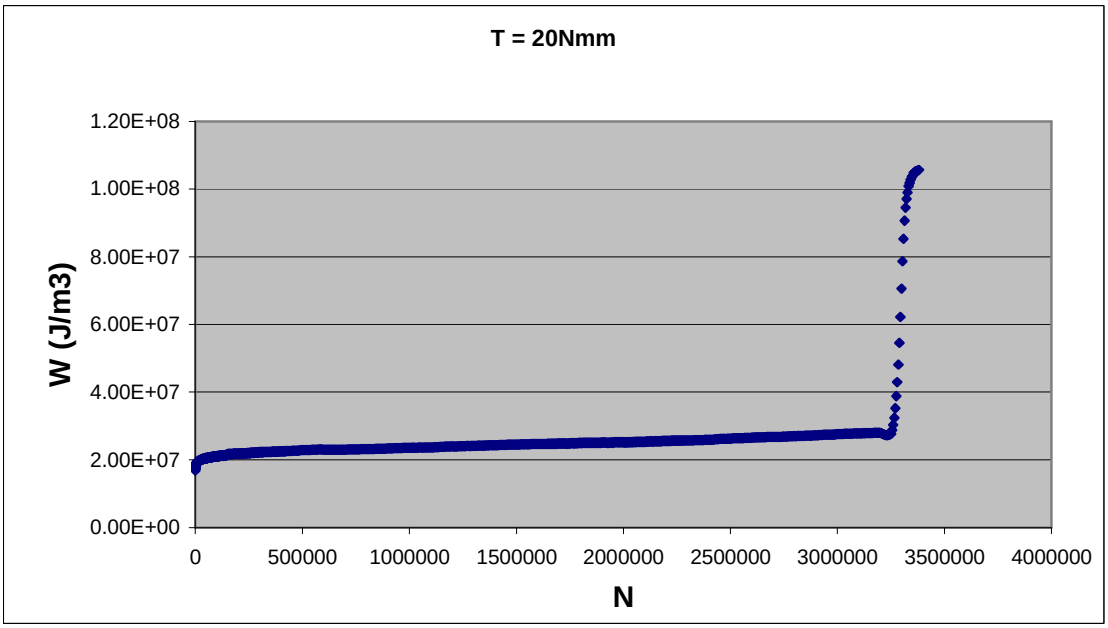


**Graph A2.12:** Dissipated energy for mortar 3, T = 20 Nmm

# Mortar 4

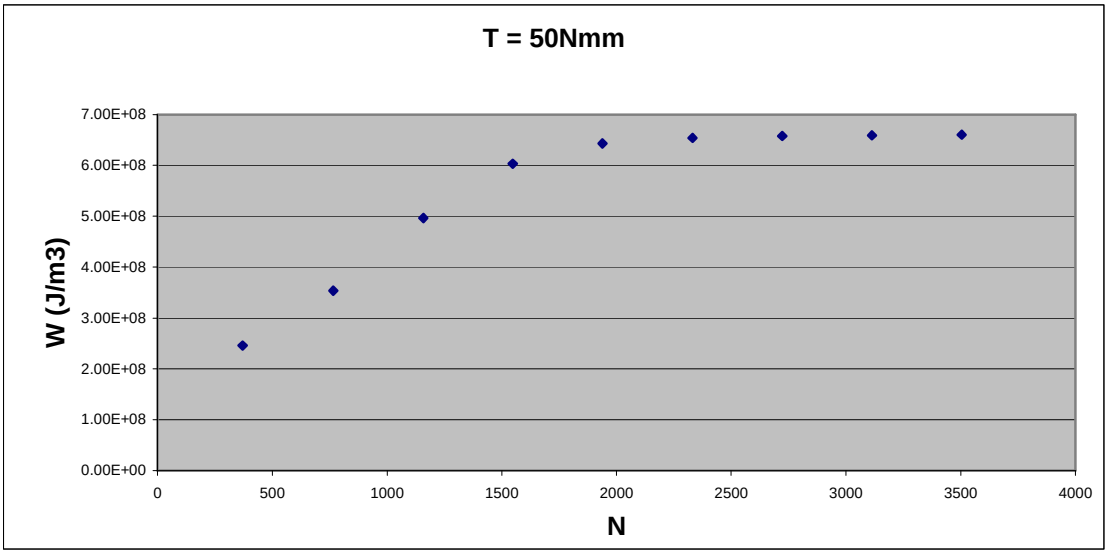


**Graph A2.13:** Dissipated energy for mortar 4, T = 50 Nmm

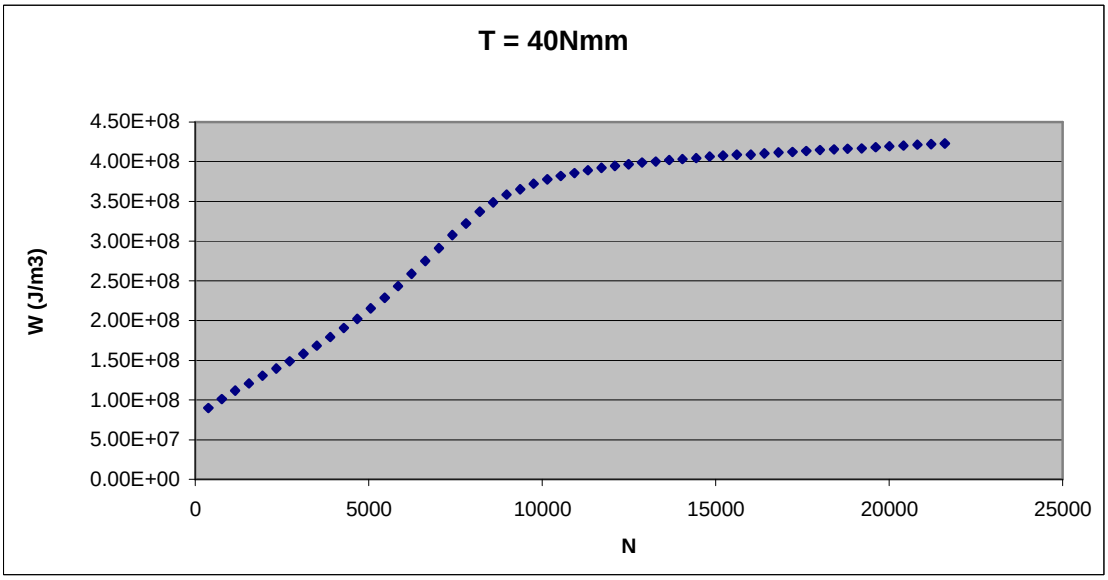


**Graph A2.14:** Dissipated energy for mortar 4, T = 40 Nmm

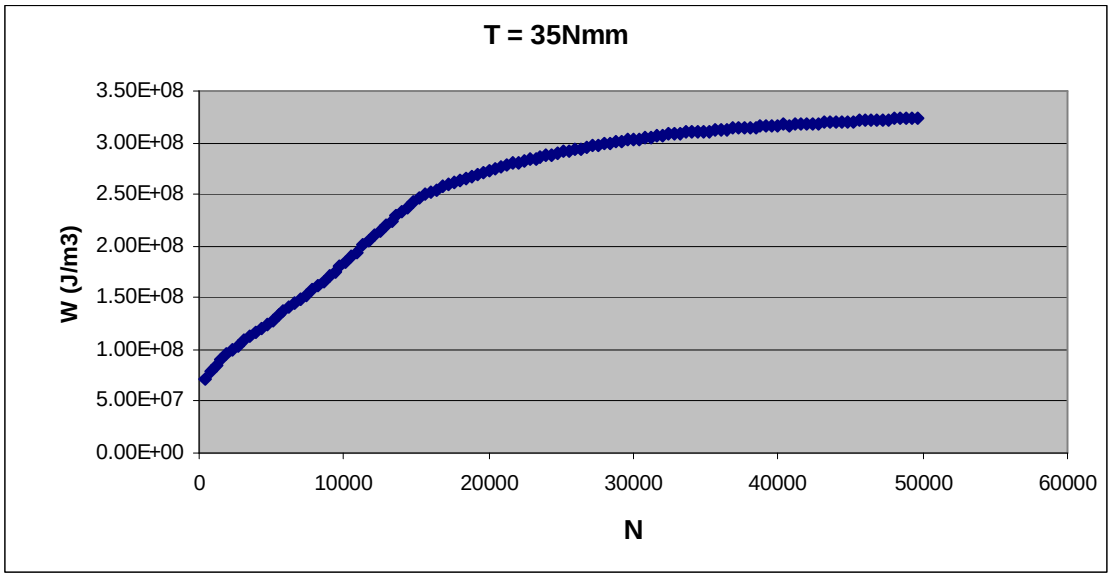


**Graph A2.15:** Dissipated energy for mortar 4, T = 35 Nmm

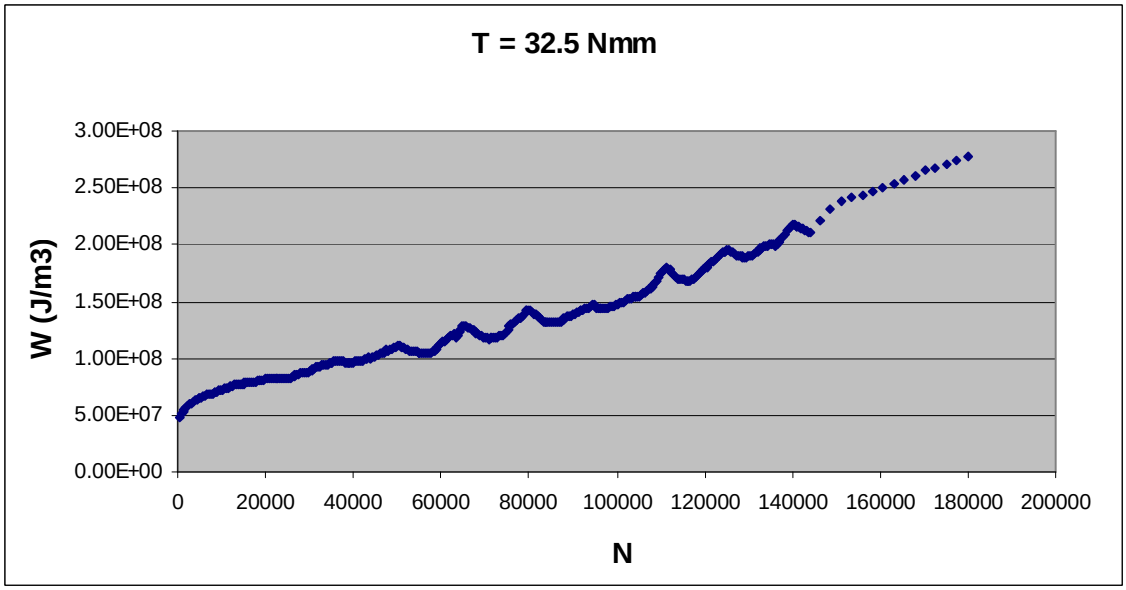


**Graph A2.16:** Dissipated energy for mortar 4, T = 32,5 Nmm

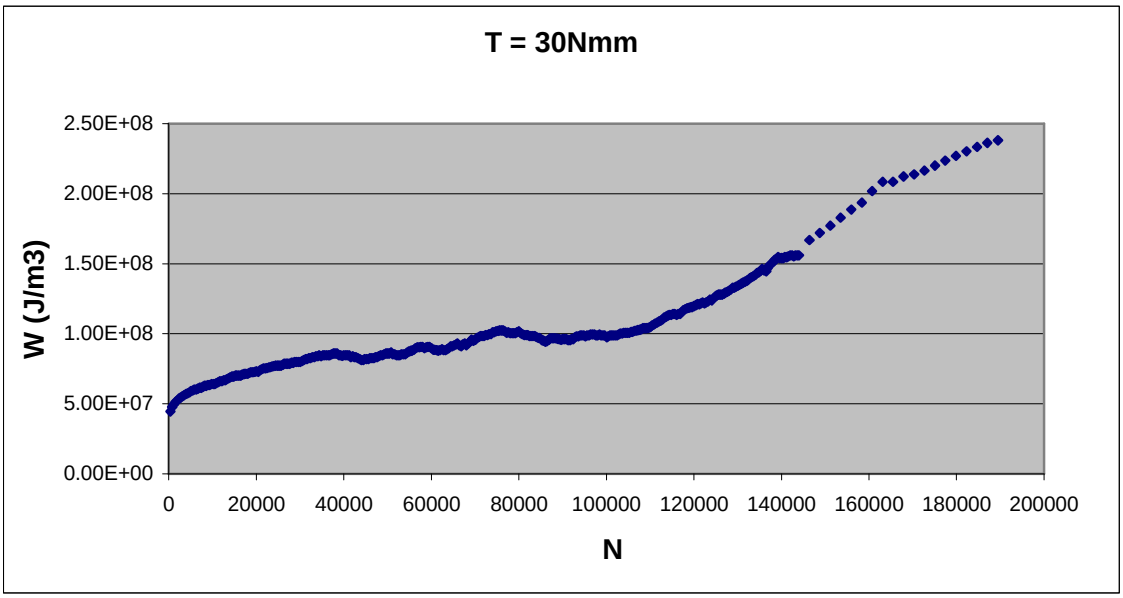


**Graph A2.17:** Dissipated energy for mortar 4, T = 30 Nmm